Doctoral Dissertation

Metabolomics-based approach to identify important shelf life-related metabolite in full-ripe ‘Queen’ pineapple (*Ananas comosus* cv. Queen)

Muhammad Maulana Malikul Ikram

June 2022

Division of Advanced Science and Biotechnology

Graduate School of Engineering,

Osaka University

List of Abbreviations

(*in alphabetical order*)

ANOVA	Analysis of variance
GC	Gas chromatography
MS	Mass Spectrometry
MSTFA	*N*-methyl-*N*-trimethylsilyl-trifluoroacetamide
OPLS	Orthogonal Projection to Latent Structure
PCA	Principal Component Analysis
RMSEE	Root-Mean-Square-Error of Estimation
RMSECv	Root-Mean-Square-Error of Cross-validation
RATA	Rate-All-That-Apply
QqQ	Triple quadrupole
VIP	Variable Importance in Projection

Table of Contents

Chapter 1
General introduction

1.1 Importance of pineapple

Pineapple is an important commodity in tropical fruit industries with the market value could reach 14.7 billion USD and production volume of approximately 28.3 million metric tons in the world, making it the third-most abundant tropical fruit after banana and mango (http://www.fao.org/faostat/en/#data/QC/). Pineapple is popular due to its mild sweet and acid flavor (United Nations 2016). Due to its popularity, pineapple market has grown annually by around 3% over the past 10 years (Altendorf 2017). Countries that have the highest consumption are Brazil, Philippines, Indonesia, India, and China (Mulderij 2018). All of these countries mainly obtained the pineapple from their own production.

Aside from above countries that mainly consume pineapple within their own country, there are also countries that need to import pineapple for consumption. The top importer countries are United States, Netherlands, Japan, Belgium, Canada, and United Kingdom (United Nations 2016). Top importer countries might obtain their pineapple from Costa Rica, Philippines, Ecuador, Panama, Mexico, and other top exporting countries which the total export volume accounts for 9 to 9.5 million tonnes (United Nations 2016).

1.1.1 Important pineapple cultivar

Pineapple has numerous varieties or cultivar that derived from different groups. Each variety or cultivar have different distributions depends on the production zone that linked to the climate conditions (United Nations 2016). Nowadays, the most widespread commercial cultivars are Smooth Cayenne that accounted for majority production of pineapple worldwide. Not only that, but there are also other commercial cultivars that available in the market, such as MD2 ‘Extra Sweet’, Queen Victoria, Sugarloaf, and Red Spanish pineapple, with each cultivar might have different sensory profile between each other as shown in Figure 1.1 (United Nations 2016). Among these commercially important pineapple cultivars, Queen Victoria, or known as ‘Queen’ cultivar is one of the under-utilized pineapple that has distinct and superior organoleptic with high enough production to be exported to Europe, thus explained the potential as important pineapple export cultivar in the world (United Nations 2016).

Figure 1.1 Several commercially important pineapple cultivars in the world (from left to right: Smooth Cayenne, Red Spanish, Queen Victoria)

1.2 Pineapple ripening process

Fruit ripening process can be classified into two groups based on the respiration rate and ethylene productions, namely climacteric and non-climacteric group (Paul et al. 2012). Climacteric fruit, such as banana, and mango, can further ripened after harvested from the tree, and mainly indicated by the burst of ethylene production and increase of respiration rate during ripening process of the fruit (Symons et al. 2012). In contrast, non-climacteric fruit such as pineapple cannot ripened after harvested from the plant and also did not have the increase of ethylene production and respiration rate during ripening process (Symons et al. 2012; Kader 1999). These processes are shown in Figure 1.2.

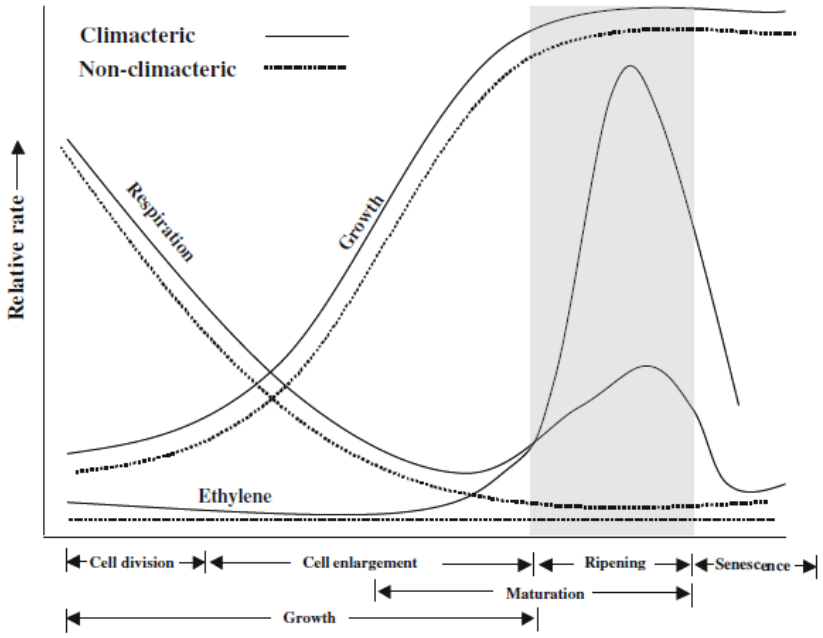

Figure 1.2. Respiration rate of climacteric and non-climacteric (Reprinted/adapted by permission from Springer Nature Customer Service Centre GmbH: Springer Nature, The fading distinctions between classical patterns of ripening in climacteric and non-climacteric fruit and the ubiquity of ethylene—An overview, by Vijay Paul et al, 2012)

Due to its non-climacteric characteristic, pineapple should be harvested at the intended ripening stage according to the purpose. Pineapple ripening stage can be divided into five stages according to the peel color changes shown in Figure 1.3 (Agricultural Standards Unit United Nations Economic Commission for Europe 2013). The classification was divided as follows: C0 stage contains 0% yellow color, C1 stage contain 0%–25% yellow color, C2 stage contain 25%–50% yellow color, C3 stage contain 50%–75% yellow color, and C4 stage contain 75%–100% yellow color (Agricultural Standards Unit United Nations Economic Commission for Europe 2013). Mainly, pineapple was harvested as mature green stage (C1-stage) for export to fulfill the worldwide consumption, while the full ripe yellow stage (C4-stage) for domestic consumption. But nowadays, we can also find full ripe pineapple (C4-stage) in the export country and classified as a 'premium' product with a higher price (Steingass et al. 2015c). However, even though full-ripe pineapple is sold as premium, the shelf-life of these product remain as a hindrance to increase the export volume of full-ripe pineapple. Compared to C1-stage pineapple that have around 3-weeks of shelf life, C4-stage pineapple only have 1-week of shelf life, thus the distribution is limited to the air cargo and increasing the distribution cost (Dhar et al. 2008).

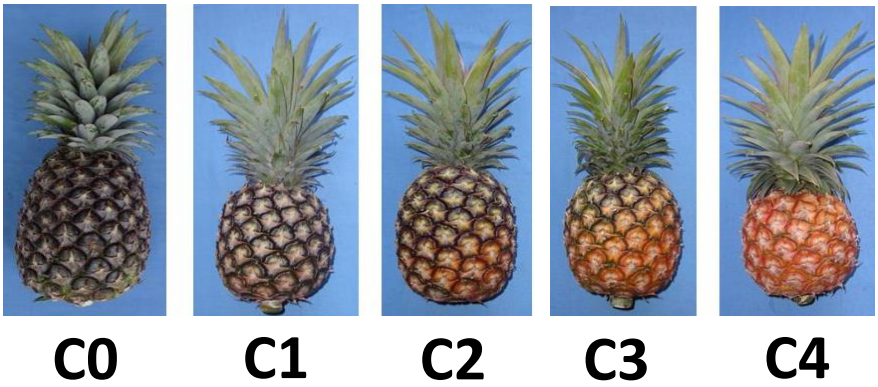

Figure 1.3. Ripening classification of pineapple based on UNECE FFV-49

1.3 Metabolomics approach

Metabolomics is a comprehensive profiling of metabolites within biological system, such as cells, tissue, and organisms, that reflect its molecular quality thus can be used to elucidate changes or differences in biological system (Putri and Fukusaki 2014; Hanifah et al. 2018). Due to its usefulness to detect various metabolites at one-time, metabolomics has been widely used in many fields, such as medical field, synthetic biology, agriculture, and also food sciences (Takeuchi et al. 2018; Fathima et al. 2018; Anjaritha et al. 2019). Based on its target metabolites, metabolomics research can be divided into two groups, namely targeted metabolomics and untargeted metabolomics (Schrimpe-rutledge et al. 2016). Targeted metabolomics focusing on specific class compound of metabolites such as volatile compound, or amino acid compound, to answer the biological problems in the sample, while untargeted metabolomics, or also known as non-targeted metabolomics, focusing on all the metabolite peak that can be obtained from one biological sample, whether it can be identified or not (including unknown metabolite) (Schrimpe-rutledge et al. 2016).

In metabolomics analysis, instrument that commonly used are nuclear magnetic resonance (NMR) and chromatography coupled with mass spectrometry, e.g., gas chromatography-mass spectrometry (GC-MS) and liquid chromatography-mass spectrometry (LC-MS) (Li et al. 2021). Among these instruments, GC-MS is frequently chosen due to its relatively low cost, high reproducibility, high stability, and convenient data processing even though it required additional derivatization method to be able to analyze broad range of metabolites (Putri and Fukusaki 2014). Analysis of metabolomics

also required big database of metabolites for identification of the metabolites that contained in the sample. Identification was conducted by comparing the retention time, retention time index (obtained via calculation with n-alkene peaks or fatty acid methyl ester solution), and fragment pattern with in-house library or online database, including National Institute of Standard and Technology (NIST), Fiehn library, MassBank, Golm Metabolome Database, and Wiley Database (Want and Metz 2017; Hill et al. 2015). Big metabolites data that obtained from GC-MS and annotation process were further subjected to multivariate analysis for easier understanding and to be able to gain key information that were hidden in complex-metabolites data (Putri and Fukusaki 2014). Common methods in multivariate analysis for metabolomics are principal component analysis (PCA) to see the general trend obtained from the metabolites data in the sample, and also projection to latent structures (PLS) to correlate and obtain the connection between the explanatory variables (in this case metabolite data) and response variable (quantifiable phenotypic characteristics, e.g., weight, color, firmness, etc) (Teoh et al. 2015).

1.3.1 Pineapple metabolomics

There are numerous studies that used metabolomics to study about pineapple fruit. Studies about ripening process of pineapple was conducted to evaluate the ripening process and its relation to volatile, phenolic, and fatty acids (Steingass et al. 2015a; Steingass et al. 2015b; Ogawa et al. 2018; Hong et al. 2021). Other studies were focused on the he changes in metabolites profile after coincident with postharvest internal browning due to cold storage, and also metabolite marker study on pineapple fruitlet core rot disease (Luengwilai et al. 2018; Barral et al. 2019). Not only in the flesh and peel

part, application of metabolomics in pineapple also can be found on pineapple leave to elucidate the taxonomy and difference N-P-K ratio (Cassago et al. 2022; Chen et al. 2021). However, among the above-mentioned studies, there was no study that use metabolomics as a basis to prolong pineapple shelf-life, more specifically to Queen cultivar.

1.4 Objective and strategy

Therefore, the objective of this research is to investigate important metabolites that responsible for shelf life of full ripe Queen cultivar pineapple based on metabolomics approach. To achieve this objective, three strategies were performed. First strategy is to justify which pineapple is important and beneficial to be studied by combining metabolomics and sensory evaluation. Knowing which pineapple (cultivar and ripening stage), the study of ripening process using metabolomics was conducted to elucidate which metabolites that responsible to the changes is 'Queen' pineapple shelf-life along ripening. Finally, the important metabolites that obtained from the second strategy was added to the 'Queen' pineapple fruit to see the direct effect of this metabolites to the pineapple shelf-life.

1.5 Thesis outline

This thesis is divided into five chapters. Chapter 1 explained the importance of pineapple, which pineapple cultivar is important in the pineapple industry, pineapple ripening process due to its non-climacteric character, previous studies on pineapple metabolomics, and the objective of this study.

Chapter 2 described the application of GC-MS-based metabolomics in combination with sensory evaluation to elucidate which pineapple is preferable to the consumer in

term of ripening stage and cultivars. Moreover, metabolites that responsible to sensory profile are proposed using orthogonal projection to latent structures (OPLS) regression analysis.

Chapter 3 focused on the investigation of ‘Queen’ pineapple ripening process using GC-MS-based metabolomics. Similar with the strategy in chapter 2, OPLS was conducted between metabolites as explanatory variable and ripening stage as response variable to identify which metabolites are responsible to the ripening process, specifically to the decrease of shelf-life along ripening process.

Chapter 4 discussed the effect of metabolites that responsible to the shelf-life of ripening by the addition of these metabolites to the ‘Queen’ pineapple. Through physicochemical analysis that determine the freshness of pineapple (i.e., weight and color changes) and metabolomics analysis with the comparison to the day 0 (fresh sample), the effect of shelf-life related metabolites to the pineapple fruit were elucidated.

Chapter 5 present the conclusion of this study and future perspectives that were proposed from this study.

Chapter 2
Comparative metabolomics and sensory evaluation of pineapple (*Ananas comosus*) reveal the importance of C4-pineapple

2.1 Introduction

In contrast to banana and mango, which exhibit an increase in respiration rate and ethylene production during ripening, pineapples are categorized as non-climacteric fruits, therefore the ripening process is stopped after harvest (Jiang and Song 2010; Kader 1999). The ripening stage of pineapple can be divided into five stages, from C0 to C4, based on the color of its peel, according to the United Nations Economic Commission for Europe (UNECE) Standard for pineapple (FFV-49). While C4 fruits can currently be exported at a higher price, C1 fruits are typically sold as an export product. (Agricultural Standards Unit United Nations Economic Commission for Europe 2013; Ahmad and Siddiqui 2015).

Worldwide, there are numerous cultivars of pineapple, the three most popular being Smooth Cayenne, Red Spanish, and Queen (Steingass et al. 2015c). These different in cultivars and ripening stages may have sensory profiles that differ from one another (Shoda et al. 2013). These various sensory profiles could result in variable consumer acceptance rates. Understanding consumer tastes is crucial for creating foods that are widely accepted. Based on the sample's metabolite profile, the sensory profile can be researched. Gas chromatography/mass spectrometry (GC-MS) has made it possible to analyze numerous hydrophilic small-molecule components associated to the flavor and aroma of food at once due to comprehensive metabolite analysis of biological samples. Numerous metabolomics studies have already shown a connection between certain foods

and drinks, like shrimp and Japanese tea, using sensory assessment that correlated with metabolomics data. (Putri et al. 2021; Pongsuwan et al. 2007).

Previous research have described the many stages of pineapple ripening, its metabolite profile, and its relationship with sensory qualities. (Shoda et al. 2013; Pongsuwan et al. 2007). However, there are not any comprehensive studies that combine various cultivars and ripening phases with metabolomic analysis and sensory evaluation to explain the unique traits of pineapple diversity. Therefore, this study used GC-MS analysis and sensory evaluation to profile the metabolites and sensory characteristics of different pineapple cultivars and ripening phases. The results of this study should serve as a foundation for employing metabolites to enhance pineapple quality by correlating pineapple taste with cultivar or ripening stage.

2.2 Materials and Method

2.2.1 Plant materials

Two sample sets of the pineapple (*Ananas comosus*) were taken for this study. The sensory assessment and GC-MS analyses were conducted using the first set. In the GC-MS analysis, extra samples were taken from the second set. According to the UNECE FFV-49 classification, the phases of ripening were categorized. Smooth Cayenne and Red Spanish were the two cultivars included in the first sampling batch. Red Spanish was harvested from Indonesia at the C1, C3, and C4 ripening stages. Smooth Cayenne, which was imported from the Philippines, was found in a local store in Japan at the ripening stages C1 and C4. Queen and Smooth Cayenne were the two cultivars included in the second sampling set. The Smooth Cayenne cultivar has three ripening stages—C1, C3,

and C4—and was available in Indonesia or from a local Japanese retailer that imported its products from Taiwan and Japan. Queen cultivars originated in Japan and were purchased from a local retailer there. They have one ripening stage, known as the C1 stage. Before further examination, all samples were kept at 4 °C for storage. Table 2.1 and Figure S2.1, respectively, offer an in-depth sampling of data and images.

Table 2.1. Sample set for pineapple sensory evaluation and GC-MS analysis

Country	Cultivar	Ripening stage	Label	Picture label
Indonesia (North Sulawesi)	Red Spanish	C1	IoC1	A
		C4	IoC4	B
		C1	IrC1	C
		C3	IrC3	D
		C4	IrC4	E
Philippine	Smooth Cayenne	C1	PhC1	F
		C4	PhC4	G
Indonesia (West Java)	Smooth Cayenne	C3	IC3	H
Taiwan	Smooth Cayenne	C4	TC4	I
Japan	Smooth Cayenne	C4	JC4	J
	Queen	C1	JC1	K
Indonesia (West Java)	Smooth Cayenne	C4	IC4	L

Samples A–G were used for sensory evaluation and GC-MS analysis. Samples H–L were used for additional samples in the GC-MS analysis.

2.2.2 Sensory evaluation by Rate-All-That-Apply (RATA) test and its sample preparation

The pineapple was split into four symmetrical pieces after being skinned, and the core was taken out. The pineapple flesh was then divided into pieces that were around 2 x 1.5 x 1.5 cm. Before the panelists received their samples, three flesh cubes from each

sample were put in clear plastic cups and marked with a random three-digit code. At Osaka University, sensory assessments were performed over the course of two sessions. The Graduate School of Engineering at Osaka University recruited 28 panelists (12 women and 16 men; 22 Japanese; 5 Indonesian; 1 Malaysian; 22-53 years of age); they had a 60-minute training session to become familiar with sensory characteristics before the test (semi-trained panelists). Panelists were asked to score the strength of sensory qualities using a five-point scale in the Rate-All-That-Apply (RATA) test sensory evaluation, with the samples being presented in a randomized order. The participants were asked to rinse their lips with water before testing a new sample. Based on prior research, the definitions of the sensory qualities considered in this evaluation are provided in Table S2.1 (Supplementary Information) (Schulbach et al. 2007; Koppel and Chambers Iv 2010; Threlfall et al. 2007).

2.2.3 Sample preparation for GC-MS analysis

The pineapple fruit's core and crown were removed, leaving only the fruit's flesh. The flesh of the pineapple was divided into cubes measuring 2 x 1.5 x 1.5 cm. These flesh cubes were divided into top, middle, and bottom portions. They were then wrapped in aluminum foil, lyophilized with liquid nitrogen, and put in a 50 mL freeze-crushing tube (made by Yasui Kikai, Osaka, Japan) with metal beads. The tube was then crushed into powder using a multi-bead shocker at 2000 rpm for 20 seconds (Yasui Kikai). Three duplicates from each pineapple sample totaling 5 mg were weighed into a 2 mL microtube (n = 3). All samples were extracted using 1 mL of the extraction solvent (methanol: chloroform: ultrapure water 5:2:2 v/v/v) containing 100 µg/mL ribitol as an internal standard, along with one empty microtube that served as a blank. Centrifugation was used

to separate the solid components of this mixture for three minutes at 10.000 rpm at 4 °C after it had been incubated for 30 minutes at 37 °C and 1200 rpm. A new 1.5 mL microtube was used to transfer 600 µL of supernatant, and 300 µL of ultrapure water was added. The microtube was then centrifuged for three minutes at 10.000 rpm, 4 °C. The aqueous and organic solvent layers were able to be separated thanks to centrifugation. 20 µL were transferred from the aqueous layer into fresh 1.5 mL microtubes for the analysis of sucrose, and 100 µL were transferred for the analysis of all metabolites, before the tubes were sealed with perforated caps. Additionally, for quality control (QC) samples, 100 µL of each sample were combined into a 50 mL falcon tube. For each analysis, 20 µL and 100 µL aliquots of the QC samples were also created. All samples, QC, and a blank were placed in a centrifugal concentrator (Taitec, Saitama, Japan) and spun under vacuum for 30 minutes for the sucrose analysis and 75 minutes for the analysis of all metabolites. The concentrated materials were lyophilized over night after being frozen in liquid nitrogen. The derivatization procedure was likewise carried out similarly to earlier investigations (Parijadi et al. 2018).

2.2.4 GC-MS analysis

A GCMS-QP2010 Ultra (Shimadzu, Kyoto, Japan) outfitted with an AOC-20i/s autoinjector was used for the GC-MS analysis (Shimadzu). The GC-2010 was outfitted with InertCap 5MS/NP (35 m 0.25 mm, I.D. df = 0.25 m), linked to an inner seal connector (Lot No. TAYL01) (GL Sciences, Tokyo, Japan), and baked at 250 °C for an hour. Sucrose-included and sucrose-excluded assays were both carried out. 1 µL of the material was introduced into the system at 230 °C and a split ratio of 25:1 for the sucrose-included analysis. The linear velocity of the carrier gas (He) was 39.0 cm/s. The column

temperature was held at 80 °C for 4 minutes before being increased to 330 °C at a rate of 15 °C/minute for 8 minutes. 310 °C and 280 °C, respectively, were maintained as the interface and ion source temperatures. Using the electron ionization (EI) technique and a 70.0 V filament bias voltage, ions were produced. With an event time of 0.15 seconds, spectra covering the mass range *m/z* 85–500 were captured. Prior to analysis, a standard alkene mixture (C_8-C_{40}) was injected to determine the retention index (RI), which was then used for peak identification. Similar settings were employed for the sucrose-excluded analysis, with the filament-off time being different at 19.1–19.4 min to exclude the sucrose peak.

2.2.5 Data analysis

The raw data produced from the analysis was converted into.cdf format using GCMSsolution ver 4.20 (Shimadzu) before being converted to.abf format using an Abfconverter (Reifycs, Tokyo, Japan). Baseline correction, denoising, peak detection, alignment, and automatic compound annotation of the compounds with EI mass spectral library from GL-Science DB InertCap 5MS-NP, Kovats RI, 494 records (Riken, Kanagawa, Japan) and NIST-11 MS Spectral Library (NIST, Maryland, USA). were carried out using MS-DIAL (version 4.00) (Lai et al. 2018). Both automatic annotation in MS-DIAL and human annotation in GCMSsolution have similarity values set to a minimum of 70%. Co-injection analysis was used to confirm several peaks with real standards, including inositol, mannose, galactose, quinic acid, and sucrose (Wako Pure Chemical Industries Ltd., Osaka, Japan; Sigma-Aldrich Japan Ltd., Tokyo, Japan; Alfa Aesar Ltd., Heysham, UK).

2.2.6 Statistical analysis

To determine the normalized peak height, annotated metabolites were standardized to the internal standard, ribitol. These identified metabolites were subjected to multivariate analysis using SIMCA-P ver. 13 (Umetrics, Umea, Sweden) to perform principal component analysis (PCA), with autoscaling being used as a scaling approach and no transformation. Trends, clusters, and outliers can be seen using PCA, an unsupervised analysis (Jolliffe et al. 2016). Only metabolites in the QC samples with a relative standard deviation under 30% were included as explanatory factors. SIMCA-P version 13 was used to carry out an orthogonal projection to latent structure (OPLS) regression analysis (Umetrics, Umea, Sweden). Each metabolite's variable important in projection (VIP) score and coefficient value were generated from this regression analysis and will be used in the following discussion. JASP version 0.11.1 (JASP Team, Amsterdam, Netherlands) was used for the statistical analysis, which used one-dimensional analysis of variance with Tukey's post-hoc test. Significant differences were defined as those with $p < 0.05$.

2.3 Result and discussion

2.3.1 Evaluation of pineapple sensory properties from different cultivars and ripening stages

To comprehend the taste qualities of pineapples from various cultivars and ripening phases, sensory assessment was carried out. The samples used in this investigation were the Philippines Smooth Cayenne at C1 and C4 ripening stage and the

Indonesian Red Spanish at the C1, C3, and C4 ripening stages (Figure S2.1, A-G). Panelists were able to identify between pineapple in its unripe and ripening stages, according on PCA results from the sensory evaluation utilizing the 15 sensory qualities indicated earlier (Figure 2.1A). With the late-ripening phases (C3 and C4 stages) clustered on the positive side and the early-ripening stages (C1) clustered on the negative side of a score plot based on PC1 (30.5 percent contribution), the separation was demonstrated. The explanatory factors that contribute to the separation seen in the score plot are displayed in the loading plot. Sweetness, juiciness, and high acceptance are sensory qualities that contribute to the late-ripening stage, whereas stiffness and sourness were sensory qualities that contributed to the early ripening stage.

The disparities in consumer preferences across groups were investigated further. As evidenced by the high acceptability attributes in Figure S2.2, panelists from all nationalities preferred C4 stage pineapple to C1 pineapple. Due of the high acceptability in both genders and the relevance of the C4 ripening stage, gender analysis emphasizes this further (Figure S2.3). This study has demonstrated that, independent of cultivar, consumers of all sexes and nationalities prefer pineapples that are at the C4 ripening stage. The typical pineapple market, however, only offers the C1 stage. This is due in part to the C1 stage's extended shelf life (3 weeks), which contrasts with the C4 stage's shorter shelf life (approximately 1 week) (Dhar et al. 2008). Therefore, a method for extending the pineapples' shelf life during the C4 stage is required to fulfill consumer needs.

2.3.2 Metabolites contribution to different sensory profile in pineapple

The same sample set from the RATA test was used to annotate 45 peaks using GC-MS. Table S2.2 contains a list of the specific metabolites that were employed in this

study. The PCA figure in Figure 2.1B was made using these peaks as explanatory factors. Contrary to sensory evaluation, a 42.5 percent contribution from PC1 revealed a distinct distinction between the Smooth Cayenne and Red Spanish varieties. Within the cultivars based on PC2, ripening stage-based separation with a 23.5 percent contribution was also noted. Gamma-aminobutyric acid (GABA), valine, and alanine were the metabolites that contributed to the Red Spanish, according to the loading plot, while sucrose, threonic acid, and 5-hydroxytryptamine (serotonin) were the metabolites that contributed to the Smooth Cayenne. On the other hand, early ripening stage contributing metabolites were quinic acid, malic acid, and isocitric acid+citric acid, while the late-ripening stage contributing metabolites were asparagine, serine, and glycine.

To forecast the value of the Y-variable (response variable) by using the X-variable, regression analysis with orthogonal projection to latent structures (OPLS) is frequently utilized (explanatory variable) (Putri and Fukusaki 2014). OPLS regression analysis also revealed metabolites that were significantly impacted by the variation in the response variable. (Putri and Fukusaki 2014). With sensory value as the response variable and annotated metabolites as the explanatory variable, OPLS regression analysis was carried out to examine the contribution of metabolites responsible for the sensory features. The R^2 value, which indicates the linearity of the model, and Q^2, which indicates the model's capacity for prediction, were used to assess the model's quality. A good model will be defined as having an R^2 value more than 0.6 and a Q^2 value larger than 0.5. (Alexander et al. 2015). All models (sweetness, juiciness, acceptability, sourness, and firmness) were shown to have R^2 and Q^2 values greater than 0.869 and 0.803, respectively, indicating that the models accurately described these relationships (Figure S2.4).

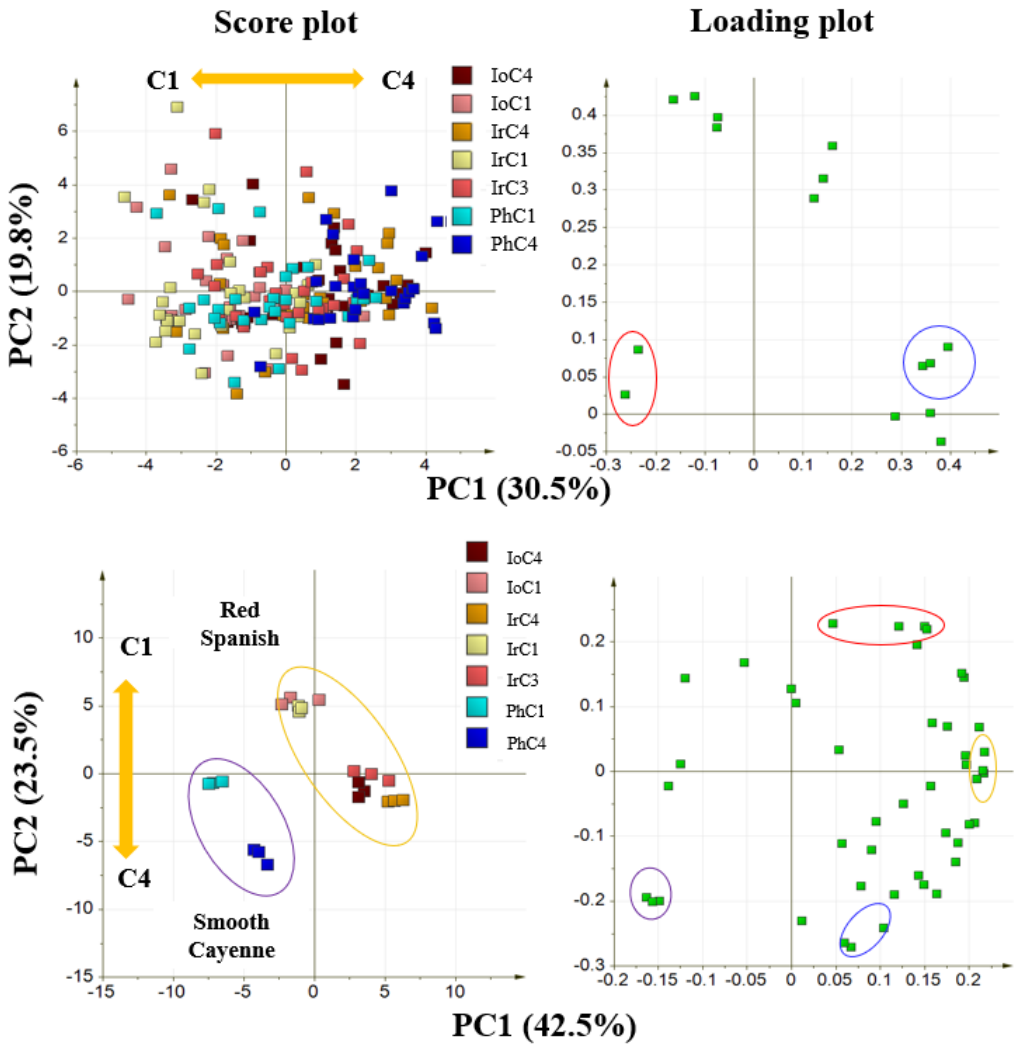

Figure 2.1. PCA results from RATA samples. (A) Sensory evaluation result. Panelists consist of 28 people were used as a dataset. Explanatory variables used in PCA were 15 auto-scaled sensory attributes data. (Left) Score plot showed separation from different ripening stages. Legends in the score plot represent the sample and colored based on Table 2.1. (Right) Loading plot corresponds to the separation in the score plot. Blue circle represents sweetness, juiciness, and high acceptability, while red circle represents sourness and firmness. (B) GC-MS analysis result. Explanatory variables used in PCA were 45 auto-scaled annotated metabolites data. (Left) Score plot showed separation from

different cultivars on PC1 and different ripening stages on PC2. Legends in the score plot represent the sample and colored based on Table 2.1. (Right) Loading plot corresponds to the separation in the score plot. Red circle represents quinic, malic, isocitric acid+citric, and ascorbic acids. Yellow circle represents GABA, valine, and alanine. Blue circle represents asparagine, serine, and glycine, while purple circle represents sucrose, threonic acid, and 5-hydroxytryptamine.

Table 2.2. Metabolites with high VIP score and positive coefficient value from sweetness, juiciness, and acceptability model from OPLS regression analysis.

VIP metabolites	VIP score Sweetness	VIP score Juiciness	VIP score Acceptability
Asparagine	2.001	1.812	2.047
Serine	1.759	1.450	1.901
Glycine	1.677	1.227	1.775
Threonic acid	1.331	1.805	1.324
Sucrose	1.154	1.670	1.187
5-Hydroxytryptamine (Serotonin)	1.033	1.693	1.165

These metabolites were selected based on a VIP score of more than 1.0 and have a positive coefficient value on sweetness-juiciness-acceptability attributes.

Table 2.3. Metabolites with high VIP score and positive coefficient value from sourness and firmness model from OPLS regression analysis.

VIP metabolites	VIP score Sourness	VIP score Firmness
Isocitric acid+Citric acid	1.218	1.943
Malic acid	1.804	1.518
Ascorbic acid	1.819	1.999
Quinic acid	1.123	1.051

These metabolites were selected based on a VIP score of more than 1.0 and have a positive coefficient value on sourness-firmness attributes.

The VIP score, which is computed for each explanatory variable, is used to illustrate which sensory characteristics have a strong link with specific metabolites. These models are built using OPLS regression analysis. The performance of the developed OPLS regression model benefits considerably from metabolites with VIP scores greater than one. Common metabolites among these three models with VIP scores of more than one and positive regression coefficients were selected in order to assess the metabolites that contribute to the positive sensory qualities (sweetness-juiciness-high acceptance). Similarly, metabolites were also used to assess the sensory qualities that contributed negatively (sourness-firmness). The favorable and negative characteristics of these metabolites are listed in Tables 2.2 and 2.3, respectively. Asparagine, serine, glycine, threonic acid, sucrose, and 5-hydroxytryptamine (serotonin) were the metabolites implicated with sweetness-juiciness-high acceptance. Asparagine and serine were also revealed to be important with sweetness, supporting earlier findings (Schiffman et al.

1981). Other fruits like tomatoes, strawberries, and mangoes, as well as their sweetness, were found to be impacted by an increase in glycine (Sung et al. 2019; Keutgen and Pawelzik 2008; Sorrequieta et al. 2010). In addition to serving as the fruit's main source of energy, sucrose is also recognized as the primary sugar present in fruit (Colaric et al. 2005). Interestingly, this is an intriguing first research on the relationship between threonic acid and 5-hydroxytryptamine (serotonin) and pineapple fruit sweetness, juiciness, and high acceptance. However, further evidence is required to assess how much affection these components have for the sensory qualities.

In contrast, isocitric, citric, malic, ascorbic, and quinic acids were involved in the sourness and firmness of pineapple fruit. These findings were consistent with earlier research that claimed malic and citric acids were responsible for the acidity of fruits (Colaric et al. 2005). Ascorbic acid, also known as vitamin C, is acidic (Iqbal et al. 2004; Szent-Györgyi 1933). Malic acid has reportedly been found to positively correlate with hardness in kiwifruit. However, the hardness of kiwi fruits was adversely associated with quinic acid. (Nakanishi et al. 1990). The variations in fruits could be the cause of the variance in correlation to the prior study. Therefore, more research is required to confirm the connection between these metabolites and pineapple firmness. Additional research was done to determine how these metabolites accumulated depending on the stage of ripening (C1 and C4 stage). Increased levels of metabolites associated to acidity and hardness in both the Smooth Cayenne pineapple from the Philippines (Figure S2.6A) and the Indonesia Red Spanish pineapple (Figure S2.5A) demonstrated that these metabolites were higher accumulated in the C1 stage compared to the C4 phases. The sensory evaluation found that pineapples in the C1 stage were sourer and stiffer than pineapples in the C4 stage, which was supported by the accumulation of metabolites related to

sourness and hardness (Figure 2.1A). Similar trends in the accumulation of metabolites linked to sweetness, juiciness, and high acceptability were seen (Figures S2.5B and S2.6B), which demonstrated that these metabolites accumulated higher in the C4 stage than the C1 stage. Although these findings imply that the ripening stage had a noticeable impact on the sensory profile, not all metabolite accumulation in the various ripening stages was associated with the modification of the sensory profile.

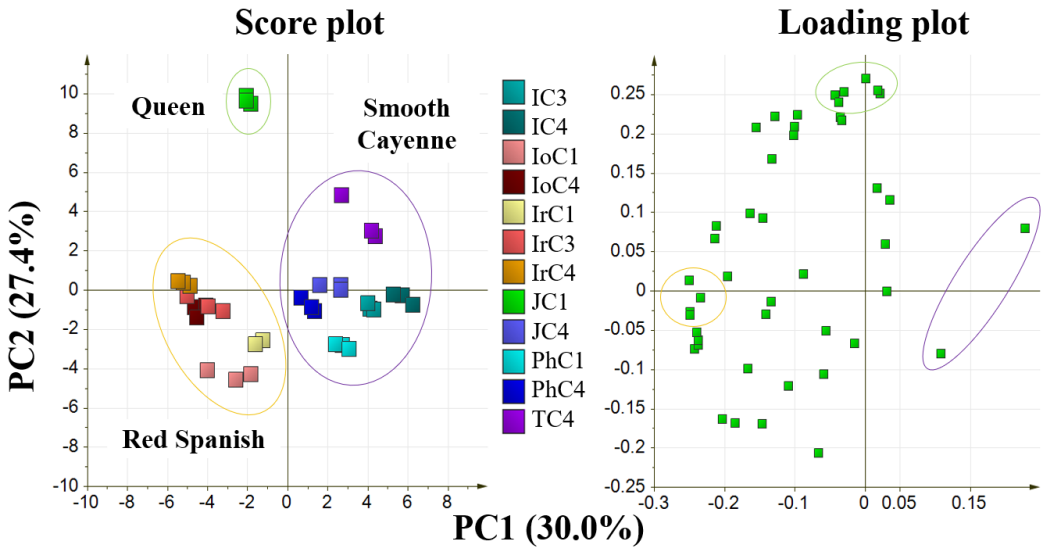

Figure 2.2. PCA result from GC-MS analysis using all samples. Explanatory variables used in PCA were 45 auto-scaled annotated metabolites data. (Left) Score plot showed separation from different cultivars. Legends in the score plot represent the sample and colored based on Table 2.1. (Right) Loading plot corresponds to the separation in the score plot. Green circle represents threonine, serine, and methionine. The purple circle represent sucrose, maleic acid, and threonic acid, and the yellow circle represents alanine, fructose, and GABA.

2.3.3 Pineapple cultivars accumulate varying metabolites

Five more samples were used to confirm the distribution of metabolites from various cultivars, as shown in Figure S2.1 (H-L). 45 metabolites were correctly identified by GC-MS analysis for use in the multivariate analysis as explanatory factors. The ripening stage does not have as much of an impact as varietal differences, as seen by the PCA score plot in Figure 2.2. Smooth Cayenne was plotted on the positive side of the first principle component, Red Spanish on the negative side, and the Queen cultivar cluster more on the upper side of PC1. The metabolite accumulation for each cluster is displayed on the loading plot. Smooth Cayenne accumulate threonic acid, maleic acid, and sucrose. Red Spanish was accumulating fructose, GABA, and alanine, while the Queen cultivar accumulate threonine, serine, and methionine. Similar results were obtained from this experiment with Smooth Cayenne accumulating sucrose and threonic acid, while Red Spanish accumulated GABA and alanine.

The prior metabolites with a high VIP score and a favorable coefficient value from the OPLS regression analysis were used to predict the sensory values of this additional sample. Figure 2.3 displays bar graphs of these metabolites for all samples. Among the samples utilized in the sensory evaluation, C4 fruits had the highest asparagine intensity (Figure 2.3A). Japan C4 Smooth Cayenne (JC4), Taiwan C4 Smooth Cayenne (TC4), and Japan C1 Queen (JC1) samples scored higher in the supplementary sample than Indonesia C3 and C4 Smooth Cayenne samples (IC3 and IC4). Glycine and serine showed comparable results (Figures 2.3B and 2.3C, respectively), with the exception of Philippine C1 Smooth Cayenne (PhC1). The high relative intensities of glycine and serine

in PhC1 pineapple might explain its clustering behavior on sensory evaluation of this cultivar shown in Figure 2.1A.

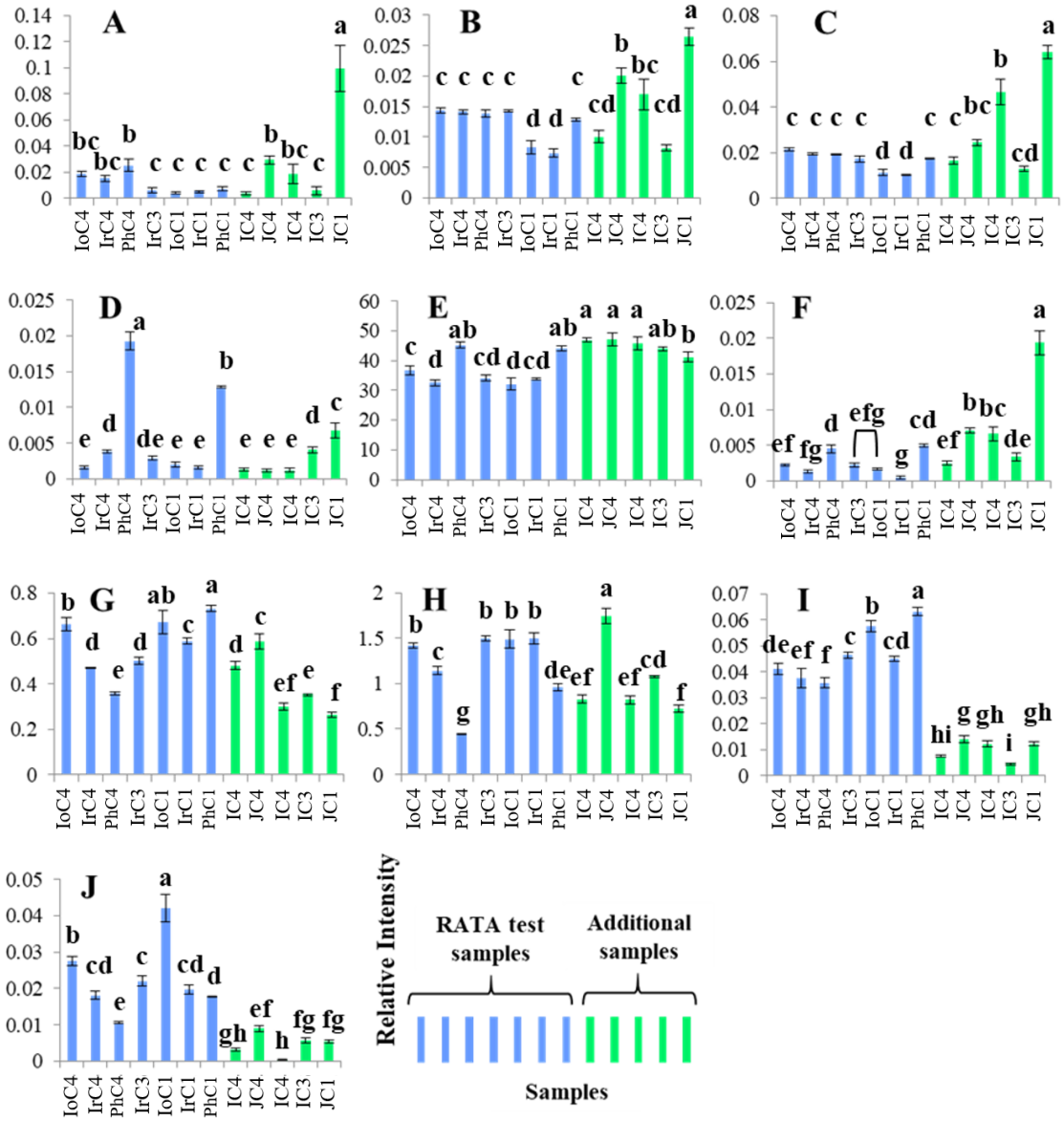

Figure 2.3. Bar graph of sensory-related metabolites from all samples. From left to right: IoC4, IrC4, PhC4, IrC3, IoC1, IrC1, PhC1, IC4, JC4, TC4, IC3, and JC1. (A) Asparagine, (B) glycine, (C) serine, (D) threonic acid, (E) sucrose, (F) 5-hydroxytryptamine, (G) malic acid, (H) isocitric acid+ citric acid, (I) ascorbic acid, and (J) quinic acid. The horizontal

axis represents the sample, and the vertical axis represents the normalized relative intensity with the internal standard. The blue bar graph shows the sample that was used in the RATA test, while the green bar graph shows the additional sample. The error bar represents the standard deviation from the relative intensity value. Different letters indicate significant differences ($p < 0.05$) based on Tukey's test mean comparison.

The C1 Smooth Cayenne from the Philippines was not grouped with the C1 stage pineapple, but rather between the C1 and C4 stages. As a result, this cultivar will probably produce sweetness and juiciness similar to pineapple in the C4 stage. The sample from the Philippines had the highest relative intensity of all the samples tested in the sensory test for threonic acid (Figure 2.3D). Furthermore, among the extra samples, Indonesia C3 Smooth Cayenne (IC3) and Japan C1 Queen were higher, indicating that it might be sweeter and juicier than the other cultivars. The Smooth Cayenne cultivar (Philippine C1, Philippine C4, Indonesia C3, Taiwan C4, Japan C4, Indonesia C4) employed in this study was sweeter than Red Spanish (Indonesia C1, Indonesia C3, Indonesia C4) and Queen (Japan C1), regardless of the country of origin, according to sucrose accumulation in Figure 2.3E. Regardless of their ripening stage, the pineapples from the Philippines (C1 and C4 Smooth Cayenne), Japan (C4 Smooth Cayenne and C1 Queen), and Taiwan (C4 Smooth Cayenne) accumulate higher serotonin levels than the pineapples from Indonesia (C1, C3, C4 Red Spanish; C3 and C4 Smooth Cayenne). In Indonesian oval fruits (IoC1 and IoC4) and C1 fruits, the relative intensity of malic acid (Figure 2.3G) was higher, indicating that malic acid may be a distinctive metabolite of these cultivars. But Japan C1 Queen accumulates low-intensity malic acid, indicating that this fruit has low acidity and low firmness. The two main organic acids found in pineapples are isocitric acid and citric

acid. (Saradhuldhat and Paull 2007). The relative intensity of this compound in our investigation indicates that it varies for each cultivar. In comparison to the other cultivars, the Red Spanish cultivar accumulated more isocitric acid+citric acid. Additionally, the Japan C4 Smooth Cayenne (JC4) accumulates higher levels of citric and isocitric acids, which may indicate the presence of a particular metabolite unique to the JC4 cultivar. It was challenging to use ascorbic acid (Figure 2.3I) and quinic acid (Figure 2.3J) to predict the sensory characteristics of additional pineapple samples. It's likely that other parameter, such the storage environment, contributed to the variation in quinic acid and ascorbic acid relative intensity. The quantity of ascorbic acid in fruit juice that has been stored changes depending on how long it has been held, according to a prior investigation. (Kabasakalis et al. 2000). Intriguingly, compared to other C1 stages and even other C4 stages, the Japan Queen C1 pineapple accumulates higher levels of sweetness, juiciness, and high acceptability-related metabolites and lower levels of sourness and firmness-related metabolites. This result may indicate that the 'Queen' cultivar is more preferable from its green-ripe (C1) stage till full-ripe (C4) stage and supports the specific organoleptic of the 'Queen' cultivar. It should be highlighted that this method only makes predictions based on metabolite levels, as determined by the findings of the OPLS regression analysis. Therefore, additional sensory analysis is necessary to verify these findings..

2.4 Conclusion

In this study, pineapples from various cultivars and ripening stages were subjected to sensory analysis and metabolite profiling. According to the findings, stiffness and sourness contributed to the early ripening stage (C1), whereas sweetness, juiciness, and

high acceptance contributed to the late ripening stage (C3 and C4 stage). Regardless of cultivar, demographic analysis of the sensory evaluation revealed that both genders and nationalities in this study preferred late ripening stage (C4 stage) pineapple over early ripening stage (C1 stage). The significance of the C4 stage fruit in the pineapple business was thus shown by this study. Quinic, malic, isocitric, citric, and ascorbic acids were metabolites that accumulated in each ripening stage and led to the early ripening of pineapple fruits., while asparagine, glycine, and serine contributed to the late ripening of pineapple fruits. It has been demonstrated that various pineapple cultivars create various metabolites. Sucrose, maleic acid, and threonic acid are all accumulated by smooth cayenne. While Queen accumulates threonine, serine, and methionine, Red Spanish accumulates alanine and GABA. It should be highlighted that this study offered the foundation for recognizing important distinctions between various pineapple types. The results and explanation may be enhanced by more research employing a comprehensive set of pairings between pineapple cultivars (three cultivars) and ripening phases (C1 for Queen, C1, C3, and C4 for Red Spanish, and C1 and C4 for Smooth Cayenne). The metabolomics approach may also be able to anticipate the sensory features of pineapple by understanding the metabolites that correlate with sensory attributes. Improvements in the pineapple industry can be anticipated based on these metabolites and sensory characteristic data, either through directed breeding techniques or genetic engineering to generate a more palatable pineapple. This study further demonstrated the distinctive organoleptic of the 'Queen' cultivar by its greatly accumulated sweetness, juiciness, and high acceptability-related metabolites. It also supported the significance of C4-stage pineapple fruit. Further research into the ripening process, particularly on "Queen"

pineapple, may be able to identify the metabolites that are responsible for the C4-stage pineapple fruit's short shelf life.

Chapter 3

GC-MS-based metabolite profiling to monitor ripening-specific metabolites in 'Queen' pineapple (*Ananas comosus*)

3.1 Introduction

Non-climacteric fruit produces low levels of ethylene and doesn't exhibit a significant peak in respiration rate during the ripening process, in contrast to climacteric fruit, which depends on ethylene bursts during ripening (Hui et al. 2010; Kader 1999). Additionally, other than degreening, ethylene treatment has no impact on non-climacteric fruit (removal of chlorophyll) (Symons et al. 2012). Non-climacteric fruit also lacks the ability to continue ripening after harvest, making it crucial to harvest at the optimum stage of ripeness to guarantee high-quality fruit. (Kader 1999). According to the United Nations Economic Commission for Europe (UNECE) Standard for pineapple (FFV-49), the ripening stage of a pineapple is classified into 5 stage, from green-ripe to full-ripe, as shown in Figure 3.1. (Agricultural Standards Unit United Nations Economic Commission for Europe 2013). Pineapple is usually exported in the C1 stage (Ahmad and Siddiqui 2015), while the fully ripe fruit (C4 stage) is mainly for domestic consumption. Individual fruits combine to form the pineapple fruit. These distinct fruits, which each emerged from a single flower, were covered with a hard, polygonal layer that is known as pineapple peel (Medina and García 2005). There are leaves that can be employed for pineapple vegetative reproduction on top of the fruit, which are known as pineapple crowns. Along with the fruit harvest, this crown portion is frequently harvested (Medina and García 2005). During the development of the pineapple fruit, the crown and peel were formed.

Therefore, study of the pineapple peel and crown is required in addition to the analysis of the pineapple flesh in order to fully comprehend the pineapple ripening process. The changes in the metabolite composition of pineapple from various ripening stages are currently little understood (Kamol et al. 2016). Understanding the ripening process of pineapples can be advanced by keeping track of metabolite changes using methods like metabolomics, a thorough study of metabolites.

Figure 3.1. Pineapple sample from all ripening stages. From left to right: C0 until C4 stages.

Currently, only climacteric fruits such banana, mango, capsicum, dates, avocado, peach, climacteric melon, and mangosteen were the main subjects of recent studies on fruit ripening metabolomics. (Yun et al. 2019; White et al. 2016; Aizat et al. 2014; Diboun et al. 2015; Pedreschi et al. 2014; Monti et al. 2016; Allwood et al. 2014; Parijadi et al. 2018). However, only a small number of non-climacteric ripening processed fruits, including cherry, blackcurrant, blueberry, non-climacteric melon, and pineapple, had been clarified utilizing metabolomics technique (Allwood et al. 2014; Karagiannis et al. 2018; Jarret et al. 2018; Montecchiarini et al. 2019; Steingass et al. 2016; Ogawa et al. 2018). A gas chromatography-mass spectrometer (GC-MS) or a liquid chromatography-mass spectrometer were used in previous metabolomics research on non-climacteric fruit (LC-MS). In several research, volatile chemicals were measured during the ripening

process by combining headspace-solid phase microextraction (HS-SPME) with GC-MS (Allwood et al. 2014; Steingass et al. 2016). HS-SPME-GC-MS, high-performance liquid chromatography with diode array detection and electrospray ionization multiple-stage mass spectrometry (HPLC-DAD-ESI-MS^n), and electrospray ionization mass spectrometry (ESI(-)FT-ICR MS) reports on pineapple ripening have concentrated on volatile and phenolic compounds. (Ogawa et al. 2018; Steingass et al. 2014; Steingass et al. 2015a; Steingass et al. 2015b; Steingass et al. 2015c). The results of these earlier studies revealed that the phenolic patterns, including coumaroyl isocitrate and S-p-coumaryl, as well as volatile substances, like methyl 3-(methylthio)propanoate and δ-octalactone, changed as the pineapple ripened.

Prior research on the ripening of pineapples focused on the targeted examination of volatile and phenolic chemicals using a sample of the flesh. There has not yet been a study that thoroughly examined primary metabolites such sugar, organic acid, amino acid, sugar alcohol, sugar acid, and amine compounds in the pineapple's flesh, peel, and crown portions. There are several various multivariate analyses that can be utilized to suggest metabolites that are connected to ripening. Principal Component Analysis (PCA) and Orthogonal Projections to Latent Structures (OPLS) regression analysis are the two most used multivariate analyses (Werth et al. 2010; Teoh et al. 2015). By examining pineapple fruit (crown, flesh, and peel) from various ripening stages, a metabolite profiling approach using GC-MS in conjunction with PCA and OPLS was carried out in this study to track the changes of primary metabolites (sugar, organic acid, amino acid, etc.) during pineapple ripening process (Figure S3.1). Metabolites identified by GC-MS were used as an explanatory variable in the OPLS model, while ripening stages were used as a response variable. The model developed from flesh and peel samples revealed a number of

potentially significant metabolites that were associated to the ripening of pineapples. This work is crucial to completing our understanding of the ripening of pineapples and can be used as a foundation for post-harvest treatment strategies in the pineapple industry.

3.2 Materials and method

3.2.1 Plant materials

In this study, pineapple (*Ananas comosus*) fruits from Indonesia representing 5 distinct ripening phases were employed (Figure 3.1). Ethephon treatment was utilized to encourage fruit development around November or December of last year in order to maintain the same harvest time at the end of April 2019. The Mahkota Bogor "Queen" cultivar of pineapple was utilized in this study to represent an important cultivar from the pineapple industry. During the cultivation period of November 2018 – April 2019 at the Center for Tropical Horticulture Studies, Bogor Agricultural University (CENTROHS, Bogor Agriculture University), Bogor, Indonesia (minimum temperature 21 °C and maximum temperature 35 °C), three samples (biological replicates) from various plants were taken from each ripening stage for Queen cultivars. A trained panelist assisted in determining the ripening stage based on variations in peel color. Sample preparation and extraction of pineapple for GC-MS analysis.

The crown, flesh, and peel of pineapples that were harvested in Indonesia at various stages of ripeness were separated. Each component was divided into small bits and put inside a pyrex tube with parafilm that had holes cut out of it. Prior to lyophilization, samples were quenched by submerging the pyrex tubes in liquid nitrogen using the VD-

800R Freeze drier (Taitec, Saitama, Japan). Samples of freeze-dried pineapple were shipped in one day from Indonesia to Japan. Using a Multi-beads shocker, the samples were homogenized and ground into a fine powder. Based on the methodology stated in our prior study, this extraction procedure was carried out (Anjaritha et al. 2019). The extraction and lyophilization of pineapple samples (10 mg), blank samples, and quality control (QC) samples took place on the same day. Small aliquots of each sample obtained for this study were taken to create the QC samples.

All samples were extracted using a mixture of 2.5/1/1 (v/v/v) ribitol as an internal standard and ultrapure water (Wako Chemical, Osaka, Japan), chloroform (Kishida Chemical Co. Ltd., Osaka, Japan), and methanol (Wako Chemical, Osaka, Japan). After 30 minutes of incubation at 37 °C and 1200 rpm, the mixture was centrifuged for 3 minutes at 40 °C. A new 1.5 mL microtube was filled with 600 µL of supernatant, and 300 µL of water was added to the mixture. 400 µL of the supernatant from the sample combination was transferred to a fresh microtube and sealed with a holed cover after being centrifuged for 3 minutes at 40 °C. Following an overnight lyophilization, the sample mixture's solvent was evaporated for an hour at room temperature. Each sample was examined three times (n=3). Lyophilized materials were mixed with 100 microliters of methoxyamine hydrochloride (20 mg/mL in pyridine) and then incubated in a thermomixer at 30 °C for 90 minutes. The samples were then treated with 50 µL of N-methyl-N-trimethylsilyl-trifluoroacetamide (MSTFA) (GL Sciences) and incubated for 30 minutes at 37 °C.

3.2.2 GC-MS analysis

On a GC-MS QP2010 Ultra (Shimadzu, Kyoto, Japan) fitted with an InertCap 5 MS/NP column, GC-Q/MS analysis was carried out (GL Sciences). Prior to analysis, the mass spectrometer was tuned and calibrated. The injection temperature was 230 °C, and 25:1 (v/v) split mode was used to inject one microliter of the derivatized sample. He was the carrier gas, and the flow rate was 1.12 mL/min with a 39 cm/sec linear velocity. The column temperature was maintained at 80 °C for two minutes, then increased to 330 °C at a rate of 15 °C/minute for six minutes. Temperatures for the ion source and transfer line were 250 °C and 200 °C, respectively. At a voltage of 0.94 kV, electron ionization (EI) produced ions. At 10000 u/s (check value), spectra were captured for the mass range *m/z* 85–500. Prior to analysis, a reference alkane mixture (C_8–C_{40}) was introduced for peak identification.

3.2.3 GC-MS data analysis

Using the GCMS solution software package, the raw data from the analysis was transformed to the AIA file (Shimadzu). MS-DIAL ver. 4.00 was used to perform peak alignment, peak filtering, and peak annotation using the GCMS-5MP Library (Riken, Kanagawa, Japan). Peak confirmation of key metabolites, including inositol, mannose, galactose, and melezitose, was carried out by co-injection with real standards (Wako Pure Chemical Industries Ltd, Osaka, Japan; Sigma-Aldrich Japan Ltd, Tokyo, Japan; Alfa Aesar Ltd, Heysham, United Kingdom).

3.2.4 Statistical analysis

The GC-MS analysis of annotated metabolites was pre-treated by internalizing each metabolite peak height (ribitol). Using SIMCA-P+ version 13, normalized data were autoscaled without alteration and subjected to PCA (Principal Component Analysis) (Umetrics, Umea, Sweden). Unsupervised analysis known as principal component analysis is helpful as a dimension-reduction approach to quickly identify patterns, clusters, and outliers (Werth et al. 2010). In addition to PCA, a Projections to Latent Structures (PLS) regression model that is built using the maximum correlation between the explanatory variable (x-variable) and response variable (y-variable) provides ranking of metabolites connection with a certain quantitative trait (Geladi and Kowalski 1986; Nitta et al. 2017). In particular, Orthogonal Projections to Latent Structures (OPLS) regression model is helpful for condensing a large number of variables to a small number of latent variables (Teoh et al. 2015). OPLS (Orthogonal Projections to Latent Structures) analysis were performed on parts that exhibit PCA-detected ripening patterns using SIMCA-P+ version 13. Variable importance in projection (VIP) was estimated for each metabolite based on OPLS analyses. Using JASP Version 0.11.1, the top five VIP-scoring metabolites in each pineapple portion were statistically analyzed using analysis of variance (ANOVA) and Tukey's post hoc test (JASP Team, Amsterdam, Netherlands). To assess the variances in mean VIP metabolite values across all ripening stages, a statistical analysis was undertaken. If $p<0.05$, differences were deemed significant.

3.3 Result and discussion

3.3.1 GC-MS and principal component analysis of pineapple from different ripening stages

Using a GC-MS instrument, a metabolite profiling technique was able to identify 351 metabolite peaks in the crown, 297 metabolite peaks in the flesh, and 359 metabolite peaks in the peel of the fruit. Using MSP Library with RI and EI-MS from our laboratory experimental data, 85 peaks in the crown part, 74 peaks in the flesh part, and 73 peaks in the peel part were annotated among those peaks. The analysis of metabolites from QC samples with RSD more than 20% was stopped (Zhao et al. 2019). The number of annotated metabolites in the crown section was 56, in the flesh part was 47, and in the peel part was 54 after metabolites with RSD higher than 20 percent were excluded. A complete list of these metabolites during ripening analysis is shown in Table S3.1.

The score plot from PCA for pineapple at various ripening stages (C0 to C4 stages) as seen in three separate regions of the pineapple is shown in Figure 3.2. Figures 3.2b and 3.2c demonstrate two separate clusters along PC1 in the flesh and peel portion. Ripe fruit samples (C3 and C4 stages) formed a discrete cluster from samples that were less ripe (C0 to C2 stages). This tendency was explained by variations in the flesh and peel portions of 63.9 and 53.3%, respectively. The pineapple crown portion, nevertheless, does not exhibit this pattern across all major components. The metabolite accumulation in the less-ripe and more-ripe samples for the flesh and peel parts, respectively, was depicted by a loading plot in Figures 3.2b and 3.2c. This score plot's metabolite intensities were normalized using ribitol as an internal standard. The internal standard was chosen because it is absent from samples of pineapple and is stable in a solution of many solvents. Each

part's annotated metabolites were subjected to PCA and OPLS analysis. Using metabolites as the explanatory variables, principal component analysis (PCA), a multivariate data analysis, might display the variation between the samples According to the PCA, there are two main phases of pineapple ripening: C0-C2 stages (early ripening), and C3-C4 stages (late ripening). The aforementioned tendencies were only seen in flesh and peel samples; there was no discernible tendency of ripening in the crown portion. It was previously suggested that the crown's photo-assimilation appeared to come from its own photosynthesis rather than from the fruit (Sanewski et al. 2018). Additionally, it is commonly known that pineapple maturity began towards the bottom rather than the top. (Joy and Rejuva TA 2016). Therefore, it is believed that there is no connection between the crown section and fruit ripening.

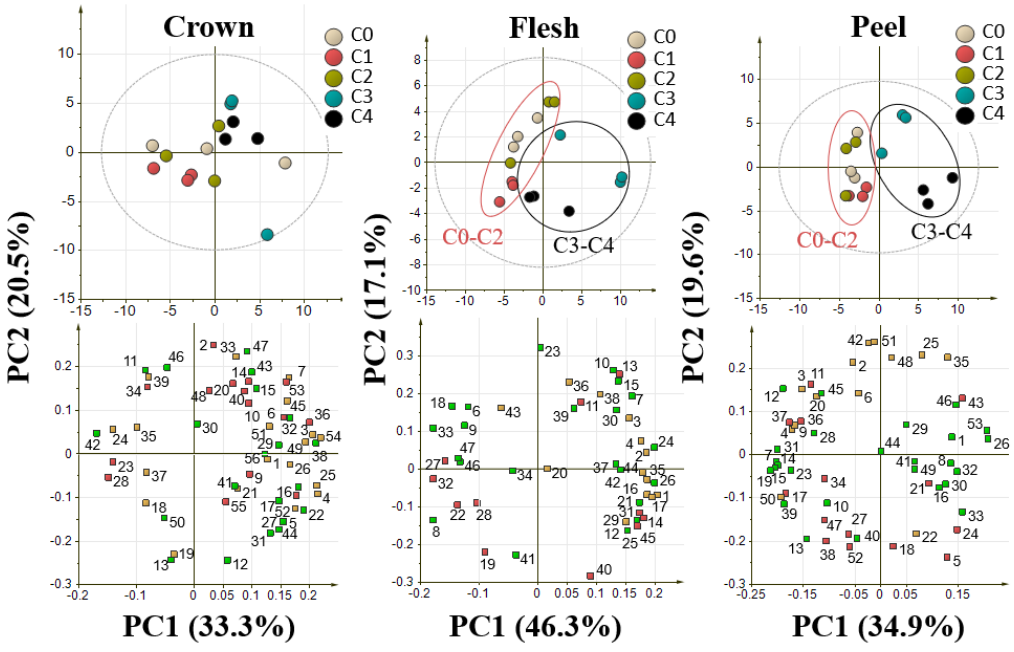

Figure 3.2. PCA result from flesh, crown and peel parts of pineapple from different ripening stages. Variables used for PCA were 56, 47, and 54 annotated metabolites by GC-MS from crown, flesh, and peel parts respectively. Data was auto scaled prior to PCA.

(a) Score and loading plot from the crown part; (b) Score and loading plot from the flesh part; (c) Score and loading plot from the peel part. Legends represent the samples and colored as follows: brown: C0 stage, red: C1 stage, green: C2 stage, blue: C3 stage, black: C4 stage. Upper part show score plot; Bottom part show loading plot. Loading plot was colored based on metabolite classes: green: sugars; red: organic acids; yellow: amino acids and amines.

3.3.2 Orthogonal projection to latent structures of pineapple ripening process

To find metabolites that are strongly influenced by the process associated to the response variable, orthogonal projection of latent structures (OPLS) regression analysis was carried out (Putri and Fukusaki 2014). In this work, the model was built utilizing the pineapple flesh and peel as latent variables. Based on the PCA results from the previous analysis, which showed that the crown component was unable to exhibit any ripening process trends, the crown part was not examined. Ripening stages from C0 as 1, C1 as 2, C2 as 3, C3 as 4, and C4 as stages 5 were utilized as response variables to create the model, while compounds annotated by GC-MS analysis were employed as the explanatory variables. A training set of C0 to C4 ripe pineapples taken in April 2019 was utilized to create the model (Figure 3.3). Cross-validation with one replicate left out was used to validate the model.

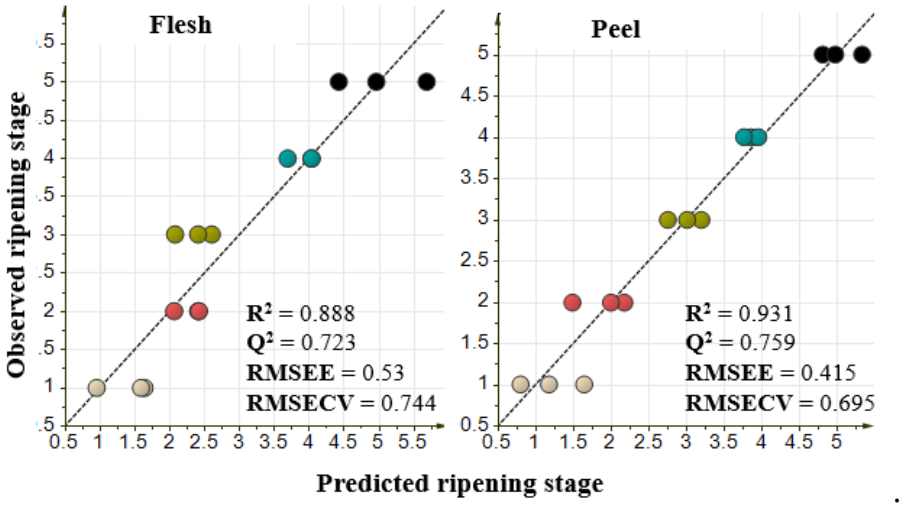

Figure 3.3. OPLS results from flesh and part of pineapple. Explanatory variables in flesh part are 47 metabolites, while in peel part are 54 metabolites. Response variable for both models is the ripening stages with numbered as follows: C0 stage as 1, C1 stage as 2, C2 stage as 3, C3 stage as 4, and C4 stage as 5. Value of R^2, Q^2, RMSEE, and RMSECv were used to evaluate the model. (a) OPLS model of flesh part; (b) OPLS model of peel part.

Figure 3.3 displays the created OPLS regression model, which has R^2 values of 0.888 and 0.931 for the flesh and peel parts, respectively. The score of Variable Important in Projection in the OPLS regression analysis indicated which metabolites were statistically significant for the models (VIP). VIP-rated metabolites are those that are deemed crucial for the model. (Putri and Fukusaki 2014) (Table S3.2). Contributing metabolites were chosen based on the five highest VIP scores. The top five VIP scores were used to choose the contributing metabolites. In the flesh model, the top five VIP metabolites were melezitose, inositol, xylonic acid, gluconic acid, and raffinose. In the peel, the top VIP metabolites were inositol, mannose, galactose, sucrose, and aspartic acid. Melezitose, xylonic acid, gluconic acid, and sucrose, among these highest VIP

metabolites in both flesh and peel, have a favorable link with the stages of ripening, but inositol, raffinose, mannose, galactose, and aspartic acid showed a negative correlation with the ripening process (Figure 3.4).

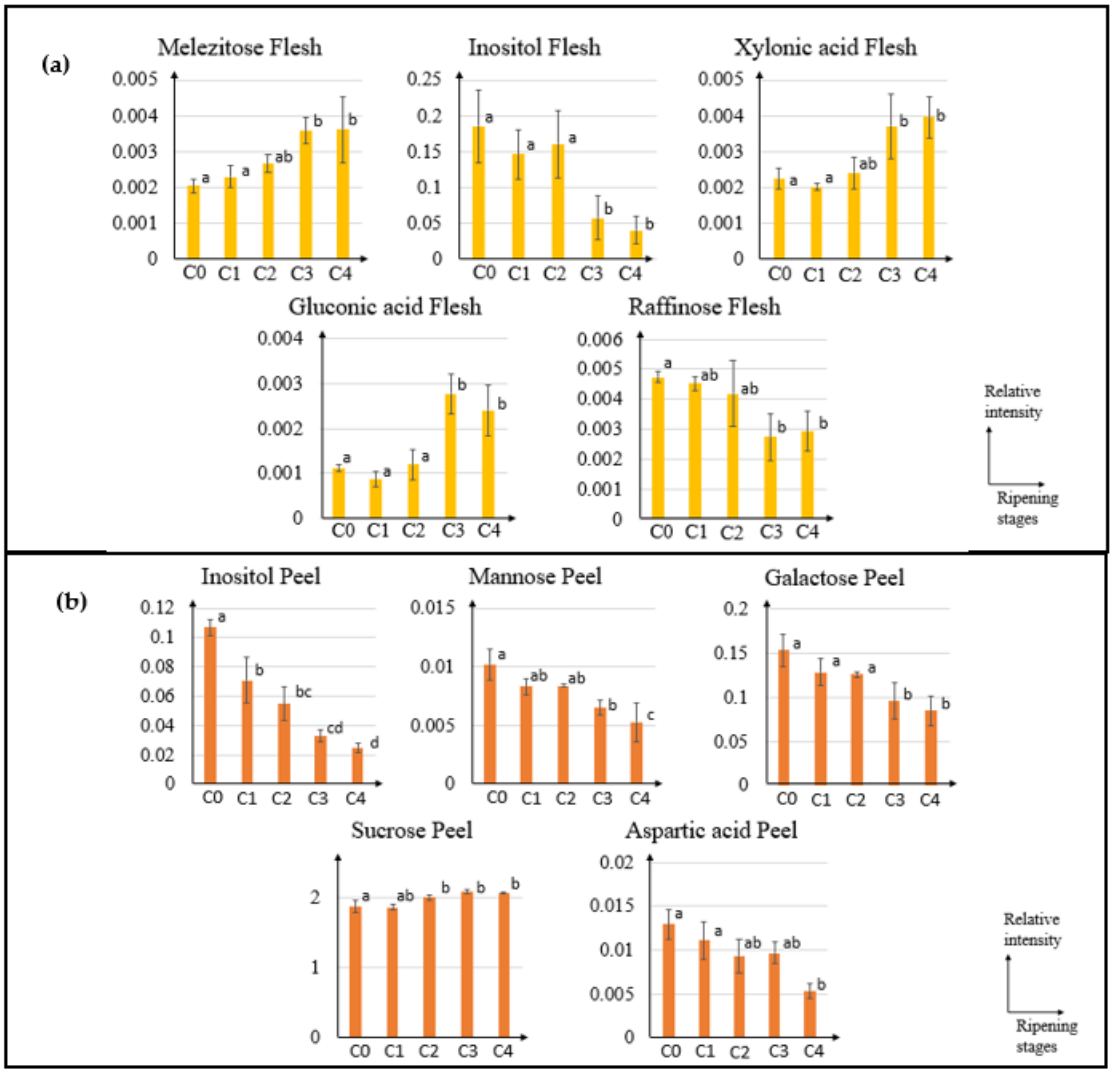

Figure 3.4. Bar graph of five highest VIP metabolites related to pineapple ripening process in (a) flesh and (b) peel part. The relative intensity of the five highest VIP metabolites was normalized by the internal standard. Vertical axis represents metabolites relative intensity and horizontal axis represents ripening stages. Significant differences (p<0.05) are indicated with the different letters.

OPLS regression analysis was used in additional study to find possibly significant metabolites associated with the ripening process. Because OPLS regression analysis is a supervised multivariate analysis, it is well known to be more effective at illuminating the link between the response variable and explanatory variable (Putri and Fukusaki 2014). There are various factors in the OPLS regression model depicted in Figure 3.3 that could be used to gauge the model's overall quality. These variables are R^2, $Q^{2,}$ RMSEE, and RMSECv. The square of the correlation coefficient between the observed value and the projected value in a regression is known as R^2. (Alexander et al. 2015). Q^2 is known to be a reliable parameter for model predictivity (Parijadi et al. 2018; Alexander et al. 2015). The numbers to assess accuracy, prediction, and model resilience are RMSEE, or Root Mean Square Error of Estimation, and RMSECv, or Root Mean Square Error of Cross-validation (Alexander et al. 2015; Fausto Rivero-Cruz et al. 2017). A good model would have the R^2 value should be greater than 0.6, the Q^2 value should be greater than 0.6, and the RMSEE and RMSECv values should be low (Alexander et al. 2015). From metabolites annotated in the flesh, peel, and crown, we created 3 OPLS models. In contrast to the crown model, which displayed R^2 values of 0.896, Q^2 values of 0.432, RMSEE values of 0.509, and RMSECv values of 1.066, the created model of flesh and peel displayed R^2 values of more than 0.6, higher than 0.6, and a low value of RMSEE and RMSECv. These findings showed that only the peel and flesh model is viable and fits the data well. The low Q^2 value in the crown model demonstrated that it is impossible to predict the stages of pineapple ripening using samples from the crown section. This is consistent with the PCA's findings previously.

3.3.3 ‘Queen’ pineapple metabolite changes along the ripening process

The variable importance in the projection (VIP) scores could be used to determine contributing metabolites associated with ripening phases. The five VIP metabolites with the highest scores are melezitose, inositol, xylonic acid, gluconic acid, and raffinose in the flesh and inositol, mannose, galactose, sucrose, and aspartic acid in the peel, respectively. Figure 3.4 depicts the dynamic of these VIP metabolites relative intensity along the ripening of the pineapple (normalized with ribitol). It has been demonstrated that these metabolites change as the pineapple ripens, either increasing or decreasing. The level of raffinose in the flesh portions was determined by these VIP metabolites and was consistent with the earlier findings, which shown a decreasing level during the ripening process (Farcuh et al. 2017). This study presents the dynamics of inositol, melezitose, xylonic acid, and gluconic acid in the flesh component during the ripening process in addition to the previously documented metabolites that correspond with the ripening process. The osmotic pressure in blueberry fruit, also known as inositol or myo-inositol, has been discovered to be regulated by inositol, keeping the turgor and fruit firmness between the firm cultivar and soft cultivar (Montecchiarini et al. 2019). Additionally, inositol may undergo an oxidation process that results in D-glucuronic acid, which is a significant precursor of the cell wall in Arabidopsis (Siddique et al. 2014). As a result, the presence of inositol may also be related to the fruit's cell wall. Melezitose has been implicated in the osmoregulation system. (Panizzi and Parra 2012). The mechanisms underlying these two metabolites, however, to control the osmoregulation system throughout the pineapple ripening process may differ when compared to inositol, based on the relative intensity trend.

It was discovered that the relative intensity of xylonic acid increased as the fruit ripened (Figure 3.4a). Oxidative stress rose as fruit ripened, which may cause some fruit modifications including skin color changes or fruit softening. Ascorbic acid, a fruit antioxidant, may therefore act to maintain the reduction-oxidation equilibrium in a balanced state (Decros et al. 2019). According to the previous study, xylonic acid is a byproduct of ascorbic acid breakdown, which accounts for the rise in xylonic acid throughout the ripening process (Musara 2019). It was discovered that raffinose levels dropped as the ripening of the pineapple progressed (Figure 3.4). According to a recent study, which supports this finding, the raffinose level likewise drops when the Japanese plum non-climacteric cultivar ripens (Farcuh et al. 2017). According to their findings, the degree of raffinose in non-climacteric fruit may be related to its capacity to slow down the oxidative process as fruit ripens (Farcuh et al. 2017). Therefore, the reduction-oxidation process occurring during the ripening phase may also be related to the quantity of raffinose in addition to xylonic acid. It has been demonstrated that the gluconic acid concentration rises when the pineapple ripens past its prime (Figure 3.4a). This rise may have been brought on by the increased availability of carbon molecules in the final stages of pineapple ripening (Paliyath et al. 2019). Additionally, cell wall disintegration, a change in the makeup of the cuticle, and the pH of the host cells may all have an impact on the strength of the gluconic acid and contribute to the fungi's aggressive colonization (Paliyath et al. 2019). Therefore, a condition that could secrete gluconic acid and cause the pH of fruit, including apple and mango, to become acidic could be indicated by the presence of this gluconic acid. (Alkan and Fortes 2015; Davidzon et al. 2010).

Mannose is the second-highest VIP-scoring metabolite in peel after inositol. It is well known that mannose is a part of the hemicellulose found in plant cell walls (Moirangthem and Tucker 2018). The earlier publication stated that mannose concentration reduced as fruits developed, which is consistent with our findings displayed in Figure 3.4b (Dheilly et al. 2016). Similar to how mannose levels decreased, aspartic acid levels decreased with the ripening of bananas and pineapples (Wu et al. 2018a). Along with glutamic acid, aspartic acid was recognized as a source of the umami flavor (Zgola-Grześkowiak and Grześkowiak 2012). In addition to being the source of umami flavor, aspartic acid levels may be related to the amount of free auxin in fruits, which influences how ripe they become (Bernales et al. 2019). t was discovered that aspartic acid was conjugated with indole acetic acid (IAA), which caused degradation of the IAA hormones (Bernales et al. 2019).

In addition to the previously noted metabolites, this study discovered that the shift in sucrose and galactose levels in the peel portion may be related to the ripening of the pineapple. This study demonstrated that during the ripening process, the sucrose content in the pineapple peel component increased (Figure 3.4b), in contrast to a prior study that noted an increase in sucrose in the pineapple flesh (Ogawa et al. 2018). According to previous reports, the peel's sucrose content is lower than that of the flesh. (Siti Roha et al. 2013). In strawberry fruit, a non-climacteric fruit, sucrose not only contributes to sweetness but also plays a role in controlling fruit development and ripening (Jia et al. 2013). The major enzymes in the abscisic acid (ABA) hormones pathway may express at higher levels as a result of sucrose buildup, which could then use ABA hormones to accelerate the ripening of non-climacteric fruit (Fuentes et al. 2019). Figure 3.4b depicts

the declining trend in galactose as the fruit ripens. The relationship between galactose and the plant cell wall may help to explain this. Galactose is the main non-cellulosic sugar in the cell wall and dramatically decreased during fruit ripening, according to a prior study (O'Donoghue et al. 2009; Ogasawara et al. 2007). Numerous biological activities, including cell wall loosening, texture alterations, flavor development, chlorophyll destruction, and pigment buildup take place throughout the ripening process (Osorio et al. 2013). Therefore, the outcome of this study revealed that the intensity of metabolites that might be involved in textural changes, cell wall metabolism, the oxidation process, and the generation of plant hormones is affected by the ripening process in pineapple (Steingass et al. 2014; Kumar et al. 2016; Wu et al. 2018a).

3.4 Conclusion

Principal component analysis (PCA) could be used to distinguish between C0-C2 phases and C3-C4 stages based on metabolite data obtained from GC-MS analysis, however the crown section did not exhibit an association with the ripening process. Metabolites that may be connected to the ripening of the pineapple are discovered using orthogonal projection to latent structures (OPLS) regression analysis on the pineapple's flesh and peel. Melezitose, inositol, xylonic acid, gluconic acid, and raffinose were determined to be the five most important metabolites in the flesh, while inositol, mannose, galactose, sucrose, and aspartic acid are the five most important metabolites in the peel. The firmness and shelf life of pineapple were recognized to be affected by these metabolites' involvement in the metabolism of plant cell walls and osmoregulation system, in addition to the redox defence system and non-climacteric ripening hormones. In future applications, these VIP metabolites could be exogenously given to control particular

effects, such as the addition of polyamine and ascorbic acid to control fruit's shelf life, as demonstrated in the earlier publications (Sharma et al. 2017; Golly et al. 2019). In addition, it was possible to control the amount of metabolites with post-harvest treatment, such as controlling inositol, galactose, and raffinose through cold or heat treatment (Yun et al. 2013; Bustamante et al. 2016; Anjaritha et al. 2019). It should be mentioned that the 'Queen' cultivar was the only one the study focused on. Future research on other well-known cultivars, such as "Smooth Cayenne," is still required to further the understanding of the ripening process for pineapples. However, by regulating significant metabolites influenced by the ripening process, this study might serve as a foundation for tackling the post-harvest problem in the pineapple industry.

Chapter 4

Effect of inositol and melezitose as a potentially important metabolites related with shelf-life in C4-stage ‘Queen’ pineapple

4.1 Introduction

As mentioned previously, full-ripe pineapple or C4-stage pineapple are more susceptible to deterioration compared to C1-stage thus the storage time of full-ripe pineapple can only reach around 1-week (Steingass et al. 2016). For elucidating the metabolites that possibly responsible to the shelf-life of ‘Queen’ pineapple, not only finding the possible important compound, but external application as a validation might be needed. Chemical treatments to prolong shelf-life of fruits are not uncommon in the field of postharvest studies. Previous reports applied essential oil to prolong shelf-life of strawberry and also application of flavonol to maintain banana fruit quality (Rahmawati et al. 2017; Yang et al. 2019). Study of fresh-cut fruit to elucidate the external chemical application might be beneficial to limit sample number in the condition of restricted sample availability. Previous study of fresh-cut fruit (eggplants and peach) showed significant alteration of metabolites, for example, the change in chlorogenic acid that is related to browning conditions, or dehydroascorbate and alanine, which might be important for fruit taste and organoleptic quality (Tosetti et al. 2012; Liu et al. 2021). Due to the contact of the inner flesh part with the external chemical, edible coating is one of the preferred methods to study the effect of chemical treatments. Edible coatings comprise a thin layer of edible material that is applied to the surface of food (Escamilla-García et al. 2018). The use of edible coatings can help to prevent water loss, deterioration of other

physicochemical parameters (e.g., color changes and weight loss), and even microbial damage (Shiekh et al. 2013).

Chitosan is one of the most widely used edible coatings. Chitosan is a polymer derived from chitin that is present in the shells of crustaceans (e.g., shrimp and crab). It is non-toxic and biodegradable, with antimicrobial and antifungal activities (Shiekh et al. 2013; Escamilla-García et al. 2018). Chitosan is commonly used as an edible coating for fresh fruits, such as banana, strawberry, papaya, and litchi, as well as in other foods such as fish fillets (Shiekh et al. 2013; Feng et al. 2016). Moreover, the result from chapter 3 reported that inositol and melezitose, a saccharide group metabolite, might play a role in controlling osmotic pressure, serving a similar purpose as edible coating. Both of these saccharides can be found naturally in plant, with inositol is synthesized from glucose by myo-inositol-1-phosphate synthase and inositol-1-phosphatase, while melezitose from sucrose by α-glucosidase/glucosyltransferase (Wu et al. 2018b; Garcia-Gonzalez et al. 2019). Thus, a combination of chitosan and these saccharides could be beneficial for retaining freshness in fresh-cut pineapples. To evaluate the treatment of fruits with edible coatings, common approaches have analyzed physical, chemical, and microbiological parameters (Xing et al. 2016; Escamilla-García et al. 2018; Taghinezhad and Sharabiani 2018). However, limited information is available regarding the effect of edible coating on the metabolites in fruits. Global metabolite change studies, or metabolomics, are powerful tools to gain a deep insight into the mechanism of phenotypic or biological changes that occur in the biological samples (Putri and Fukusaki 2014). Analyzing primary metabolites could also reflect the quality characterization of fruits that might be linked to the changes after post-harvest treatment (Allegra et al. 2018). In this context, this study aimed to evaluate the physicochemical quality of fresh-cut pineapple and correlate it with primary

metabolite changes evaluated using GC-MS-based metabolite profiling after treatment with chitosan, saccharide, and a combination of both treatments. The results presented in this study provide insights into metabolite changes that occur after the edible coating treatment of pineapple and provide a basis for the development of further post-harvest treatments of pineapple in the food industry.

4.2 Material and methods

4.2.1 Plant materials

Pineapple (*Ananas comosus* cv. Queen) from Okinawa, Japan, was purchased from a Japanese market. The crown and bottom of the fruits were cut before removing the core. The unpeeled fruits were then cut into cubes of approximately 2 × 2.5 cm. Two cubes were placed in plastic cups and labeled according to the treatment. One treatment group was replicated five times (five cups). Each cube was soaked in 1 mL of the treatment solution and air dried for 1 h. The excess solution was dried using a hand towel and stored under dark room conditions for five days [23.6 ± 0.5°C; relative humidity (RH) 40.0 ± 10.4%]. Chitosan solution (1.25%) was prepared by dissolving 1.25 g of chitosan powder in 100 mL of 0.5% v/v glacial acetic acid. Chitosan was dissolved by stirring on a hot plate (50–60 °C). Inositol solution (15 mg/L as endogenous concentration) was prepared by dilution from 20,000 mg/L of inositol (0.4 g in 20 mL of pure water). Melezitose solution (5 mg/L as endogenous concentration) was prepared by dilution from 20,000 mg/L of melezitose (0.4 g in 20 mL of pure water). Chitosan-melezitose solution was prepared by diluting the melezitose stock solution to 5 mg/L melezitose using a 1.25% chitosan solution. Chitosan was purchased from Sigma-Aldrich (St. Louis, MO, USA).

Inositol was obtained from Tsuno Group (Wakayama, Japan). Melezitose was purchased from Alfa Aesar (Heysham, UK). Glacial acetic acid was obtained from Wako Pure Chemical Industries (Osaka, Japan).

4.2.2 Physicochemical analysis

The weight of the cut fruit samples in plastic cups was determined on days 0, 3, and 5 using a digital balance (Shimadzu, Kyoto, Japan). The results were reported as weight percentage compared to weight on day 0: weight (%) = (final weight)/(initial weight) × 100. Flesh and peel color measurements were conducted using a Konica Minolta CM-2500d mobile spectrophotometer (Konica Minolta, Tokyo, Japan) using the CIELAB scale on the same day as the weight determination (L* = lightness, a*= green to red color, b* blue to yellow color). Color changes were calculated using the ΔE2000 equation in a Microsoft Excel macro provided by Edgardo Garcia (http://rgbcmyk.com.ar/en/xla-2/).

4.2.3 Sample preparation, extraction, and derivatization

Fresh-cut pineapple after cutting (day 0) and storage (day 5) were wrapped in aluminum foil and frozen in liquid nitrogen before being placed into a Pyrex tube for lyophilization using VD-800F (Taitec, Saitama, Japan); all samples were prepared in triplicates. Freeze-dried samples were ground using a multi-bead shocker (Taitec) to homogenize the samples. The extraction method was conducted according to chapter 2 and chapter 3, with some modifications. Briefly, pineapple samples (5 mg) were extracted using 1 mL of a mixture of methanol (Wako Chemical, Osaka, Japan), chloroform (Kishida Chemical Co. Ltd., Osaka, Japan), and ultrapure water (Wako Chemical, Osaka, Japan) at a ratio of 2.5:1:1 (v/v/v) containing 100 µg/mL internal standard (ribitol). A

blank microtube was also included as a blank sample. The extraction mixture was incubated for 30 minutes at 37 °C and 1200 rpm on Thermomixer comfort (Eppendorf, Hamburg, Germany), followed by centrifugation at 10,000 rpm for 3 minutes at 4 °C. The supernatant (600 µL) was transferred to a new microtube, and 300 µL of ultrapure water was added before centrifugation under the same conditions. Next, 50 µL of the supernatant was transferred into a new microtube and closed with holed caps, and another 50 µL was pooled from each sample into falcon tubes for QC preparation before being distributed again into QC microtubes. All samples, including blank and QC, were allowed to evaporate at room temperature for 45 minutes, followed by lyophilization overnight. The overnight extracted sample was then derivatized using 100 µL of methoxyamine hydrochloride (20 mg/mL in pyridine) at 30 °C for 90 minutes. Finally, 50 µL of *N*-methyl-*N*-trimethylsilyl-trifluoroacetamide (GL Science, Tokyo, Japan) was added to the sample and incubated at 37 °C for 30 minutes prior to moving the sample into GC-MS vials.

4.2.4 GC-MS analysis and data treatment

GC-MS analysis was performed on a GC-MS TQ8030 (Shimadzu, Kyoto, Japan) equipped with an InertCap 5MS/NP Proguard 5 m (35 m × 0.25 mm, I.D. df = 0.25 µm; GL Sciences, Tokyo, Japan). The instrument was tuned and calibrated prior to analysis. One microliter of the derivatized sample was taken from the GC-MS vial and injected in 25:1 (v/v) split mode at an injection temperature of 230 °C. The linear velocity of the carrier gas (He) was 39.0 cm/seconds. The column temperature was maintained at 80 °C for 4 minutes, raised to 330 °C at a rate of 15 °C/minutes, and maintained at 330 °C for 8 minutes. The temperatures of the interface and ion source were 310 °C and 280 °C,

respectively. Ions in GC-MS were generated by electron ionization (EI) with a filament bias voltage of 70.0 V, and the recorded spectra were scanned over the mass range (*m/z*) of 85–500 with 0.15 seonds event time. A standard alkene mixture (C_8–C_{40}) was injected before analysis to calculate the retention index (RI) used for peak identification.

The raw GC-MS data were converted into .cdf format using GCMSsolution version 4.20 (Shimadzu, Kyoto, Japan) and further converted into .abf format using an Abfconverter (Reifycs, Tokyo, Japan). Baseline correction, denoising, peak detection, alignment, and automatic peak annotation were conducted using MS-DIAL (version 4.20) (Lai et al., 2018) in .abf format. Peak annotation was conducted using RI and mass spectral information of the compounds with EI mass spectral library from GL-Science DB Inert Cap 5MS-NP, Fiehn RI, 494 records (RIKEN, Kanagawa, Japan), NIST-11 MS Spectral Library (NIST, Maryland, USA), and the Mass Bank of North America Database (https://mona.fiehnlab.ucdavis.edu/). Similarity values were set to a minimum of 70% for automatic annotation using MS-DIAL and manual annotation. Peaks that were confirmed with authentic standards were inositol, galactose, quinic acid, sucrose, and mannose by co-injection analysis (Wako Pure Chemical Industries Ltd.; Sigma-Aldrich Japan Ltd., Tokyo, Japan; Alfa Aesar Ltd.).

4.2.5 Statistical analysis

The obtained metabolites (annotated and unknown) were normalized to ribitol as an internal standard to obtain the normalized peak height information. These normalized peak values were screened using two parameters: (1) relative standard deviation (RSD) below 30%, and (2) the concentration of compounds in the QC samples was more than three times that of the blank samples. Compounds obtained from the screening were then

auto-scaled and subjected to multivariate analysis, principal component analysis (PCA), and orthogonal projection to latent structures (OPLS) regression analysis, using SIMCA-P version 13 (Umetrics, Umea, Sweden). The key variables in the projection (VIP) score for each metabolite were calculated using the OPLS regression analysis to identify the important metabolites during model construction. The p-value between metabolites and treatments was calculated using the statistical analysis package provided by the RIKEN team (http://prime.psc.riken.jp/compms/others/main.html#Statistics) (Matsuo et al. 2017). Based on the p-values, important metabolites were statistically analyzed to evaluate the differences between treatments by analysis of variance (ANOVA) with Tukey's post hoc test performed using JASP version 0.11.1 (JASP Team, Amsterdam, Netherlands). Differences were considered significant at $P < 0.05$.

4.3 Results and discussion

4.3.1 Optimization between inositol and melezitose

The optimal concentrations of inositol and melezitose were determined by evaluating two concentrations between high-concentration sugar solutions (20,000 mg/L) and endogenous concentrations (15 mg/L for inositol and 5 mg/L for melezitose) (Yang et al. 2019). In a previous study, Yang et al. used 20,000 mg/L icariin, a flavonol, to coat bananas (Yang et al. 2019). Here, the endogenous concentration (15 mg/L for inositol and 5 mg/L for melezitose) was determined by comparing the relative intensity of the inositol and melezitose peaks with the standard addition confirmation peak obtained in chapter 3. Color changes were selected as the parameters to select the best candidate between the

inositol and melezitose solutions, and between the Yang-based concentration (20,000 mg/L) and endogenous concentration (15 mg/L for inositol and 5 mg/L for melezitose) (Lin et al. 2018). Figure 4.1 shows the change in the color of the flesh and peel after treatment with the sugar-coated solution. A photograph of the fresh-cut pineapple treated with sugar-based coating solution is presented in Figure S4.1. In the flesh part, melezitose retained the color better than inositol at both 20,000 mg/L and 5 mg/L concentrations, while the treated peel part did not show any significant difference between the treatments.

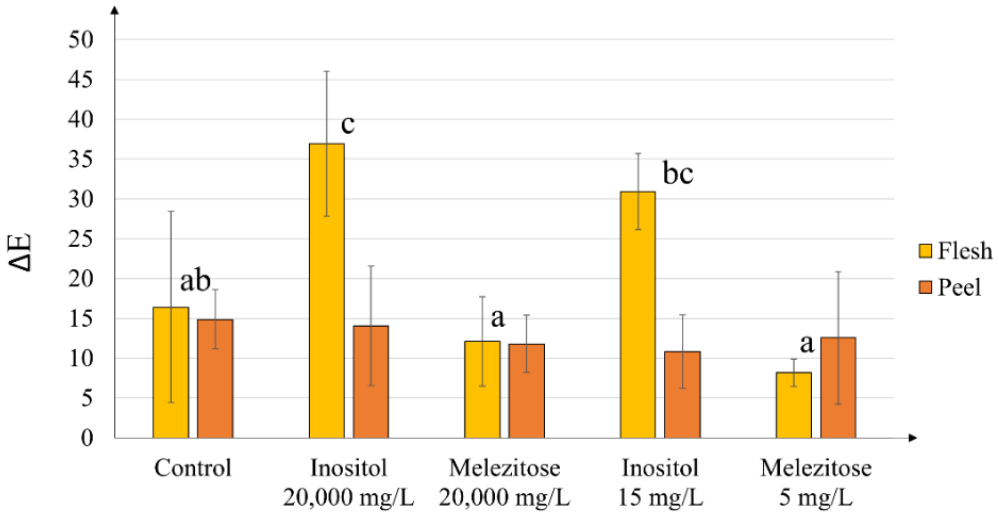

Figure 4.1. Changes in the color of the flesh and peel of fresh-cut pineapples treated with sugar-based coating solution (X-axis represents the sample, from left to right: control, inositol 20,000 mg/L, melezitose 20,000 mg/L, inositol 15 mg/L, and melezitose 5 mg/L). Yellow and orange bars represent the flesh and peel color, respectively. Significant differences ($p < 0.05$) are indicated with different letters based on Tukey's HSD.

Inositol and melezitose are known to play roles in osmoregulation (Panizzi and Parra 2012; Montecchiarini et al. 2019). The regulation of osmotic pressure in fruit

underlies the maintenance of turgor, which plays an important role in regulating fruit firmness in blueberry fruit (Montecchiarini et al. 2019). To select the appropriate sugar for application in fresh-cut pineapple, color changes were used as parameters of quality (Lin et al. 2018). Changes in the flesh color after treatment with inositol and melezitose indicated that fruits retained flesh color better after treatment with melezitose than inositol (Figure 4.1). Flesh color after the treatment with inositol markedly increased, with the flesh color changing from yellow to red (Figure S4.1). It is possible that the addition of inositol facilitates microbial contamination in fresh-cut pineapple. This hypothesis is supported by a previous report that showed inositol is needed by microbes to produce phosphatidylinositol, a structural component in the membrane, or as a precursor for other important phospholipids (Reynolds 2009). The comparison of two concentrations, namely Yang-based (20,000 rpm) and endogenous-based (15 mg/L for inositol and 5 mg/L for melezitose), following melezitose treatment did not show significant differences in color changes in the flesh and peel parts of the fresh-cut pineapple. Therefore, the minimum amount, or endogenous-based concentration, of melezitose was chosen for analysis in comparison with chitosan.

4.3.2 Physicochemical changes during storage

The appearance of fresh-cut pineapple after treatment with chitosan, melezitose, and a combination of both solutions, and subsequent storage is shown in Figure 4.2. Size shrinkage and color changes were observed from day 0 compared to day 5. Both parameters were chosen due to its importance to reflect the fruit quality, in addition to other parameter such as taste and nutritional quality (Nunes and Emond 2007; Barrett et al. 2010). Size shrinkage indicated weight loss during storage, which is one of the

parameters used to evaluate fruit conditions after storage (Bierhals et al. 2011). As shown in Figure S4.2, the weight percentage was compared to the initial weight of the fruit for each treatment to evaluate weight loss. After three days of storage, all treatments showed a heavier weight relative to day 0 compared to the control (no treatment). The weight of the control showed a bigger gap on day 5 compared to other treatments, with the biggest difference being observed with the chitosan-melezitose treatment. However, these differences were not considered statistically significant, even though a trend was observed ($p>0.05$).

Another parameter for evaluating fruit conditions after storage is color change (Lin et al. 2018). In this study, flesh and peel color were measured to investigate the effects on the different parts of the fruit (Figure S4.3). Flesh color changes (Figure S4.3A) were calculated using the flesh color difference relative to day 0. On day 3 of storage, chitosan treatment was able to retain flesh color significantly compared to the control, while the chitosan treatment itself did not differ significantly from other treatments. On day 5, all treatments showed reduced changes in color, indicating a better ability to retain color compared to the control ($p>0.05$). Peel color changes were also calculated from days 0, 3, and 5 (Figure S4.3B). At day 3 of storage, none of the treatments differed from the control. However, on day 5, chitosan-melezitose treatment was able to retain peel color significantly compared to melezitose treatment, which did not differ from the control treatment ($p>0.05$). Similar trend was also observed in Smooth Cayenne cultivar that there are no significant changes in weight, flesh and peel color changes.

Chitosan is widely used as an edible coating to protect food or fruit from bacterial contamination, oxidative stress, and other deterioration processes during storage (Bavaresco et al. 2017; Escamilla-García et al. 2018; Taghinezhad and Sharabiani 2018;

Adiletta et al. 2021). Previous research also evaluated the effects of the application of chitosan coating on the pineapple fruit and processed pineapple products (Ibrahim et al. 2014; Treviño-Garza et al. 2017; Minh Phuoc 2020). However, a study on chitosan coating on pineapple fruit products using a metabolomics approach had not previously been conducted. Therefore, to our knowledge, this study is the first to evaluate the metabolite changes in pineapple fruit products after treatment with chitosan incorporated with melezitose (chitosan-melezitose).

Previous studies on chitosan application showed significant changes in weight loss and color changes in oranges and papaya fruit (Escamilla-García et al. 2018; Taghinezhad and Sharabiani 2018). However, the effect of chitosan treatment on pineapple is different from other fruits. Fresh-cut pineapple treated with chitosan showed different results depending on the solution applied (Treviño-Garza et al. 2017). This study found that the weight of the fresh-cut pineapple samples did not significantly differ between the uncoated group and the chitosan supplemented with pullulan and linseed mucilage group up to day 6 of storage. In addition, these chitosan treatments did not show a significant difference in color changes up to day 6 (L* and b* spectrum) (Treviño-Garza et al. 2017). These findings correlate well with the changes in weight (Figure S4.2) and color (Figure S4.3) observed in the present study up until day 5 that showed no significant difference between treated and untreated samples, suggesting that the effects of chitosan treatment may not differ from the changes observed in the uncoated samples.

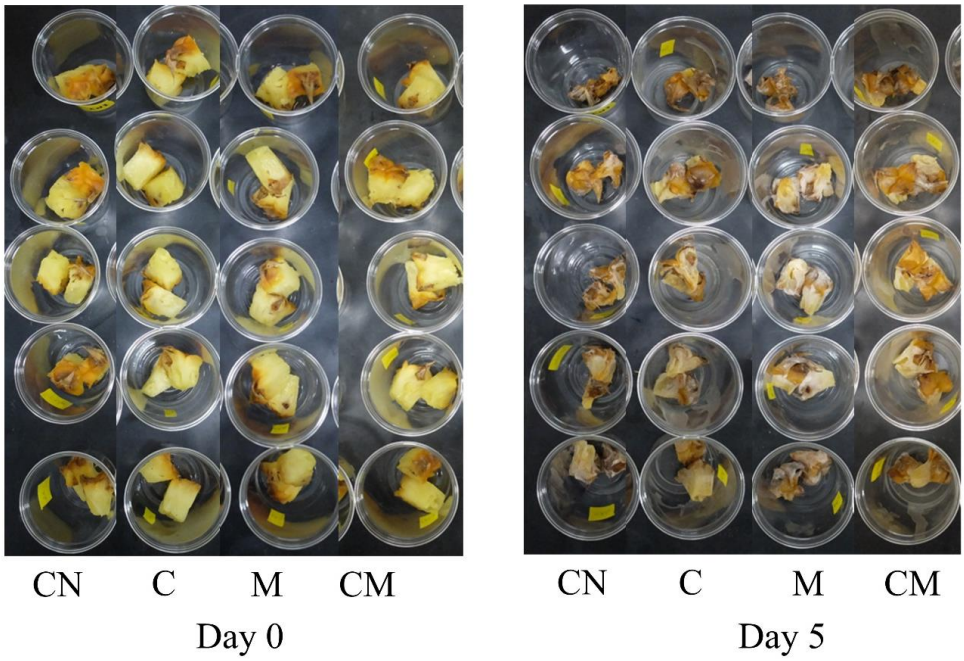

Figure 4.2. Fresh-cut untreated (CN) and chitosan- (C), melezitose- (M), and chitosan-melezitose (CM)-treated pineapple cv. Bogor, stored from day 0 until day 5.

4.3.3 Multivariate analysis of treated pineapple

Metabolite profiling using GC-MS was able to detect 370 metabolite peaks in the flesh-peel part of the cut pineapple. Among these peaks, 56 peaks were annotated using the MSP library by using the retention index compared to the alkene mix prior to the analysis and the respective mass spectra. Metabolites in the QC sample with an RSD of more than 30% and an intensity of less than 3-fold the blank were excluded from the analysis. These metabolites were normalized using the internal standard, ribitol, which was chosen due to the fact that it is not present in the pineapple sample and is stable in the extraction solution. After screening, 33 annotated metabolites and 59 unknown

metabolites were used for further multivariate analysis. A complete list of these metabolites is provided in Table S4.1.

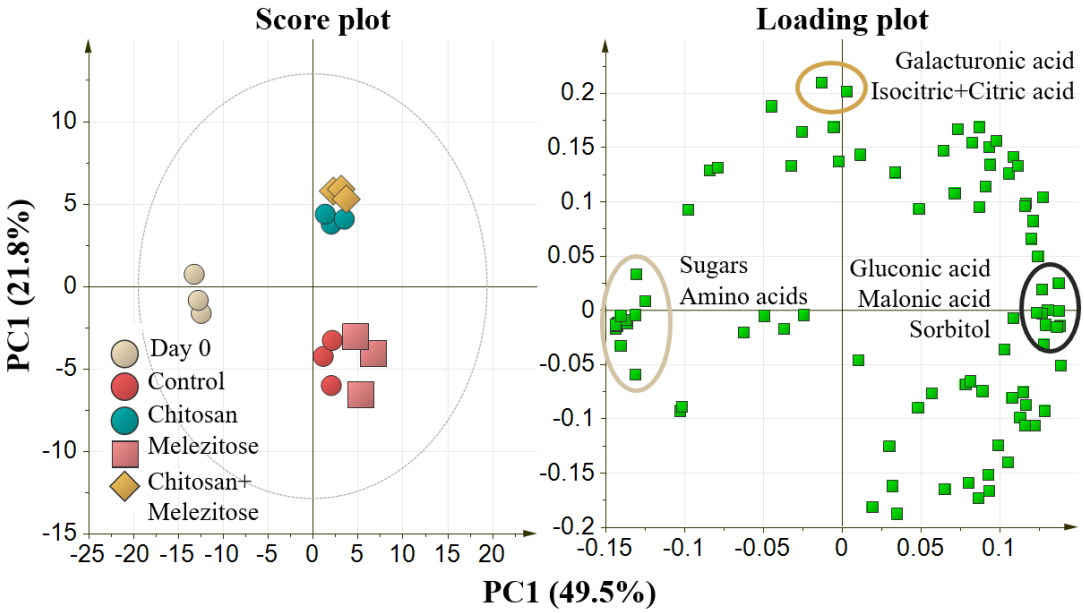

Figure 4.3. PCA results (score and loading plot) of fresh-cut pineapple subjected to coating treatments. The variables used for PCA included 33 annotated metabolites with 59 unknowns obtained from GC-MS analysis. Data was auto-scaled prior to analysis. Brown circle: day 0, red circle: control no treatment, blue circle: chitosan, red square: melezitose 5 mg/L, yellow diamond: chitosan-melezitose. Highly abundant annotated metabolites from each cluster were indicated by a circle in the loading plot. Brown: sugars and amino acids; black: gluconic acid, malonic acid, and sorbitol; yellow: galacturonic acid and isocitric+citric acid.

Figure 4.3 shows the score plot from the PCA of cut pineapple cv. Queen on day 0, control pineapple, and pineapple after treatment with chitosan, melezitose, and chitosan-melezitose. PCA is an unsupervised analysis that is useful for observing global trends in samples (Werth et al. 2010). The score plot in Figure 4.3 shows that the samples were

separated based on the day of storage in PC1 with 49.5% variance, while the chitosan-based treatment clustered separately in the positive value of PC2 with 21.8% variance. From this experiment, chitosan treatment gives more prominent effect to the pineapple cut fruit than melezitose alone. However, even chitosan could not maintain cut fruit condition closer to the day 0 (fresh) condition as shown in PC1. The loading plot in Figure 4.3 shows that metabolite accumulation corresponded to clustering in the score plot. The annotated metabolites that were highly abundant on day 0 were sugars and amino acids, while the metabolites that were abundant on day 5 were gluconic acid, malonic acid, and sorbitol. The metabolites that separated the chitosan-based treatment were galacturonic acid and isocitric+citric acid, while the metabolites that were abundant in the melezitose and control treatments were mannitol and propylene glycol.

In the present study, observation was stopped on day 5 due to a significant drop (approximately 40–50%) in the weight of fruit, indicating a deteriorated condition in all treatments. Prolonging storage time may allow for the metabolite status of the fruits to become similar across all samples, while the focus of this study was the metabolite profile differences between treatments after storage. Metabolites acquired from GC-MS analysis (33 annotated metabolites and 59 unknowns) were used to construct PCA score plots and loading plots to visualize the changes in metabolite profiles after treatment with chitosan, melezitose, and chitosan-melezitose, as shown in Figure 4.3. The PCA score plot showed that the main separation factor was the storage time (day 0 and day 5 after treatment), as shown in PC1, and the second factor that separated the samples was chitosan treatment, as shown in PC2. From the loading plot, day 0 samples contained high sugars (sucrose, glucose, sorbose, and fructose) and amino acids (alanine, valine, and tyrosine). These results indicate that these sugar and amino acid levels can be used as indicators of

pineapple freshness during storage. Accumulation of amino acids and sugars has also been found in other fruits, such as peaches (Brizzolara et al. 2020). Further analysis of chitosan treatment in the PCA plot (Figure 4.3) showed that chitosan-treated samples accumulated higher levels of galacturonic acid and isocitric+citric acid than the non-chitosan-treated samples. Galacturonic acid, isocitric acid, and citric acid may also indicate the freshness of pineapple products because galacturonic acid is known as a precursor metabolite of pectin, a component of plant cell walls, and citric acid levels correspond with the titratable acidity of pineapple fruit, which is commonly used as a quality parameter for pineapples. (Bethke et al. 2015; Minh Phuoc 2020).

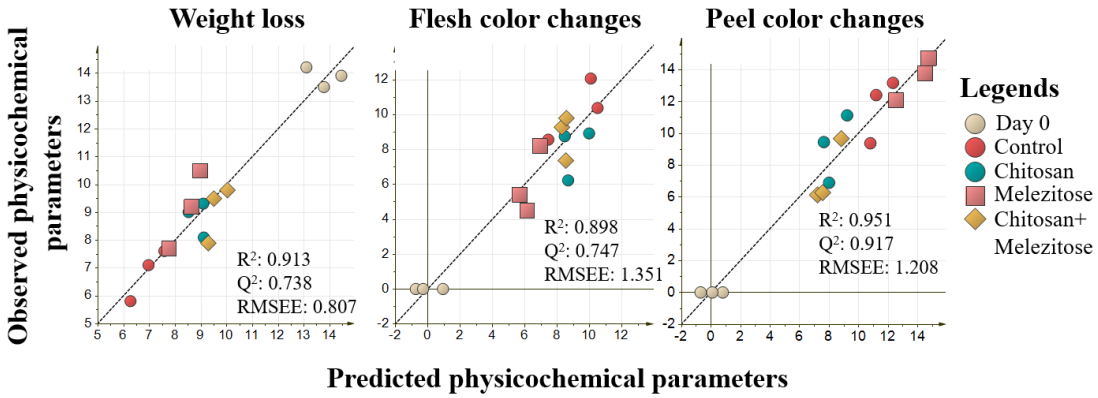

Figure 4.4. Orthogonal projection to latent structures (OPLS) regression analysis of fresh-cut pineapple. Explanatory variables are 33 annotated metabolites with 59 unknowns and response variables are weight, flesh color, and peel color data. Values of R^2, Q^2, and RMSEE were used to evaluate the models.

The identification of metabolites that were highly influenced in the shelf-life analysis was conducted using OPLS regression analysis (Teoh et al. 2015). Metabolites (annotated and unknown) were used as explanatory variables, while weight, flesh color changes, and peel color changes were used as response variables. The constructed models

(Figure 4.4) showed good linearity with R^2 values of 0.913, 0.898, and 0.951 for weight, flesh color, and peel color, respectively. Small deviations or errors are indicated by the root mean square error of estimation (RMSEE) for each model. Potentially important metabolites that correlated with changes in physicochemical parameters were evaluated further using OPLS regression analysis, which can explain the relationship between response and explanatory variables (Teoh et al. 2015). The OPLS regression models for weight, flesh color changes, and peel color changes are shown in Figure 4.4. The R^2, Q^2, and RMSEE values were used to evaluate the quality of the constructed models. The R^2 and Q^2 values over 0.6 were considered to represent good model criteria. RMSEE was used to evaluate the accuracy and model robustness, with a lower RMSEE score indicating a better model (Alexander et al. 2015). Statistically important metabolites for the models were also indicated by variable important in projection (VIP) scores. Metabolites with a VIP score of more than one are considered important for model construction. Metabolites with high VIP scores are listed in Table S4.2.

4.3.4 Metabolites changes after treated with chitosan and melezitose

Metabolites that were affected by the treatments were selected from previous VIP metabolites by calculating the p-value between treatments. Metabolites that did not differ significantly from day 0 but differed significantly from the control were chosen to explain the effect of coating treatments. A list of the affected metabolites is provided in Table 4.1. The affected metabolites were separated into three groups, as shown in Figure 4.5. The first group (Figure 4.5A) comprised metabolites that accumulated on day 0 and were retained after 5 days of storage in chitosan-melezitose compared to the control treatment,

namely inositol, quinic acid, and sucrose, in addition to galacturonic acid. The second group (Figure 4.5B) showed metabolites that accumulated on day 0 but increased significantly after 5 days of storage compared to the control (sorbitol and xylitol). The last group comprised (Figure 4.5C) metabolites (isobutyl acetate and fucose) from the control treatment group that showed low accumulation on day 0, which increased significantly after 5 days of storage compared to the other groups.

Table 4.1. List of the high VIP-score metabolites affected by the chitosan and chitosan-melezitose treatments, comparison between day 0 and control.

Metabolite	***p*-value**	
	Day 0 vs Chitosan	**Day 0 vs Chitosan-Melezitose**
Inositol	**0.162**	**0.399**
Quinic acid	0.009	**0.239**
Unknown 40	**0.222**	0.001
Unknown 42	**0.094**	0.006
Metabolite	**Control vs Chitosan**	**Control vs Chitosan-Melezitose**
Inositol	**0.039**	0.111
Sorbitol	**0.013**	**0.002**
Sucrose	0.204	**0.013**
Isobutyl acetate	**0.012**	**0.017**
Fucose	**0.023**	**0.019**
Unknown 43	**0.032**	0.059
Xylitol	**0.007**	**0.001**

Bold numbers indicate the importance of metabolites (insignificant compared to day 0 and significant compared to control)

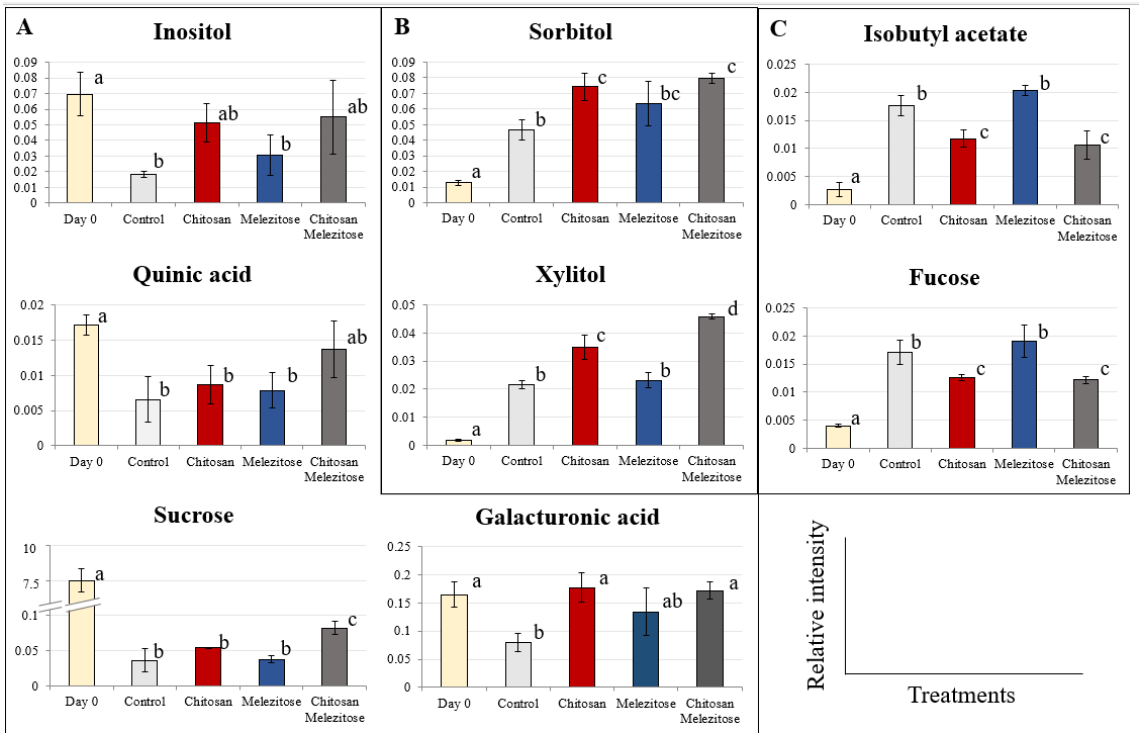

Figure 4.5. Bar graph of the affected metabolites after chitosan-melezitose coating treatments. Metabolites with different trends were divided into A, B, and C groups. The relative intensity was normalized using an internal standard. The vertical axis represents the relative intensity of metabolites, and the horizontal axis represents the treatments. Significant differences ($p < 0.05$) are indicated with different letters based on Tukey's HSD.

Metabolites affected by chitosan-melezitose treatment were chosen based on the p-value score with two parameters: (1) insignificant difference compared with day 0, and (2) significant difference compared with the control. The first criterion was used to select the metabolites that were retained in the fresh sample and were more likely to be correlated with the fresh sample. The second criterion was used to select metabolites that could be used as markers to evaluate the degree of deterioration. A list of the affected

high VIP-score metabolites is provided in Table 4.1. Among all the affected high VIP-score metabolites, only inositol, quinic acid, sucrose, isobutyl acetate, fucose, sorbitol, and xylitol were found to be affected by chitosan-melezitose treatment, in addition to galacturonic acid that affected by melezitose-treatment. The relative intensities of above-mentioned metabolites are shown in Figure 4.5. Inositol was previously reported to regulate osmotic pressure in blueberry fruits, thereby regulating turgor pressure to regulate weight loss in fruits (Montecchiarini et al. 2019). Moreover, inositol may also be linked to the precursor of the plant cell wall, as shown in a study on Arabidopsis (Siddique et al. 2014). Therefore, the accumulation of inositol in the chitosan-melezitose sample and day 0 sample may indicate the integrity of the cell wall under these two conditions (Figure 4.5A).

Compared to chitosan treatment alone, melezitose addition affected the accumulation of quinic acid and sucrose (Table 4.1). Quinic acid is one of the main organic acids in pineapple fruit, and it also showed to be accumulated in the early stages of kiwi fruit ripening process (Marsh et al. 2009; Lobo and Paull 2017). The presence of quinic acid may induce the production of nicotinamide (vitamin B3), which may play a role in antioxidant activity (Kamat and Devasagayam 1999; Pero et al. 2009). This study also found similar result in chapter 2 that mentioned stored pineapple samples accumulated a lower level of quinic acid compared to fresh samples. The accumulation of sucrose on day 0 represented the sweetness of the fruit when it was first cut (Figure 4.5A). After 5 days of storage, all treatments induced a significantly lower level of sucrose compared to day 0. This trend was in line with those of previous studies that showed lower sucrose intensity after the storage of other fruits, such as apples (Brizzolara et al. 2020). However, among all the treatments, chitosan-melezitose treatment resulted in the

accumulation of the highest level of sucrose. This result shows the effectiveness of chitosan-melezitose in retaining sucrose levels compared to the control treatment. The accumulation of quinic acid and sucrose by the addition of melezitose to chitosan provides insights into the possibility of melezitose to influence antioxidant capability on pineapple fruits in addition to the previous reports that shown melezitose may be involved in osmoregulation (Akšić et al. 2014). Moreover, melezitose-treated pineapple in day 5 was found to have galacturonic acid, precursor metabolites to plant cell walls materials, relative intensity similar to day 0 pineapple, indicating the potential of melezitose to retain the freshness of pineapple (Bethke et al. 2015).

Sorbitol is a sweet sugar that determines the sweetness of Japanese fruits, together with sucrose (Itai et al. 2015). The accumulation of sorbitol, shown in Figure 4.5B, may be indicative of the sweetness of the stored cut fruit. However, in contrast with sucrose, the sorbitol concentration on day 0 was lower than that after 5 days of storage. Therefore, the role of sorbitol may not only be related to sweetness but also to the fact that it is a sugar alcohol that has a protective effect against oxidative stress in pineapple fruits (Paul et al. 2014). Similar to sorbitol, xylitol can also be used as a sugar substitute because of its sweetness, which has an intensity equivalent to that of sucrose, in addition to a low caloric value (Rehman et al. 2018). Despite its similarity to sucrose, xylitol may prevent the browning/oxidation process due to the absence of aldehyde or ketone groups (Ahuja et al. 2020). Compared to other sugars, xylitol can be used to prevent microbial contamination because it cannot be digested by microbes (Ahuja et al. 2020). Both xylitol and sorbitol can act as humectants to prevent water and moisture loss during storage, thus allowing the product to retain its weight (Young and O'Sullivan 2011). Two other important metabolites that were affected by chitosan-melezitose treatment were

previously annotated as unknown metabolites. Further studies were conducted by comparing their mass spectra to another database (i.e., Fiehn Database: https://mona.fiehnlab.ucdavis.edu/) with a similarity score of over 700. From the mass spectra database, unknown 10 was putatively identified as isobutyl acetate, while unknown 13 was putatively identified as D-fucose. Both metabolites accumulated after 5 days of storage and showed higher levels in the control group than in the chitosan-treated groups (Figure 4.5C). Isobutyl acetate is an aromatic ester commonly found in melons and plums (Pino and Quijano 2012; Farcuh et al. 2017). The accumulation of isobutyl acetate was correlated with the process of senescence in melons and indicated the short shelf life of these fruits (Obando-Ulloa et al. 2009; Farcuh et al. 2017). Another possible reason for isobutyl acetate accumulation is fermentation from yeast contamination (Jackson 2008). Thus, in the current study, the accumulation of isobutyl acetate may be related to senescence in fresh-cut pineapples or yeast fermentation in fresh-cut fruits. Fucose is a monosaccharide that constitutes the plant cell wall (Yamaki et al. 1983). A previous study found an increase in fucose in date palm fruits during storage (Cherif et al. 2021). An increase in fucose was also observed during the chilling of injured peach fruits and its ripening process (Brizzolara et al. 2020). Therefore, fucose accumulation in the control group may be correlated with senescence or deterioration in fresh-cut pineapples. The lower accumulation of both isobutyl acetate and fucose after chitosan-melezitose treatment may explain the ability of the solution to prevent the deterioration of fresh-cut pineapples. The previous analysis of the metabolites affected by chitosan-melezitose treatment showed that these changes in primary metabolites may contribute to the different processes involved in fruit deterioration. Chitosan added with melezitose treatment may modulate osmotic balance (inositol, sorbitol, and xylitol), cell wall-related

metabolites (inositol, fucose, and galacturonic acid), and antioxidant-related compounds (quinic acid and xylitol), resulting in changes in the sweetness and aroma of fresh-cut pineapples (sucrose and isobutyl acetate). While previous reported only mentioned the ability of melezitose in osmoregulation system (Panizzi and Parra 2012; Akšić et al. 2014), this study showed that melezitose addition might work synergistically with chitosan to influence metabolites relative intensity that related with cell wall-related metabolism and antioxidative process even though further analysis still needed to confirm the antioxidant properties of melezitose. This study also opens the possibility for food researcher to analyze the food safety of melezitose as a preservative due to the inability of food-grade melezitose in the market.

4.4 Conclusion

This study shows that melezitose was able to maintain flesh color better than inositol. The addition of melezitose to the chitosan-based coating treatment may affect the weight and color of fresh-cut pineapple after storage for five days under ambient conditions. Although the physicochemical changes were not statistically significant, the metabolites acquired from GC-MS analysis showed significant changes through the PCA score plot, separating chitosan-treated sample and non-chitosan-treated sample with day 0. Further evaluation of chitosan-melezitose treatment showed that inositol, quinic acid, sucrose, sorbitol, xylitol, isobutyl acetate, and fucose were the most affected metabolites and may be involved in osmoregulation, plant cell-wall metabolism, and the antioxidative process, thereby affecting the sweetness and aroma of fresh-cut pineapple during storage. These findings suggest that the application of chitosan-based coating in pineapple fruit may modulate the primary metabolites related to osmoregulation,

antioxidant protection, and cell wall-related processes. More specifically, the addition of melezitose to chitosan may not only related to affect osmoregulation as previously reported, but might also affect the antioxidant protection and cell wall metabolism by influencing quinic acid, xylitol, and galacturonic acid accumulation, thereby affecting the fruit ability to retain sucrose. Although the physicochemical changes were not statistically significant in this study, trends in the changes of weight and color can be seen and supported by the changes in metabolite levels. Moreover, further experiment will be needed to determine the antioxidant protection effect of melezitose and cell wall metabolism, such as 2,2-diphenyl-1-picrylhydrazyl (DPPH) radical scavenging activity for evaluating antioxidant activity. Regardless, this study provides a basis to use melezitose as the additive in chitosan-based coating and become an alternative to current post-harvest treatments of pineapple to prevent post-harvest losses.

Chapter 5

Conclusion

This study showed the application of metabolomics-based research to characterize different pineapple cultivars based on their metabolite profile, monitor metabolite changes during ‘Queen’ pineapple ripening process, and elucidate the effect of specific metabolites in ‘Queen’ pineapple postharvest process. From the consumer perspective, pineapple ripening stage was more important and affected the sensory profile compared to pineapple cultivar, with the C4-stage or full-ripe pineapple being more preferable than C1-stage or green-ripe pineapple. With the help of metabolomics, asparagine, serine, glycine, threonic acid, sucrose, and serotonin were shown to be correlated with high acceptability attributes in pineapple sensory evaluation. Interestingly, all of these metabolites were found to be high in ‘Queen’ pineapple. Further evaluation of ‘Queen’ pineapple ripening process found that inositol and melezitose, saccharide group compounds, were changed and correlated with ripening, and might contribute to the shelf-life of pineapple. External application of inositol and melezitose to ‘Queen’ pineapple showed that melezitose was giving a more prominent effect than inositol. With the addition of chitosan, melezitose and chitosan might act synergistically to changes metabolite intensity that correlated with shelf-life of pineapples, such as galacturonic acid, inositol, sucrose, quinic acid, sorbitol, and xylitol. It must be noted that the scope of chapter 3 and 4 in this dissertation only applies to ‘Queen’ cultivar, thus the changes of metabolites in ripening stage and the addition effect of melezitose to other cultivar such as ‘Smooth Cayenne’ might give different result. Nevertheless, the finding of melezitose

in this study that play a role in influencing the changes of metabolites related with oxidative process, and cell wall metabolism complement the previously known function of melezitose in regulating osmotic pressure in plants. The relation of melezitose to oxidative process or cell wall metabolism will be needed to confirm by additional experiment, such as DPPH radical scavenging activity.

Currently, the most common pineapple to be exported is the green-mature pineapple. However, this research indicates that the consumer prefers C4-stage pineapple or the full ripe pineapple, even in Japan. Therefore, to tackle the short shelf-life problem in full-ripe pineapple, including ‘Queen’ cultivar, the findings in this study open a new possibility for pineapple postharvest researchers to use melezitose as a raw material or additives for pineapple coatings to prolong the shelf life of ‘Queen’ pineapple. Even though the effect of melezitose is not apparent in the physicochemical parameter, the changes in metabolites relative intensity indicate positive trends, shown by the increase of metabolite related with shelf-life. Thus, additional formulation or combination with another bioactive compound is still needed to prolong ‘Queen’ pineapple shelf life.

Acknowledgement

First, I would like to praise Allah The Almighty, The Lord of the Universe, The Most Gracious, and The Most Merciful for all the blessings that I have continuously received since birth until now.

I would like to express my gratitude and thankfulness to Prof. Eiichiro Fukusaki, Assoc. Prof. Shuichi Shimma, Assist. Prof. Sastia Prama Putri. Their guidance, in experiments, and in life, helped me to stay motivated to finish my Master and Doctor program in Osaka University and giving me opportunity here in Japan.

I would like to acknowledge Prof. Sobir Ridwani and Dr. Fenny Martha Dwivany for the guidance, advice, and support during my study, Prof. Toshiya Muranaka and Prof. Kazuhito Fujiyama for their insightful comments to improve the quality of my doctoral dissertation from various perspectives. I would like to thank also MEXT for the financial support throughout my study.

To Pramesti Istiandari, my wife that also struggle together to finish PhD with me, thank you for your understanding and support until now. To Della, Hadi, Sri, Fitri, Fira, Kak Jalu Nael, Abi, Marvin for always be there (in lab mainly) as a place to share laughter together. To Kak Anja, Kak Mega, Kak Kadar, Kak Wisman, Moke, Ploy, Sana, for teaching me metabolomics and how to handle the daily life in Japan. To Mizuno-kun, Arisa, Riley, Watanabe-kun, Arakawa-san, Ikuta-kun, Kitani-san, and all food team members from 2017-2022 that always helping each other and share great memories together. Finally, I would like to express my gratitude and love to my family, Alm. Mbah Roni, Alm. Mbah Uti, Ibu, Mbak Sita, Mbak Lia, Mas Lana, De Akbar for always loving me, pray the best for me, even though I always act recklessly to them.

References

Adiletta, G., Di Matteo, M., Petriccione, M.: Multifunctional role of chitosan edible coatings on antioxidant systems in fruit crops: A review. *Int. J. Mol. Sci.*, **22**, 1–18 (2021).

Agricultural Standards Unit United Nations Economic Commission for Europe: UNECE Standard on the marketing and commercial quality control of Pineapples - Explanatory Brochure. *Agric. Stand. Unit*, 26 (2013).

Ahmad, M.S., Siddiqui, M.W.: *Postharvest quality assurance of fruits*, Springer (2015).

Ahuja, V., Macho, M., Ewe, D., Singh, M., Saha, S., Saurav, K.: Biological and pharmacological potential of xylitol: A molecular insight of unique metabolism. *Foods*, **9**, 1–24 (2020).

Aizat, W.M., Dias, D.A., Stangoulis, J.C.R., Able, J.A., Roessner, U., Able, A.J.: Metabolomics of capsicum ripening reveals modification of the ethylene related-pathway and carbon metabolism. *Postharvest Biol. Technol.*, **89**, 19–31 (2014).

Akšić, M.F., Tosti, T., Nedić, N., Marković, M., Ličina, V., Milojković-Opsenica, D., Tešić, Ž.: Influence of frost damage on the sugars and sugar alcohol composition in quince (*Cydonia oblonga* Mill.) floral nectar. *Acta Physiol. Plant.*, **37**, 1701 (2014).

Alexander, D.L.J., Tropsha, A., Winkler, D.A.: Beware of R(2): Simple, Unambiguous Assessment of the Prediction Accuracy of QSAR and QSPR Models. *J. Chem. Inf. Model.*, **55**, 1316–1322 (2015).

Alkan, N., Fortes, A.M.: Insights into molecular and metabolic events associated with fruit response to post-harvest fungal pathogens. *Front. Plant Sci.*, **6**, 1–14 (2015).

Allegra, A., Gallotta, A., Carimi, F., Mercati, F., Inglese, P., Martinelli, F.: Metabolic profiling and post-harvest behavior of “dottato” fig (*Ficus carica* L.) fruit covered with an edible coating from O. *ficus-indica*. *Front. Plant Sci.*, **9**, 1–10 (2018).

Allwood, J.W., Cheung, W., Xu, Y., Mumm, R., De Vos, R.C.H., Deborde, C., Biais, B., Maucourt, M., Berger, Y., Schaffer, A.A., Rolin, D., Moing, A., Hall, R.D.,

Goodacre, R.: Metabolomics in melon: A new opportunity for aroma analysis. *Phytochemistry*, **99**, 61–72 (2014).

Altendorf, S.: Global Prospects for Major Tropical Fruits. *Food Outlook*, 68–81 Available at: http://www.fao.org/fileadmin/templates/est/COMM_MARKETS_MONITORING/Tropical_Fruits/Documents/Tropical_Fruits_Special_Feature.pdf.(2017).

Anjaritha, A.A., Ridwani, S., Dwivany, F.M., Putri, S.P., Fukusaki, E.: A metabolomics-based approach for the evaluation of off-tree ripening conditions and different postharvest treatments in mangosteen (*Garcinia mangostana*). *Metabolomics*, **15**, 1–16 (2019).

Barral, B., Chillet, M., Léchaudel, M., Lugan, R., Schorr-Galindo, S.: Coumaroyl-isocitric and caffeoyl-isocitric acids as markers of pineapple fruitlet core rot disease. *Fruits*, **74**, 11–17 (2019).

Barrett, D.M., Beaulieu, J.C., Shewfelt, R.: Color, flavor, texture, and nutritional quality of fresh-cut fruits and vegetables: Desirable levels, instrumental and sensory measurement, and the effects of processing. *Crit. Rev. Food Sci. Nutr.*, **50**, 369–389 (2010).

Bavaresco, L., Zamboni, M., Squeri, C., Xu, S., Abramowicz, A., Lucini, L.: Chitosan and grape secondary metabolites: A proteomics and metabolomics approach. *BIO Web Conf.*, **9**, 01004 (2017).

Bernales, M., Monsalve, L., Ayala-Raso, A., Valdenegro, M., Martínez, J.P., Travisany, D., Defilippi, B., González-Agüero, M., Cherian, S., Fuentes, L.: Expression of two indole-3-acetic acid (IAA)-amido synthetase (GH3) genes during fruit development of raspberry (*Rubus idaeus* Heritage). *Sci. Hortic. (Amsterdam).*, **246**, 168–175 (2019).

Bethke, G., Thao, A., Xiong, G., Li, B., Soltis, N.E., Hatsugai, N., Hillmer, R.A., Katagiri, F., Kliebenstein, D.J., Pauly, M., Glazebrook, J.: Pectin biosynthesis is critical for cell wall integrity and immunity in *Arabidopsis thaliana*. *Plant Cell*, **28**,

537–556 (2015).

Bierhals, V.S., Chiumarelli, M., Hubinger, M.D.: Effect of Cassava Starch Coating on Quality and Shelf Life of Fresh-Cut Pineapple (*Ananas Comosus* L. Merril cv "Pérola"). *J. Food Sci.*, **76**, E62-E72 (2011).

Brizzolara, S., Manganaris, G.A., Fotopoulos, V., Watkins, C.B., Tonutti, P.: Primary Metabolism in Fresh Fruits During Storage. *Front. Plant Sci.*, **11**, 80 (2020).

Bustamante, C.A., Monti, L.L., Gabilondo, J., Scossa, F., Valentini, G., Budde, C.O., Lara, M. V., Fernie, A.R., Drincovich, M.F.: Differential metabolic rearrangements after cold storage are correlated with chilling injury resistance of peach fruits. *Front. Plant Sci.*, **7**, 1–15 (2016).

Cassago, A.L.L., Souza, F.V.D., Zocolo, G.J., da Costa, F.B.: Metabolomics as a tool to discriminate species of the Ananas genus and assist in taxonomic identification. *Biochem. Syst. Ecol.*, **100**, 104380 (2022).

Chen, J., Zeng, H., Zhang, X.: Integrative transcriptomic and metabolomic analysis of D-leaf of seven pineapple varieties differing in N-P-K% contents. *BMC Plant Biol.*, **21**, 1–19 (2021).

Cherif, S., Le Bourvellec, C., Bureau, S., Benabda, J.: Effect of storage conditions on 'Deglet Nour' date palm fruit organoleptic and nutritional quality. *LWT*, **137**, 110343 (2021).

Colaric, M., Veberic, R., Stampar, F., Hudina, M.: Evaluation of peach and nectarine fruit quality and correlations between sensory and chemical attributes. *J. Sci. Food Agric.*, **85**, 2611–2616 (2005).

Davidzon, M., Alkan, N., Kobiler, I., Prusky, D.: Acidification by gluconic acid of mango fruit tissue during colonization via stem end infection by *Phomopsis mangiferae*. *Postharvest Biol. Technol.*, **55**, 71–77 (2010).

Decros, G., Baldet, P., Beauvoit, B., Stevens, R., Flandin, A., Colombié, S., Gibon, Y., Pétriacq, P.: Get the Balance Right: ROS Homeostasis and Redox Signalling in Fruit. *Front. Plant Sci.*, **10**, 1091 (2019).

Dhar, M., Rahman, S.M., Sayem, S.M.: Maturity and post harvest study of pineapple with quality and shelf life under red soil. *Int. J. Sustain. Crop Prod.*, **3**, 69–75 (2008).

Dheilly, E., Gall, S. Le, Guillou, M.-C., Renou, J.-P., Bonnin, E., Orsel, M., Lahaye, M.: Cell wall dynamics during apple development and storage involves hemicellulose modifications and related expressed genes. *BMC Plant Biol.*, **16**, 201 (2016).

Diboun, I., Mathew, S., Al-Rayyashi, M., Elrayess, M., Torres, M., Halama, A., Méret, M., Mohney, R.P., Karoly, E.D., Malek, J., Suhre, K.: Metabolomics of dates (*Phoenix dactylifera*) reveals a highly dynamic ripening process accounting for major variation in fruit composition. *BMC Plant Biol.*, **15**, 291 (2015).

Escamilla-García, M., Rodríguez-Hernández, M.J., Hernández-Hernández, H.M., Delgado-Sánchez, L.F., García-Almendárez, B.E., Amaro-Reyes, A., Regalado-González, C.: Effect of an edible coating based on chitosan and oxidized starch on shelf life of *Carica papaya* L., and its physicochemical and antimicrobial properties. *Coatings*, **8**, 318 (2018).

Farcuh, M., Li, B., Rivero, R.M., Shlizerman, L., Sadka, A., Blumwald, E.: Sugar metabolism reprogramming in a non-climacteric bud mutant of a climacteric plum fruit during development on the tree. *J. Exp. Bot.*, **68**, 5813–5828 (2017).

Fathima, A.M., Chuang, D., Laviña, W.A., Liao, J., Putri, S.P., Fukusaki, E.: Iterative cycle of widely targeted metabolic profiling for the improvement of 1-butanol titer and productivity in *Synechococcus elongatus*. *Biotechnol. Biofuels*, **11**, 1–12 (2018).

Fausto Rivero-Cruz, J., Rodríguez de San Miguel, E., Robles-Obregón, S., Hernández-Espino, C.C., Rivero-Cruz, B.E., Pedraza-Chaverri, J., Esturau-Escofet, N.: Prediction of antimicrobial and antioxidant activities of Mexican propolis by ^{1}H-NMR spectroscopy and chemometrics data analysis. *Molecules*, **22**, 1–17 (2017).

Feng, X., Bansal, N., Yang, H.: Fish gelatin combined with chitosan coating inhibits

myofibril degradation of golden pomfret (*Trachinotus blochii*) fillet during cold storage. *Food Chem.*, **200**, 283–292 (2016).

Fuentes, L., Figueroa, C.R., Valdenegro, M.: Recent advances in hormonal regulation and cross-talk during non-climacteric fruit development and ripening. *Horticulturae*, **5**, 45(2019).

Garcia-Gonzalez, M., Plou, F.J., Cervantes, F. V, Remacha, M., Poveda, A., Jiménez-Barbero, J., Fernandez-Lobato, M.: Efficient production of isomelezitose by a glucosyltransferase activity in *Metschnikowia reukaufii* cell extracts. *Microb. Biotechnol.*, **12**, 1274–1285 (2019).

Geladi, P., Kowalski, B.R.: Partial least-squares regression: a tutorial. *Anal. Chim. Acta*, **185**, 1–17 (1986).

Golly, M.K., Ma, H., Sarpong, F., Dotse, B.P., Oteng-Darko, P., Dong, Y.: Shelf-life extension of grape (*Pinot noir*) by xanthan gum enriched with ascorbic and citric acid during cold temperature storage. *J. Food Sci. Technol.*, **56**, 4867–4878 (2019).

Hanifah, A., Maharijaya, A., Putri, S.P., Laviña, W.A., Sobir: Untargeted Metabolomics Analysis of Eggplant (*Solanum melongena* L.) Fruit and Its Correlation to Fruit Morphologies. *Metabolites*, **8**, 49 (2018).

Hill, C.B., Dias, D.A., Roessner, U.: Current and Emerging Applications of Metabolomics in the Field of Agricultural Biotechnology. *Adv. Food Biotechnol.*, 13–26 (2015).

Hong, K., Chen, L., Gu, H., Zhang, X., Chen, J., Nile, S.H., Hu, M., Gong, D., Song, K., Hou, X., Chen, J., Yao, Q., Fan, Z., Yuan, D.: Novel Insight into the Relationship between Metabolic Profile and Fatty Acid Accumulation Altering Cellular Lipid Content in Pineapple Fruits at Different Stages of Maturity. *J. Agric. Food Chem.*, **69**, 8578–8589 (2021).

Hui, Y.H., Chen, F., Nollet, L.M.L., Guiné, R.P.F., Martín-Belloso, O., Mínguez-Mosquera, M.I., Paliyath, G., Pessoa, F.L.P., Le Quéré, J.-L., Sidhu, J.S.: *Handbook of fruit and vegetable flavors*, Wiley Online Library (2010).

Ibrahim, S.M., Nahar, S., Islam, J.M.M., Islam, M., Hoque, M.M., Khan, M.A.: Effect of Low Molecular Weight Chitosan Coating on Physico-chemical Properties and Shelf life Extension of Pineapple (*Ananas sativus*). *J. For. Prod. Ind.*, **3**, 161–166 (2014).

Iqbal, K., Khan, A., Khattak, M.M.A.K.: Biological Significance of Ascorbic Acid (Vitamin C) in Human Health-A Review. *Pakistani J. Nutr.*, **3**, 5–13 (2004).

Itai, A., Hatanaka, R., Irie, H., Murayama, H.: Effects of storage temperature on fruit quality and expression of sucrose phosphate synthase and acid invertase genes in Japanese pear. *Hortic. J.*, **84**, 227–232 (2015).

Jackson, R.S.: 8 - Postfermentation Treatments and Related Topics. In R. S. B. T.-W. S. (Third E. Jackson, ed. *Food Science and Technology*. (*pp. 418–519*). San Diego: Academic Press. (2008).

Jarret, D.A., Morris, J., Cullen, D.W., Gordon, S.L., Verrall, S.R., Milne, L., Hedley, P.E., Allwood, J.W., Brennan, R.M., Hancock, R.D.: A Transcript and Metabolite Atlas of Blackcurrant Fruit Development Highlights Hormonal Regulation and Reveals the Role of Key Transcription Factors. *Front. Plant Sci.*, **9**, 1–22 (2018).

Jia, H., Wang, Y., Sun, M., Li, B., Han, Y., Zhao, Y., Li, X., Ding, N., Li, C., Ji, W., Jia, W.: Sucrose functions as a signal involved in the regulation of strawberry fruit development and ripening. *New Phytol.*, **198**, 453–465 (2013).

Jiang, Y., Song, J.: Fruits and Fruit Flavor: Classification and Biological Characterization. *Handb. Fruit Veg. Flavors*, 1–23 (2010).

Jolliffe, I.T., Cadima, J., Cadima, J.: Principal component analysis : a review and recent developments Subject Areas. *Phil.Trans.R.Soc.A*, **374**, 1–16 (2016).

Joy, P.P., Rejuva TA, R.: *Harvesting and post-harvest handling of pineapple*, Pineapple research station, Kerala, India (2016).

Kabasakalis, V., Siopidou, D., Moshatou, E.: Ascorbic acid content of commercial fruit juices and its rate of loss upon storage. *Food Chem.*, **70**, 325–328 (2000).

Kader, A.A.: Fruit maturity, ripening, and quality relationships. In *Acta Horticulturae*. (*pp. 203–208*). International Society for Horticultural Science (ISHS), Leuven, Belgium. (1999).

Kamat, J.P., Devasagayam, T.P.A.: Nicotinamide (vitamin B3) as an effective antioxidant against oxidative damage in rat brain mitochondria. *Redox Rep.*, **4**, 179–184 (1999).

Kamol, S., Howlader, J., Dhar, G.S., Aklimuzzaman, M.: Effect of different stages of maturity and postharvest treatments on quality and storability of pineapple. *J. Bangladesh Agric. Univ.*, **12**, 251–260 (2016).

Karagiannis, E., Michailidis, M., Karamanoli, K., Lazaridou, A., Minas, I.S., Molassiotis, A.: Postharvest responses of sweet cherry fruit and stem tissues revealed by metabolomic profiling. *Plant Physiol. Biochem.*, **127**, 478–484 (2018).

Keutgen, A.J., Pawelzik, E.: Contribution of amino acids to strawberry fruit quality and their relevance as stress indicators under NaCl salinity. *Food Chem.*, **111**, 642–647 (2008).

Koppel, K., Chambers Iv, E.: Development and application of a lexicon to describe the flavor of pomegranate juice. *J. Sens. Stud.*, **25**, 819–837 (2010).

Kumar, V., Irfan, M., Ghosh, S., Chakraborty, N., Chakraborty, S., Datta, A.: Fruit ripening mutants reveal cell metabolism and redox state during ripening. *Protoplasma*, **253**, 581–594 (2016).

Lai, Z., Tsugawa, H., Wohlgemuth, G., Mehta, S., Mueller, M., Zheng, Y., Ogiwara, A., Meissen, J., Showalter, M., Takeuchi, K., Kind, T., Beal, P., Arita, M., Fiehn, O.: Identifying metabolites by integrating metabolome databases with mass spectrometry cheminformatics. *Nat. Methods*, **15**, 53–56 (2018).

Li, S., Tian, Y., Jiang, P., Lin, Y., Liu, X., Yang, H.: Recent advances in the application of metabolomics for food safety control and food quality analyses. *Crit. Rev. Food Sci. Nutr.*, **61**, 1448–1469 (2021).

Lin, M.G., Lasekan, O., Saari, N., Khairunniza-Bejo, S.: Efecto de los recubrimientos

comestibles a base de chitosano y carragenano en los frutos de longan (*Dimocarpus longan*) después de la cosecha. *CYTA - J. Food*, **16**, 490–497 (2018).

Liu, X., Zhang, A., Shang, J., Zhu, Z., Li, Y., Wu, X., Zha, D.: Study on browning mechanism of fresh-cut eggplant (*Solanum melongena* L.) based on metabolomics, enzymatic assays and gene expression. *Sci. Rep.*, **11**, 1–13 (2021).

Lobo, M.G., Paull, R.E.: *Handbook of pineapple technology: production, postharvest science, processing and nutrition*, John Wiley & Sons (2017).

Luengwilai, K., Beckles, D.M., Roessner, U., Dias, D.A., Lui, V., Siriphanich, J.: Identification of physiological changes and key metabolites coincident with postharvest internal browning of pineapple (*Ananas comosus* L.) fruit. *Postharvest Biol. Technol.*, **137**, 56–65 (2018).

Marsh, K., Boldingh, H., S. Shilton, R., A. Laing, W.: Changes in quinic acid metabolism during fruit development in three kiwifruit species, *Functional Plant Biology*, **36**, 463-470 (2009).

Matsuo, T., Tsugawa, H., Miyagawa, H., Fukusaki, E.: Integrated Strategy for Unknown EI–MS Identification Using Quality Control Calibration Curve, Multivariate Analysis, EI–MS Spectral Database, and Retention Index Prediction. *Anal. Chem.*, **89**, 6766–6773 (2017).

Medina, J.D.L.C., García, H.S.: *Pineapple: Post-harvest Operations*, Food and Agriculture Organization, United States (2005).

Minh Phuoc, N.: Synergistic Effect of Calcium Chloride and Chitosan Treatment on Physicochemical Characteristics of Pineapple (*Ananas Comosus*) Fruit During Cool Storage. *Int. J. Pharma Bio Sci.*, **11**, 24–28 (2020).

Moirangthem, K., Tucker, G.: How Do Fruits Ripen? *Front. Young Minds*, **6**, 1–7 (2018).

Montecchiarini, M.L., Margarit, E., Morales, L., Rivadeneira, M.F., Bello, F., Gollán, A., Vázquez, D., Podestá, F.E., Tripodi, K.E.J.: Proteomic and metabolomic approaches unveil relevant biochemical changes in carbohydrate and

cell wall metabolisms of two blueberry (*Vaccinium corymbosum*) varieties with different quality attributes. *Plant Physiol. Biochem.*, **136**, 230–244 (2019).

Monti, L.L., Bustamante, C.A., Osorio, S., Gabilondo, J., Borsani, J., Lauxmann, M.A., Maulion, E., Valentini, G., Budde, C.O., Fernie, A.R., Lara, M. V, Drincovich, M.F.: Metabolic profiling of a range of peach fruit varieties reveals high metabolic diversity and commonalities and differences during ripening. *Food Chem.*, **190**, 879–888 (2016).

Mulderij, R.: Overview global pineapple market. Available at: https://www.freshplaza.com/article/2194086/overview-global-pineapple-market/ [Accessed June 28, 2019].(2018).

Musara, A.: *Determination of ascorbic acid in some citrus fruits by using pencil graphite electrode*. Master Thesis, Near East University, Nicosia (2019).

Nakanishi, K., Matsudo, T., Hori, I., Komiyama, Y., Yokotsuka, K.: Relationship between Fruit Hardness in Kiwifruit and Its Juice Composition. *Nippon shokuhin kogyo gakkaishi*, **37**, 323–330 (1990).

Nitta, K., Laviña, W.A., Pontrelli, S., Liao, J.C., Putri, S.P., Fukusaki, E.: Orthogonal partial least squares / projections to latent structures regression-based metabolomics approach for identification of gene targets for improvement of 1-butanol production in *Escherichia coli*. *J. Biosci. Bioeng.*, **124**, 498–505 (2017).

Nunes, C., Emond, J.-P.: Relationship between weight loss and visual quality of fruits and vegetables. *Proc. Fla. State Hort. Soc.*, **120**, 235–245 (2007).

O'Donoghue, E.M., Somerfield, S.D., Watson, L.M., Brummell, D.A., Hunter, D.A.: Galactose metabolism in cell walls of opening and senescing petunia petals. *Planta*, **229**, 709–721 (2009).

Obando-Ulloa, J.M., Nicolai, B., Lammertyn, J., Bueso, M.C., Monforte, A.J., Fernández-Trujillo, J.P.: Aroma volatiles associated with the senescence of climacteric or non-climacteric melon fruit. *Postharvest Biol. Technol.*, **52**, 146–155 (2009).

Ogasawara, S., Abe, K., Nakajima, T.: Pepper beta-galactosidase 1 (PBG1) plays a significant role in fruit ripening in bell pepper (*Capsicum annuum*). *Biosci. Biotechnol. Biochem.*, **71**, 309–322 (2007).

Ogawa, E.M., Costa, H.B., Ventura, J.A., Caetano, L.C.S., Pinto, F.E., Oliveira, B.G., Barroso, M.E.S., Scherer, R., Endringer, D.C., Romão, W.: Chemical profile of pineapple cv. Vitória in different maturation stages using electrospray ionization mass spectrometry. *J. Sci. Food Agric.*, **98**, 1105–1116 (2018).

Osorio, S., Scossa, F., Fernie, A.R.: Molecular regulation of fruit ripening. *Front. Plant Sci.*, **4**, 1–8 (2013).

Paliyath, G., Subramanian, J., Lim, L.-T., Subramanian, K.S., Handa, A.K., Matto, A.K.: *Postharvest Biology and Nanotechnology*, New York Academy of Sciences; New York, United States (2019).

Panizzi, A.R., Parra, J.R.P.: *Insect bioecology and nutrition for integrated pest management*, CRC press (2012).

Parijadi, A.A.R., Putri, S.P., Ridwani, S., Dwivany, F.M., Fukusaki, E.: Metabolic profiling of *Garcinia mangostana* (mangosteen) based on ripening stages. *J. Biosci. Bioeng.*, **125**, 238–244 (2018).

Paul, P.K., Ghosh, S.K., Singh, D.K., Bhowmick, N.: Quality of osmotically pre-treated and vacuum dried pineapple cubes on storage as influenced by type of solutes and packaging materials. *J. Food Sci. Technol.*, **51**, 1561–1567 (2014).

Paul, V., Pandey, R., Srivastava, G.C.: The fading distinctions between classical patterns of ripening in climacteric and non-climacteric fruit and the ubiquity of ethylene-An overview. *J. Food Sci. Technol.*, **49**, 1–21 (2012).

Pedreschi, R., Munoz, P., Robledo, P., Becerra, C., Defilippi, B.G., Eekelen, H.D.L.M. van, Mumm, R., Westra, E.H., Vos, R.C.H. de: Metabolomics analysis of postharvest ripening heterogeneity of 'Hass' avocadoes. , **92**, 172–179 (2014).

Pero, R.W., Lund, H., Leanderson, T.: Antioxidant metabolism induced by quinic acid. increased urinary excretion of tryptophan and nicotinamide. *Phyther. Res.*, **23**, 335–

346 (2009).

Pino, J.A., Quijano, C.E.: Study of the volatile compounds from plum (*Prunus domestica* L. cv. Horvin) and estimation of their contribution to the fruit aroma. *Food Sci. Technol.*, **32**, 76–83 (2012).

Pongsuwan, W., Fukusaki, E., Bamba, T., Yonetani, T., Yamahara, T., Kobayashi, A.: Prediction of Japanese green tea ranking by gas chromatography/mass spectrometry-based hydrophilic metabolite fingerprinting. *J. Agric. Food Chem.*, **55**, 231–236 (2007).

Putri, S.L.E., Suantika, G., Situmorang, M.L., Christina, J., Nikijuluw, C., Putri, S.P., Fukusaki, E.: Shrimp count size: GC/MS-based metabolomics approach and quantitative descriptive analysis (QDA) reveal the importance of size in white leg shrimp (*Litopenaeus vannamei*). *Metabolomics*, **17**, 1–12 (2021).

Putri, S.P., Fukusaki, E.: *Mass spectrometry-based metabolomics: A practical guide*, CRC Press, Boca Raton (2014).

Rahmawati, D., Chandra, M., Santoso, S., Puteri, M.G.: Application of lemon peel essential oil with edible coating agent to prolong shelf life of tofu and strawberry. *AIP Conf. Proc.*, **1803**, 20037 (2017).

Rehman, S., Murtaza, M., Mushtaq, Z.: Xylitol as Sweetener. In: Merillon JM., Ramawat K. (eds) *Sweeteners. Reference Series in Phytochemistry*. (*pp. 129–149*). Springer, Cham (2018).

Reynolds, T.B.: Strategies for acquiring the phospholipid metabolite inositol in pathogenic bacteria, fungi and protozoa: Making it and taking it. *Microbiology*, **155**, 1386–1396 (2009).

Sanewski, G.M., Bartholomew, D.P., Paull, R.E.: *The pineapple: botany, production and uses* 2nd editio., CABI (2018).

Saradhuldhat, P., Paull, R.: Pineapple organic acid metabolism and accumulation during fruit development. *Sci. Hortic. (Amsterdam).*, **112**, 297–303 (2007).

Schiffman, S.S., Sennewald, K., Gagnon, J.: Comparison of taste qualities and thresholds of D- and L-amino acids. *Physiol. Behav.*, **27**, 51–59 (1981).

Schrimpe-rutledge, A.C., Codreanu, S.G., Sherrod, S.D., Mclean, J.A.: Untargeted metabolomics strategies - challenges and emerging directions. *J. Am. Soc. Mass Spectrom.*, **27**, 1897–1905 (2016).

Schulbach, K.F., Portier, K.M., Sims, C.A.: Evaluation of overall acceptability of fresh pineapple using the regression tree approach. *J. Food Qual.*, **30**, 993–1008 (2007).

Sharma, S., Pareek, S., Sagar, N.A., Valero, D., Serrano, M.: Modulatory effects of exogenously applied polyamines on postharvest physiology, antioxidant system and shelf life of fruits: A review. *Int. J. Mol. Sci.*, **18**, 1789 (2017).

Shiekh, R.A., Malik, M.A., Al-Thabaiti, S.A., Shiekh, M.A.: Chitosan as a novel edible coating for fresh fruits. *Food Sci. Technol. Res.*, **19**, 139–155 (2013).

Shoda, M., Urasaki, N., Sakiyama, S., Terakami, S., Hosaka, F., Shigeta, N., Nishitani, C., Yamamoto, T.: DNA profiling of pineapple cultivars in Japan discriminated by SSR markers. *Breed. Sci.*, **62**, 352–359 (2013).

Siddique, S., Endres, S., Sobczak, M., Radakovic, Z.S., Fragner, L., Grundler, F.M.W., Weckwerth, W., Tenhaken, R., Bohlmann, H.: Myo-inositol oxygenase is important for the removal of excess myo-inositol from syncytia induced by *Heterodera schachtii* in Arabidopsis roots. *New Phytol.*, **201**, 476–485 (2014).

Siti Roha, A.M., Zainal, S., Noriham, A., Nadzirah, K.Z.: Determination of sugar content in pineapple waste variety N36. *Int. Food Res. J.*, **20**, 1941–1943 (2013).

Sorrequieta, A., Ferraro, G., Boggio, S.B., Valle, E.M.: Free amino acid production during tomato fruit ripening: a focus on l-glutamate. *Amino Acids*, **38**, 1523–1532 (2010).

Steingass, C.B., Grauwet, T., Carle, R.: Influence of harvest maturity and fruit logistics on pineapple (*Ananas comosus* [L.] Merr.) volatiles assessed by headspace solid phase microextraction and gas chromatography-mass spectrometry (HS-SPME-GC/MS). *Food Chem.*, **150**, 382–391 (2014).

Steingass, C.B., Carle, R., Schmarr, H.G.: Ripening-dependent metabolic changes in the volatiles of pineapple (*Ananas comosus* (L.) Merr.) fruit: I. Characterization of pineapple aroma compounds by comprehensive two-dimensional gas chromatography-mass spectrometry. *Anal. Bioanal. Chem.*, **407**, 2591–2608 (2015a).

Steingass, C.B., Glock, M.P., Schweiggert, R.M., Carle, R.: Studies into the phenolic patterns of different tissues of pineapple (Ananas comosus [L.] Merr.) infructescence by HPLC-DAD-ESI-MS (n) and GC-MS analysis. *Anal. Bioanal. Chem.*, **407**, 6463–79 Available at: http://www.ncbi.nlm.nih.gov/pubmed/26215283.(2015b).

Steingass, C.B., Jutzi, M., Müller, J., Carle, R., Schmarr, H.G.: Ripening-dependent metabolic changes in the volatiles of pineapple (*Ananas comosus* (L.) Merr.) fruit: II. Multivariate statistical profiling of pineapple aroma compounds based on comprehensive two-dimensional gas chromatography-mass spectrometry. *Anal. Bioanal. Chem.*, **407**, 2609–2624 (2015c).

Steingass, C.B., Dell, C., Lieb, V., Mayer-Ullmann, B., Czerny, M., Carle, R.: Assignment of distinctive volatiles, descriptive sensory analysis and consumer preference of differently ripened and post-harvest handled pineapple (*Ananas comosus* [L.] Merr.) fruits. *Eur. Food Res. Technol.*, **242**, 33–43 (2016).

Sung, J., Suh, J.H., Chambers, A.H., Crane, J., Wang, Y.: Relationship between Sensory Attributes and Chemical Composition of Different Mango Cultivars. *J. Agric. Food Chem.*, **67**, 5177–5188 (2019).

Symons, G.M., Chua, Y.-J., Ross, J.J., Quittenden, L.J., Davies, N.W., Reid, J.B.: Hormonal changes during non-climacteric ripening in strawberry. *J. Exp. Bot.*, **63**, 4741–4750 (2012).

Szent-Györgyi, A.: Identification of Vitamin C*. *Nature*, **131**, 225–226 (1933).

Taghinezhad, E., Sharabiani, V.R.: Effect of chitosan coating on some quality properties of thomson orange during storage (A case study in Iran). *Agric. Eng. Int. CIGR J.*, **20**, 157–161 (2018).

Takeuchi, Y., Nakayama, Y., Fukusaki, E., Irino, Y.: Glutamate production from

ammonia via glutamate dehydrogenase 2 activity supports cancer cell proliferation under glutamine depletion. *Biochem. Biophys. Res. Commun.*, **495**, 761–767 (2018).

Teoh, S.T., Putri, S., Mukai, Y., Bamba, T., Fukusaki, E.: A metabolomics-based strategy for identification of gene targets for phenotype improvement and its application to 1-butanol tolerance in *Saccharomyces cerevisiae*. *Biotechnol. Biofuels*, **8**, 1–14 (2015).

Threlfall, R., Morris, J., Meullenet, J., Striegler, K.: Sensory Characteristics, Composition, and Nutraceutical Content of Juice from *Vitis rotundifolia* (Muscadine) Cultivars. *Am. J. Enol. Vitic.*, **58**, 268-273(2007).

Tosetti, R., Martinelli, F., Tonutti, P., Barupal, D.K.: Metabolomics approach to studying minimally processed peach (*Prunus persica*) fruit. *Acta Hortic.*, **934**, 1017–1022 (2012).

Treviño-Garza, M.Z., García, S., Heredia, N., Alanís-Guzmán, M.G., Arévalo-Niño, K.: Layer-by-layer edible coatings based on mucilages, pullulan and chitosan and its effect on quality and preservation of fresh-cut pineapple (*Ananas comosus*). *Postharvest Biol. Technol.*, **128**, 63–75 (2017).

United Nations: Pineapple: United Nation Conference On Trade and Development. *An INFOCOMM Commod. Profile*, **New York** &, 1–22 (2016).

Want, E.J., Metz, T.O.: MS Based Metabonomics. In J. C. Lindon, G. E. Tranter, & D. W. B. T.-E. of S. and S. (Third E. Koppenaal, eds. (*pp. 926–935*). Oxford: Academic Press. (2017).

Werth, M.T., Halouska, S., Shortridge, M.D., Zhang, B., Powers, R.: Analysis of metabolomic PCA data using tree diagrams. *Anal. Biochem.*, **399**, 58–63 (2010).

White, I.R., Blake, R.S., Taylor, A.J., Monks, P.S.: Metabolite profiling of the ripening of Mangoes *Mangifera indica* L. cv. 'Tommy Atkins' by real-time measurement of volatile organic compounds. *Metabolomics*, **12**, 1–11 (2016).

Wu, Q., Li, T., Chen, X., Wen, L., Yun, Z., Jiang, Y.: Sodium dichloroisocyanurate delays ripening and senescence of banana fruit during storage. *Chem. Cent. J.*, **12**,

1–11 (2018a).

Wu, Z.C., Zhang, J.Q., Zhao, J.T., Li, J.G., Huang, X.M., Wang, H.C.: Biosynthesis of quebrachitol, a transportable photosynthate, in *Litchi chinensis*. *J. Exp. Bot.*, **69**, 1649–1661 (2018b).

Xing, Y., Xu, Q., Li, X., Chen, C., Ma, L., Li, S., Che, Z., Lin, H.: Chitosan-based coating with antimicrobial agents: Preparation, property, mechanism, and application effectiveness on fruits and vegetables. *Int. J. Polym. Sci.*, **2016** (2016).

YAMAKI, S., SATO, Y., MACHIDA, Y.: Characteristics of Cell Wall Polysaccharides and Their Degrading Enzyme Activities in Mealy Fruit and Ishinashi Fruit of Japanese Pear (*Pyrus serotina* Rehder var. culta Rehder). *J. Japanese Soc. Hortic. Sci.*, **52**, 123–134 (1983).

Yang, J., Zhu, H., Tu, J., Jiang, Y., Zeng, J., Yang, B.: Icariin as a Preservative to Maintain the Fruit Quality of Banana During Postharvest Storage. *Food Bioprocess Technol.*, **12**, 1766–1775 (2019).

Young, N.W.G., O'Sullivan, G.R.: 5 - The influence of ingredients on product stability and shelf life. In D. Kilcast & P. B. T.-F. and B. S. and S. L. Subramaniam, eds. *Woodhead Publishing Series in Food Science, Technology and Nutrition*. (*pp. 132–183*). Woodhead Publishing. (2011).

Yun, Z., Gao, H., Liu, P., Liu, S., Luo, T., Jin, S., Xu, Q., Xu, J., Cheng, Y., Deng, X.: Comparative proteomic and metabolomic profiling of citrus fruit with enhancement of disease resistance by postharvest heat treatment. *BMC Plant Biol.*, **13**, 44 (2013).

Yun, Z., Li, T., Gao, H., Zhu, H., Gupta, V.K., Jiang, Y., Duan, X.: Integrated Transcriptomic, Proteomic, and Metabolomics Analysis Reveals Peel Ripening of Harvested Banana under Natural Condition. *Biomolecules*, **9**, 167 (2019).

Zgola-Grześkowiak, A., Grześkowiak, T.: Determination of Glutamic Acid and Aspartic Acid in Tomato Juice by Capillary Isotachophoresis. *Int. J. of Food Prop.*, **15**, 628–637 (2012).

Zhao, X., Chen, M., Zhao, Y., Zha, L., Yang, H., Wu, Y.: GC–MS-Based Nontargeted and Targeted Metabolic Profiling Identifies Changes in the *Lentinula edodes* Mycelial Metabolome under High-Temperature Stress. *Int. J. Mol. Sci.*, **20**, 2330 (2019).

List of publications

Original paper

Ikram, M.M.M.; Ridwani, S.; Putri, S.P.; Fukusaki, E. GC-MS Based Metabolite Profiling to Monitor Ripening-Specific Metabolites in Pineapple (*Ananas comosus*). Metabolites 2020, 10, 134. https://doi.org/10.3390/metabo10040134

Ikram, M.M.M.; Mizuno, R.; Putri, S.P.; Fukusaki, E. Comparative metabolomics and sensory evaluation of pineapple (*Ananas comosus*) reveal the importance of ripening stage compared to cultivar. J. Biosci. Bioeng. 2021, 12, 132. https://doi.org/10.1016/j.jbiosc.2021.08.008

Ikram, M.M.M.; Putri, S.P.; Fukusaki, E. Chitosan-based coating enriched with melezitose alters primary metabolites in fresh-cut pineapple during storage. Fro. Plant Sci. (Submitted and under review)

Presentations:

1. **Ikram, M.M.M.;** Mizuno, R.; Putri, S.P.; Fukusaki, E**.** Comparative metabolomics and sensory evaluation of Smooth Cayenne pineapple and Red Spanish pineapple *(Online presentation) 3rd Academic Exchange Seminar Shanghai Jiao Tong University and Osaka University. 2021*

2. **Ikram, M.M.M.;** Mizuno, R.; Putri, S.P.; Fukusaki, E. Comparative metabolomics and sensory evaluation of pineapple from different cultivar and ripening stage *(Online presentation) 73rd Annual Society of Biotechnology Japan Meeting. 2021*

3. **Ikram, M.M.M.;** Ridwani, S.; Putri, S.P.; Fukusaki, E. GC-MS based metabolomics approach to evaluate shelf life-related metabolites in pineapple (*Ananas comosus*) ripening process *(Online presentation) RWTH Aachen-Osaka University Symposium. 2021*

4. **Ikram, M.M.M.;** Ridwani, S.; Putri, S.P.; Fukusaki, E. GC-MS based metabolomics approach to evaluate shelf life-related metabolites in pineapple (*Ananas comosus*) ripening process *(Online presentation and online poster presentation) Metabolomics Society Online Conference. 2020*

5. **Ikram, M.M.M.;** Ridwani, S.; Putri, S.P.; Fukusaki, E. Untargeted metabolomics approach to monitor metabolite changes during pineapple ripening process *(Oral presentation) 71st Annual Society of Biotechnology Japan Meeting. 2019*

Supplementary

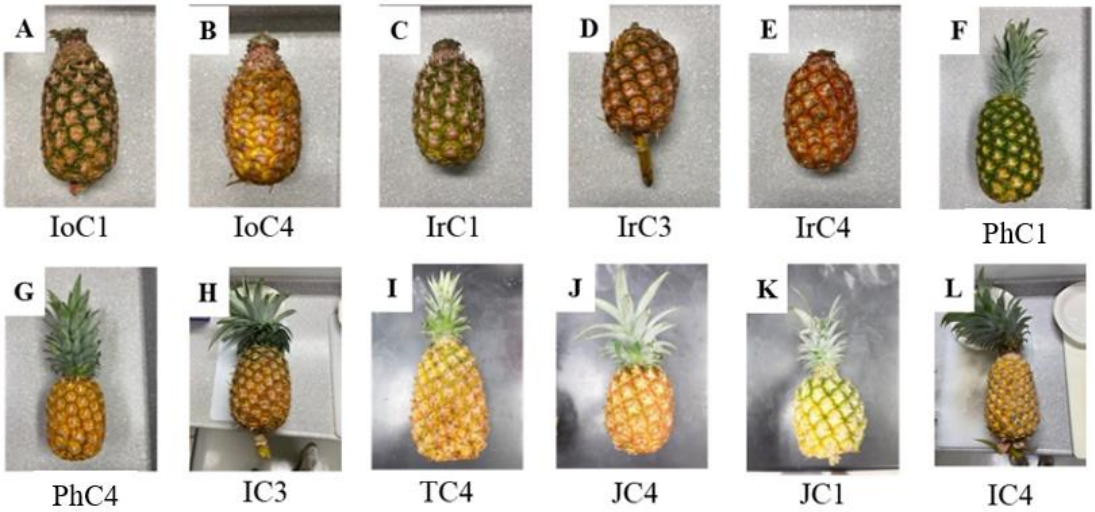

Figure S2.1. Pineapple used in this study. Pineapple samples that were subjected to RATA test (A–G) and subjected to GC-MS (A–L), (A) Indonesia Red Spanish Oval C! (IoC1), (B) Indonesia Red Spanish Oval C4 (IoC4), (C) Indonesia Red Spanish Round C1 (IrC1), (D) Indonesia Red Spanish Round C3 (IrC3), (E) Indonesia Red Spanish Round C4 (IrC4), (F) Philippine Smooth Cayenne C1 (PhC1), (G) Philippine Smooth Cayenne (PhC4), (H) Indonesia Smooth Cayenne C3 (IC3), (I) Taiwan Smooth Cayenne C4 (TC4), (J) Japan Smooth Cayenne C4 (JC4), (K) Japan Queen C1 (JC1), and (L) Indonesia Smooth Cayenne C4 (IC4).

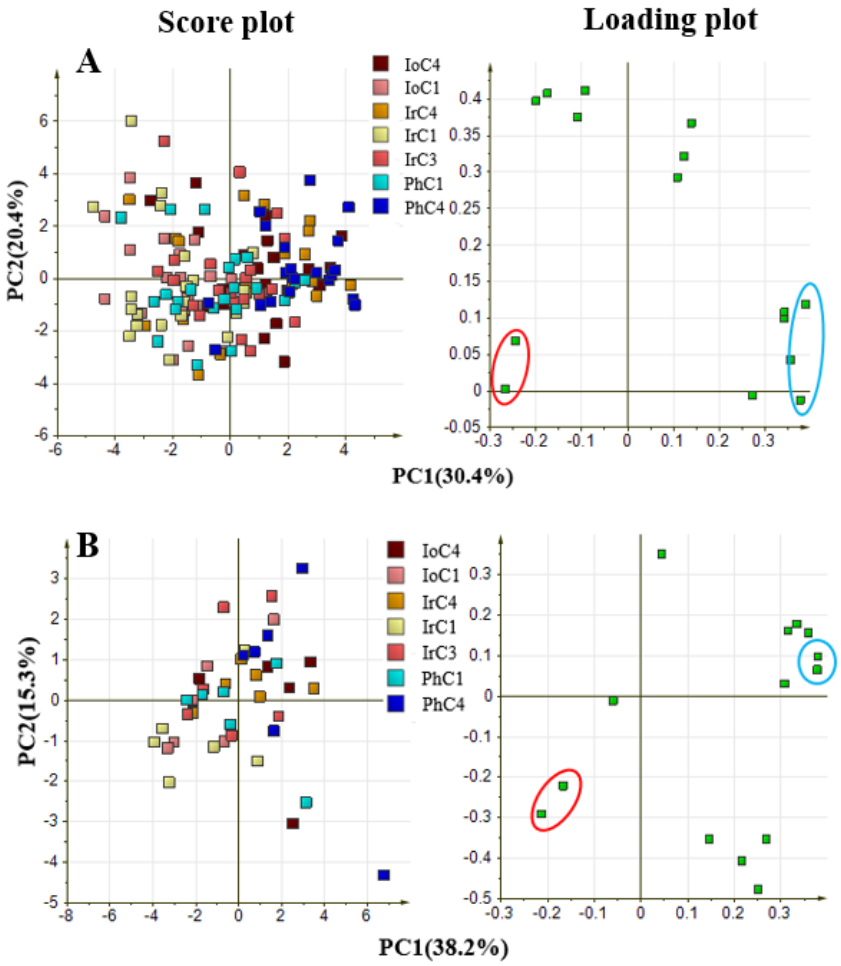

Figure S2.2. PCA result of RATA test using a different set of nationalities. (A) Results for group of 22 Japanese respondents. (B) Results for group of 5 Indonesian and 1 Malaysian respondents. Explanatory variables used in PCA were 15 auto-scaled sensory attributes data. (Left) Score plot showed separation from different ripening stages in PC1. Legends in the score plot represent the sample and colored based on Table 1. (Right) Loading plot corresponds to the separation in the score plot. Blue circle represents sweetness and high acceptability, while red circle represents sourness and firmness.

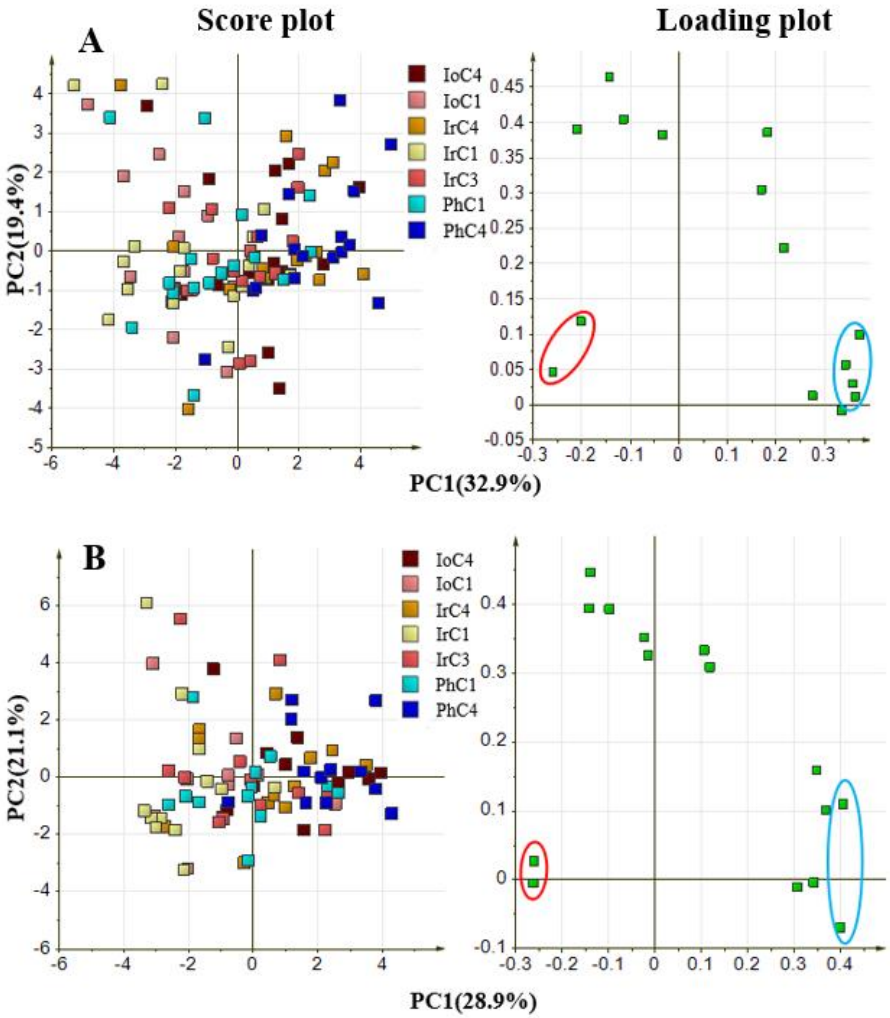

Figure S2.3. Gender PCA results of RATA test. (A) Results for group of 16 men. (B) Results for group of 12 women. Explanatory variables used in PCA were 15 auto-scaled sensory attributes data. (Left) Score plot showed separation from different ripening stages in PC1. Legends in the score plot represent the sample and colored based on Table 1. (Right) Loading plot corresponds to the separation in the score plot. Blue circle represents sweetness and high acceptability, while red circle represents sourness and firmness.

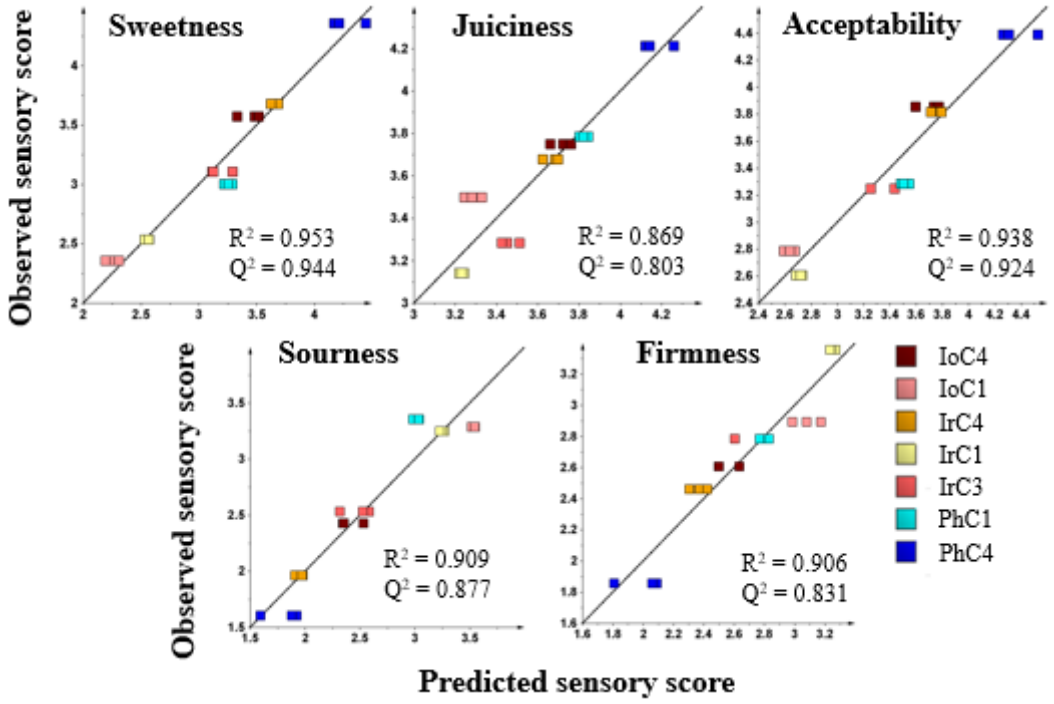

Figure S2.4. OPLS regression analysis results using RATA samples. Explanatory variables used to construct the model were 45 metabolites, with the response variables are the sensory score from 28 panelists. Value of R^2 and Q^2 were used to evaluate the model.

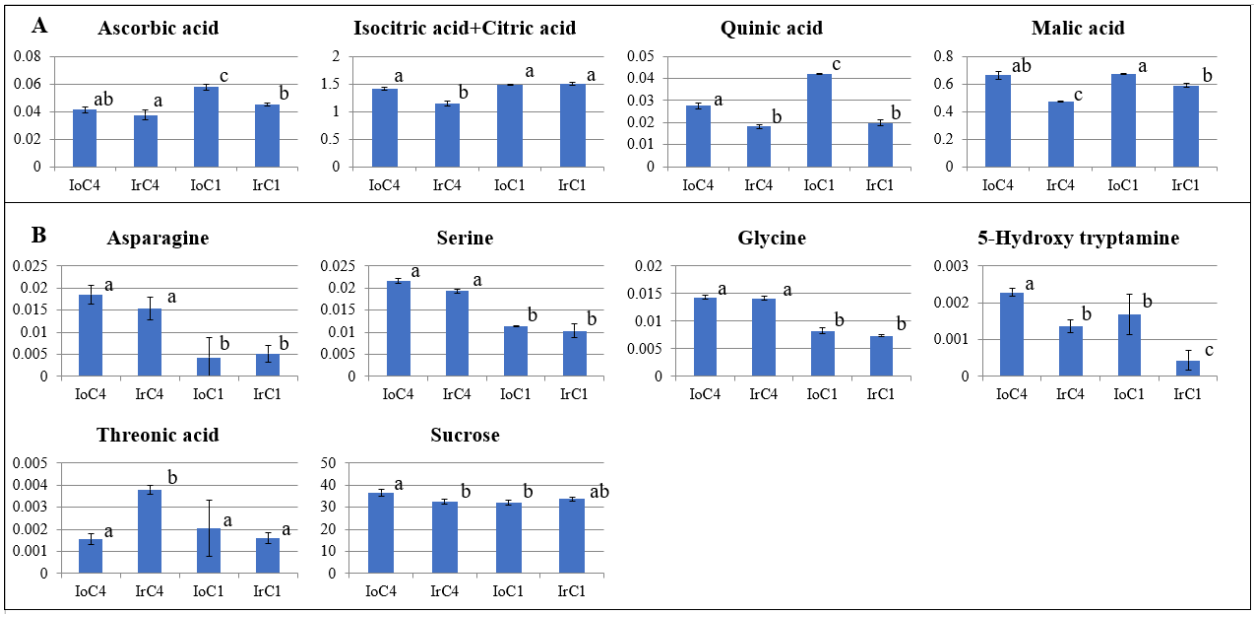

Figure S2.5. Sensory-related metabolite level on Indonesia Red Spanish C4 and C1 stage pineapple. From left to right: IoC4, IrC4, IoC1, and IrC1. (A) Bar graph of sourness and firmness-related metabolites (B) Bar graph of sweetness, juiciness, and high acceptability-related metabolites. Different letters are indicating significant differences ($p < 0.05$) based on Tukey's test mean comparison.

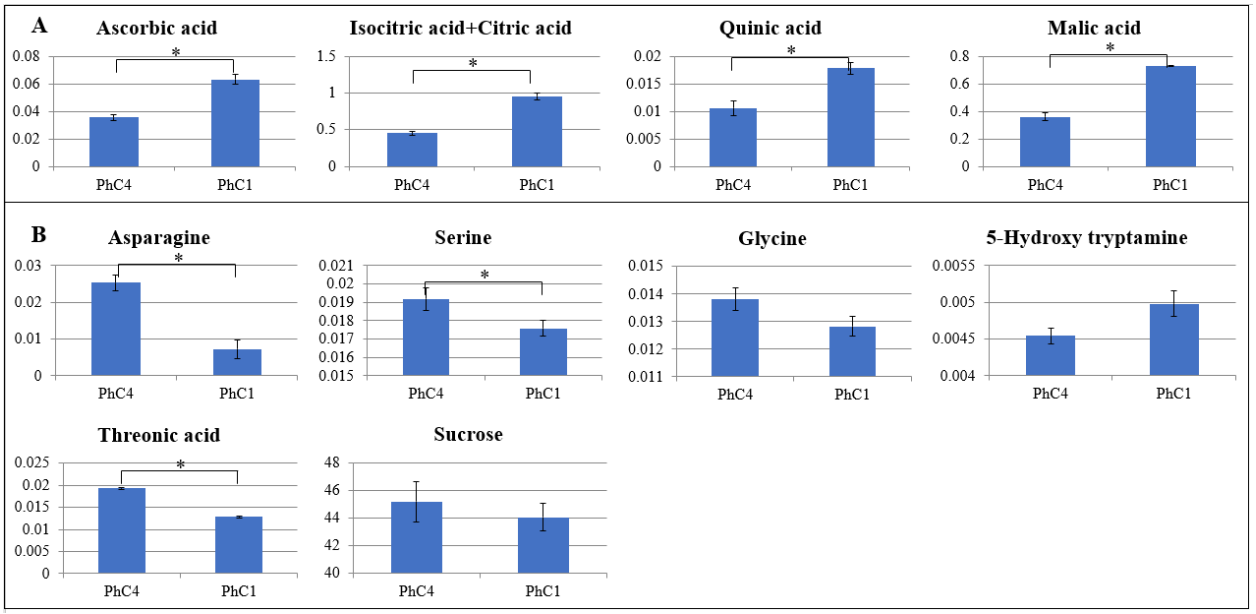

Figure S2.6. Sensory-related metabolite level on Philippine Smooth Cayenne C4 and C1 stage pineapple. From left to right: PhC4 and PhC1. (A) Bar graph of sourness and firmness-related metabolites (B) Bar graph of sweetness, juiciness, and high acceptability-related metabolites. Star marks indicating significant differences ($p < 0.05$) based on Tukey's test mean comparison.

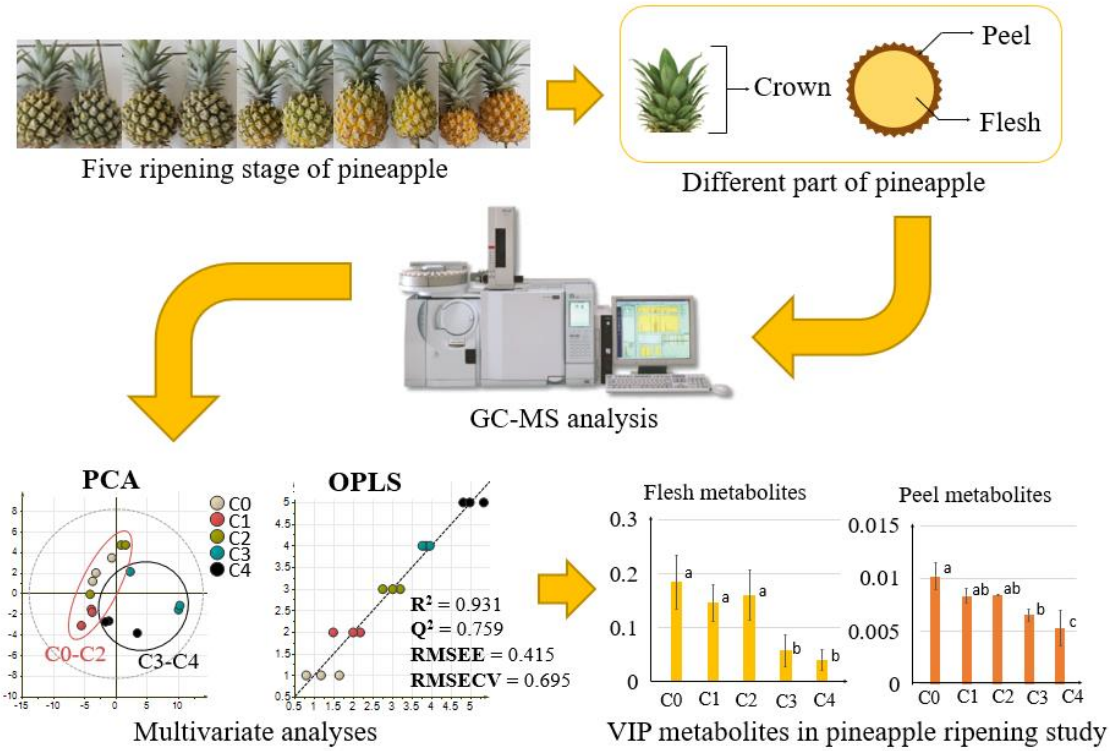

Figure S3.1. Visual experimental design on pineapple ripening study in this dissertation

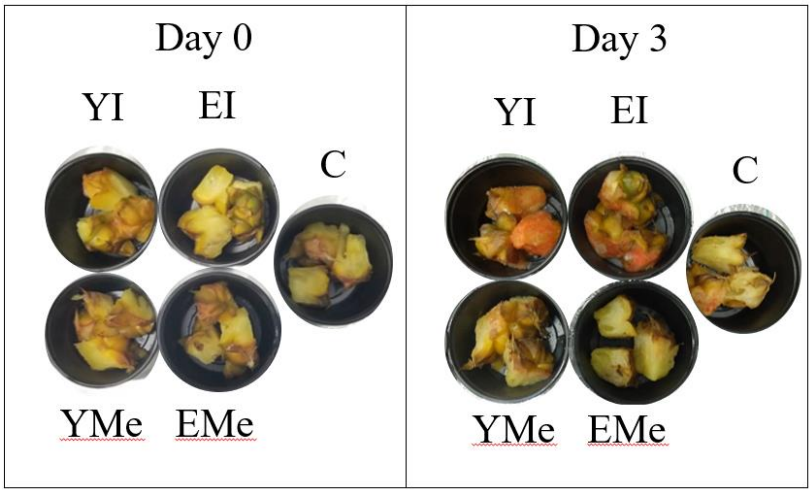

Figure S4.1. Fresh-cut pineapple picture of untreated (C), treated with Yang-based Inositol (20,000 mg/L) (YI), Yang-based Melezitose (20,000 mg/L) (YMe), Endogenous-based Inositol (15 mg/L) (EI), Endogenous-based Melezitose (5 mg/L) (EMe) and stored from day 0 until day 3.

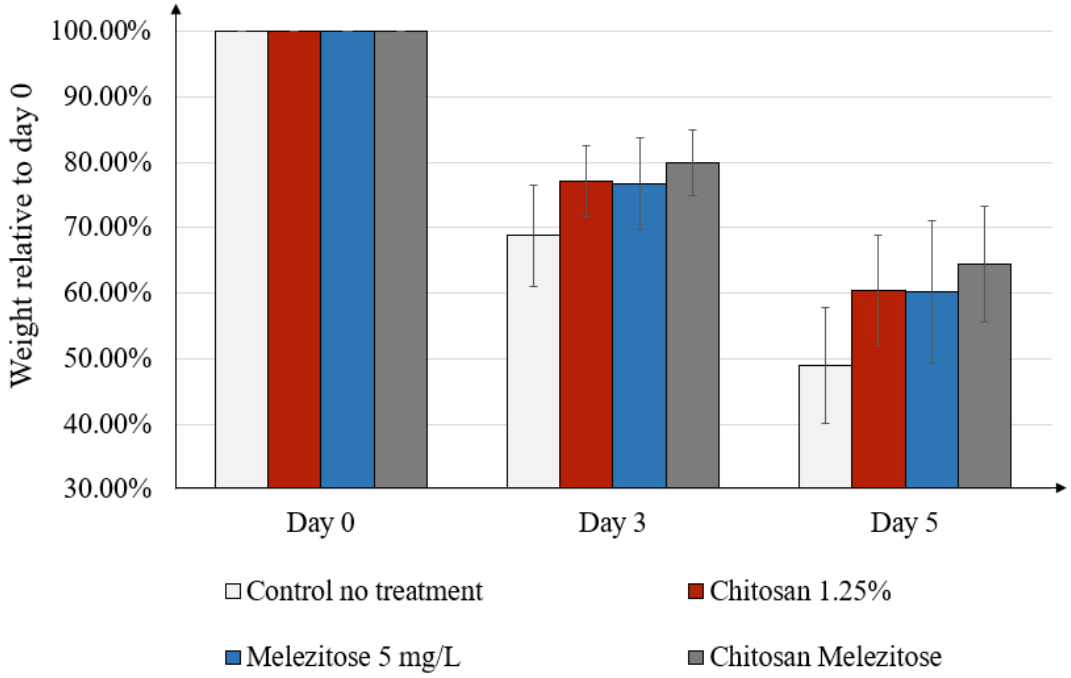

Figure S4.2. Weight difference between treatment after five days of storage

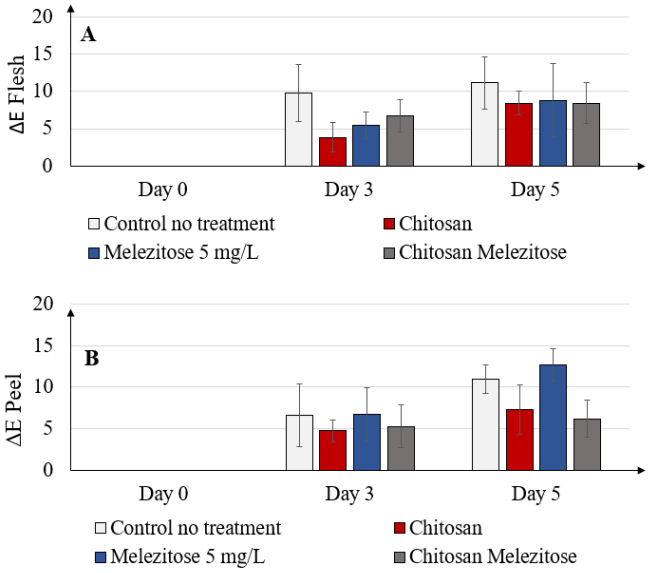

Figure S4.3. Color changes analysis calculated by using the ΔE2000 formula. (A) Flesh color changes relative to day 0 between treatments after five days of storage (B) Peel color changes relative to day 0 between treatments after five days of storage

Table S2.1. Sensory attributes for RATA test

Category	No	Attribute	Description
Aroma	1	Fruity	A general term used to describe the sweet, floral, or fruit-like aromatics associated with a blend of fruits
	2	Pineapple-like	Term to describe aromatics compounds specific to pineapple fruits, which comes from 2-methyl butanoate and methyl hexanoate
	3	Cardboard-like	Term to describe aromatic compounds related to the wet-cardboard smell packaging, commonly 2-nonenal
Taste	1	Sweetness	The fundamental taste factor associated with a sucrose solution
	2	Sourness	A fundamental taste factor of which citric acid in water is typical
	3	Salty	The fundamental taste factor associated with sodium chloride
	4	Bitter	A fundamental taste factor of which caffeine or quinine is typical
	5	Umami	The fundamental taste factor of which monosodium glutamate is typical
	6	Pineapple flavor	Intensity of “pineapple-specific” taste
	7	Banana	Intensity of “banana-specific” taste
	8	Coconut	Intensity of “coconut-specific” taste

	9	Off-flavor	Metallic taste (mouthfeel and aromatics associated "tin" cans, iron copper, or oxidized silver) or fermented taste (pungent, sweet, slightly sour, sometimes yeasty/alcohol-like)
Texture	1	Firmness	Flesh only. Amount of force required to bite completely through the sample using molar teeth
	2	Juiciness	The degree of moisture released after two chews; relative amount of juice released into the mouth
Hedonic	1	Acceptability	Term to describe the acceptance of pineapple as an overall value concurrent with all attributes

Table S2.2. Metabolites obtained from GC-MS analysis for different cultivar and different ripening stages analysis

Metabolite name	Average RT (min)	Average RI	Quant mass
Alanine	7.144	1108.07	116.1238
Valine	8.663	1224.03	144.1466
Serine	9.125	1264.08	116.0867
2-Aminoethanol	9.258	1275.57	174.1054
Phosphate	9.341	1282.76	299.0191
Isoleucine	9.554	1301.39	158.1398
Proline	9.592	1305.16	142.1438
Maleic acid	9.633	1309.16	147.1029
Glycine	9.701	1315.87	174.1054
Succinic acid	9.702	1315.94	147.0971
Serine	10.258	1370.79	204.0853
Threonine	10.532	1397.84	218.0938
b-Alanine	10.888	1436.5	174.1
Malic acid	11.445	1497.37	147.1
Methionine	11.718	1529.51	176.0958
Aspartic acid	11.727	1530.55	232.0728
Pyroglutamic acid	11.751	1533.41	156.0978
4-Aminobutyric acid	11.813	1540.86	174.105

Threonic acid	12.111	1576.14	147.1087
Glutamic acid	12.538	1628.65	246.0802
Phenylalanine	12.641	1641.81	218.0393
Xylose+Lyxose	12.874	1671.35	103.0687
Xylose	12.928	1678.33	103.0695
Asparagine	12.962	1682.62	116.1148
Lyxose	12.977	1684.44	103.068
Ribose	13.095	1699.48	103.0721
Xylonic acid	13.854	1801.9	217.0459
Isocitric acid+Citric acid	14.112	1838.58	273.0511
Quinic acid	14.47	1889.44	345.1333
Psicose+Tagatose	14.566	1903.24	103.0707
Fructose	14.633	1913.27	103.0652
Glucose	14.757	1931.8	205.0544
Lysine	14.8	1938.32	174.0985
Galactose+Glucose	14.892	1952.06	205.0511
Ascorbic acid	15.044	1974.77	147.0938
Galacturonic acid	15.224	2001.79	147.09
Glucarate	15.586	2058.4	333.0967
Inositol	16.039	2130.89	217.0554
5-Hydroxy tryptamine	18.232	2516.41	174.1061
b-Lactose	19.523	2773.76	204.0444

Trehalose	19.71	2813.14	361.125
Maltose	19.914	2856.97	361.11
Gentiobiose	20.225	2924.3	361.1194
Melibiose	20.344	2950.72	204.0481
Paeoniflorin	23.341	3512.74	361.1131

These metabolites were screened by relative standard deviation less than 30% and relative intensity more than three times compared to the blank sample. Retention indices (RI) were calculated using a standard alkene mixture (C_{10}–C_{40}). All annotated peak RI and mass spectra were compared with GL-science library and NIST 11 MS library with a 70% upwards matching score.

Table S3.1. Complete list of annotated metabolites with RSD<20% for ripening process analysis

* = metabolites that only present in either crown, flesh, or peel part

Crown				
No	**Metabolite**	**RI***	**Quantitative m/z**	**Annotation**
1	2-Aminoethanol	1275.61	174	GL-sciences library and NIST11
2	2-Hydroxypyridine	1038.83	152	GL-sciences library and NIST11
3	4-Aminobutyric acid	1541.90	174	GL-sciences library and NIST11
4	Alanine	1107.02	116	GL-sciences library and NIST11
5	Arabionose	1685.38	103	GL-sciences library and NIST11
6	Ascorbic acid*	1975.45	319	GL-sciences library
7	Asparagine	1683.48	116	GL-sciences library and NIST11
8	β-Lactose	2773.80	204	GL-sciences library and NIST11
9	Chlorogenic acid*	3169.11	345	GL-sciences library
10	Fructose 6-phosphate	2371.14	387	GL-sciences library
11	Fructose	1915.19	103	GL-sciences library and NIST11
12	Galactose	1927.13	309	GL-sciences library and NIST11
13	Galactose+Glucose	1953.42	319	GL-sciences library
14	Galacturonic acid	1981.79	333	GL-sciences library
15	Gentiobiose	2889.32	204	GL-sciences library and NIST11
16	Glucarate	2059.52	333	GL-sciences library and NIST11
17	Glucose	1933.45	319	GL-sciences library and NIST11

18	Glutamic acid	1629.50	246	GL-sciences library and NIST11
19	Glutamine*	1785.77	156	GL-sciences library
20	Glyceric acid	1340.15	147	GL-sciences library and NIST11
21	Glycine	1316.47	174	GL-sciences library and NIST11
22	Inositol	2132.57	217	GL-sciences library and NIST11
23	Isocitric acid+Citric acid	1841.85	273	GL-sciences library and NIST11
24	Isoleucine	1301.52	158	GL-sciences library and NIST11
25	Leucine*	1279.71	158	GL-sciences library and NIST11
26	Lysine	1940.35	174	GL-sciences library
27	Lyxose	1685.35	103	GL-sciences library and NIST11
28	Malic acid	1498.61	147	GL-sciences library and NIST11
29	Maltitol	2936.87	204	GL-sciences library
30	Mannitol	1967.73	319	GL-sciences library and NIST11
31	Melibiose	2949.37	361	GL-sciences library
32	Meso erythritol	1523.81	147	GL-sciences library and NIST11
33	N-Acetyl glucosamine*	2118.52	147	GL-sciences library and NIST11
34	Oxalacetic acid+Pyruvate	1050.97	174	GL-sciences library
35	Phenylalanine	1642.44	218	GL-sciences library and NIST11
36	Phosphate	1282.05	299	GL-sciences library and NIST11
37	Proline	1306.0	142	GL-sciences library and NIST11

38	Psicose+Tagatose	1905.19	103	GL-sciences library and NIST11
39	Putrescine*	1757.65	174	GL-sciences library and NIST11
40	Quinic acid	1890.97	345	GL-sciences library
41	Raffinose	3500.23	361	GL-sciences library
42	Rhamnose	1744.84	117	GL-sciences library and NIST11
43	Ribitol	1752.37	217	GL-sciences library, NIST11, and STD
44	Ribose	1700.54	103	GL-sciences library and NIST11
45	Serine	1262.93	116	GL-sciences library and NIST11
46	Sucrose	2704.68	361	GL-sciences library and NIST11
47	Threitol*	1515.11	217	GL-sciences library
48	Threonic acid	1577.02	147	GL-sciences library and NIST11
49	Threonine	1397.86	218	GL-sciences library and NIST11
50	Trehalose	2814.93	361	GL-sciences library
51	Tryptophan	2219.10	218	GL-sciences library
52	Tyrosine	1958.71	218	GL-sciences library
53	Uric acid*	2127.02	441	GL-sciences library*
54	Valine	1223.4	144	GL-sciences library and NIST11
55	Xylonic acid	1793.15	292	GL-sciences library
56	Xylose	1679.15	103	GL-sciences library and NIST11
Flesh				
No	**Metabolite**	**RI***	**Quantitative m/z**	**Annotation**
1	2-Aminoethanol	1275.39	174	GL-sciences library and NIST11

2	4-Aminobutyric acid	1541.37	174	GL-sciences library and NIST11
3	5-Hydroxy tryptamine*	2517.11	174	GL-sciences library
4	Alanine	1371.36	188	GL-sciences library and NIST11
5	Aspartic acid	1530.54	232	GL-sciences library
6	β-Lactose	2773.87	204	GL-sciences library and NIST11
7	Fructose	1915.21	103	GL-sciences library and NIST11
8	Galactinol	3075.23	204	GL-sciences library
9	Galactose	1927.03	319	GL-sciences library and NIST11
10	Galactose+Glucose	1953.44	319	GL-sciences library
11	Galacturonic acid	1981.75	147	GL-sciences library
12	Gentiobiose	2888.76	204	GL-sciences library and NIST11
13	Glucarate	2058.66	204	GL-sciences library and NIST11
14	Gluconic acid	2035.99	147	GL-sciences library
15	Glucose	1933.95	319	GL-sciences library and NIST11
16	Glutamic acid	1629.04	246	GL-sciences library and NIST11
17	Glycine	1316.22	174	GL-sciences library and NIST11
18	Inositol	2131.83	217	GL-sciences library, NIST11, and STD
19	Isocitric acid+Citric acid	1840.31	273	GL-sciences library and NIST11
20	Lysine	1939.74	174	GL-sciences library
21	Lyxose	1684.88	103	GL-sciences library and NIST11
22	Malic acid	1497.61	147	GL-sciences library and NIST11

23	Maltitol	2936.84	204	GL-sciences library
24	Maltose	2856.61	361	GL-sciences library and NIST11
25	Melezitose*	3590.08	361	GL-sciences library and STD
26	Melibiose	2949.63	361	GL-sciences library
27	Oxalacetic acid+Pyruvate	1050.55	174	GL-sciences library
28	Phosphate	1281.72	299	GL-sciences library and NIST11
29	Proline	1305.97	142	GL-sciences library and NIST11
30	Psicose+Tagatose	1905.13	103	GL-sciences library and NIST11
31	Pyroglutamic acid	1534.04	156	GL-sciences library
32	Quinic acid	1890.39	345	GL-sciences library and STD
33	Raffinose	3499.49	361	GL-sciences library
34	Rhamnose	1744.43	117	GL-sciences library and NIST11
35	Ribitol	1751.91	217	GL-sciences library, NIST11, and STD
36	Serine	1369.89	204	GL-sciences library and NIST11
37	Sorbitol	1975.10	319	GL-sciences library and NIST11
38	Spermidine*	2284.89	368	GL-sciences library
39	Sucrose	2708.22	362	GL-sciences library and NIST11
40	Threonic acid	1576.48	292	GL-sciences library and NIST11
41	Trehalose	2815.30	361	GL-sciences library
42	Turanose	2830.75	217	GL-sciences library
43	Tyrosine	1958.97	218	GL-sciences library
44	Valine	1223.06	144	GL-sciences library and NIST11

45	Xylonic acid	1802.68	103	GL-sciences library
46	Xylose+Lyxose	1671.96	103	GL-sciences library
47	Xylose	1678.61	103	GL-sciences library and NIST11
Peel				
No	**Metabolite**	**RI***	**Quantitative m/z**	**Annotation**
1	1,6-Anhydroglucose*	1726.19	204	GL-sciences library
2	2-Aminoethanol	1275.80	174	GL-sciences library and NIST11
3	2-Hydroxypyridine	1038.98	152	GL-sciences library and NIST11
4	4-Aminobutyric acid	1541.83	174	GL-sciences library and NIST11
5	α-Ketoglutaric acid*	1583.58	147	GL-sciences library
6	Alanine	1371.86	188	GL-sciences library and NIST11
7	Allose+Mannose	1936.41	273	GL-sciences library and NIST11
8	Arabionose	1685.53	103	GL-sciences library and NIST11
9	Aspartic acid	1531.03	232	GL-sciences library
10	β -Lactose	2774.12	204	GL-sciences library and NIST11
11	Fructose 6-phosphate	2371.23	387	GL-sciences library
12	Fructose	1915.69	103	GL-sciences library and NIST11
13	Galactinol	3075.95	204	GL-sciences library
14	Galactose	1927.53	319	GL-sciences library, NIST11, and STD
15	Galactose+Glucose	1953.92	319	GL-sciences library
16	Gentiobiose	2889.44	204	GL-sciences library and NIST11

17	Glucarate	2059.65	333	GL-sciences library and NIST11
18	Gluconic acid	2003.61	147	GL-sciences library
19	Glucose	1934.39	319	GL-sciences library, NIST11, and STD
20	Glutamic acid	1629.56	246	GL-sciences library and NIST11
21	Glyceric acid	1340.31	189	GL-sciences library
22	Glycine	1316.38	147	GL-sciences library and NIST11
23	Inositol	2132.77	217	GL-sciences library, NIST11, and STD
24	Isocitric acid+Citric acid	1840.73	273	GL-sciences library and NIST11
25	Isoleucine	1301.68	158	GL-sciences library and NIST11
26	Lyxose	1679.11	103	GL-sciences library and NIST11
27	Malic acid	1498.09	147	GL-sciences library and NIST11
28	Maltitol	2937.58	204	GL-sciences library
29	Maltose	2853.17	319	GL-sciences library and NIST11
30	Mannitol	1967.98	319	GL-sciences library and NIST11
31	Mannose*	1920.82	160	GL-sciences library, NIST11, and STD
32	Melibiose	2950.27	361	GL-sciences library
33	Meso erythritol	1523.84	217	GL-sciences library
34	Oxalacetic acid+Pyruvate	1051.11	174	GL-sciences library
35	Phenylalanine	1642.55	218	GL-sciences library and NIST11
36	Phosphate	1282.15	299	GL-sciences library and NIST11
37	Pyroglutamic acid	1534.56	156	GL-sciences library

38	Quinic acid	1890.97	345	GL-sciences library
39	Raffinose	3500.43	361	GL-sciences library
40	Rhamnose	1744.97	117	GL-sciences library and NIST11
41	Ribitol	1752.38	217	GL-sciences library, NIST11, and STD
42	Ribose	1700.52	103	GL-sciences library
43	Serine	1370.24	204	GL-sciences library and NIST11
44	Sinapinic acid*	2256.58	368	GL-sciences library
45	Sorbitol	1975.97	147	GL-sciences library and NIST11
46	Sorbose*	1905.65	103	GL-sciences library and NIST11
47	Sucrose	2707.94	362	GL-sciences library and NIST11
48	Threonic acid	1577.04	147	GL-sciences library and NIST11
49	Threonine	1398.00	218	GL-sciences library and NIST11
50	Trehalose	2815.29	361	GL-sciences library
51	Tyrosine	1958.86	218	GL-sciences library
52	Valine	1223.59	144	GL-sciences library and NIST11
53	Xylonic acid	1782.37	103	GL-sciences library
54	Xylose+Lyxose	1672.39	103	GL-sciences library

*Retention indices (RI) were calculated using standard alkane mixture (C_{10}-C_{40}).

Peak annotation was as follows:

- Comparison of the retention indices (RI) and their mass spectra with GL-science library,
- 80% upwards matching to NIST11 library
- Co-injection with authentic standard by spiking into extracted samples.

Table S3.2. Metabolites with VIP score (more than 1) and its coefficients

Flesh				Peel			
No	Metabolite	VIP Score	Coefficients	No	Metabolite	VIP Score	Coefficients
1	Melezitose	1.805	0.086	1	Inositol	1.858	-0.088
2	Inositol	1.784	-0.085	2	Mannose	1.712	-0.066
3	Xylonic acid	1.736	0.075	3	Galactose	1.700	-0.053
4	Gluconic acid	1.689	0.069	4	Sucrose	1.661	0.079
5	Raffinose	1.687	-0.070	5	Aspartic acid	1.627	-0.066
6	Threonic acid	1.617	0.090	6	Galactose+Glucose	1.596	-0.065
7	β-Lactose	1.553	-0.076	7	1,6-Anhydroglucose	1.535	0.071
8	Quinic acid	1.457	-0.058	8	Tyrosine	1.423	-0.044
9	Oxalacetic acid+Pyruvate	1.378	-0.054	9	Allose+Mannose	1.377	-0.036
10	Melibiose	1.373	0.042	10	Melibiose	1.360	-0.050
11	Malic acid	1.248	-0.057	11	4-Aminobutyric acid	1.294	-0.036
12	Galactose	1.241	-0.048	12	Glucose	1.292	-0.023
13	Maltose	1.203	0.033	13	Pyroglutamic acid	1.267	-0.031
14	Turanose	1.200	0.046	14	Meso erythritol	1.247	0.036
15	Galacturonic acid	1.145	-0.106	15	Raffinose	1.230	-0.025
16	2-Aminoethanol	1.019	0.013	16	Galactinol	1.216	-0.043
17	Gentiobiose	1.004	0.058	17	Fructose	1.215	-0.027
				18	Quinic acid	1.205	-0.055
				19	Xylose+Lyxose	1.198	0.090
				20	Lyxose	1.196	0.015
				21	Glutamic acid	1.155	-0.043
				22	Threonic acid	1.067	-0.034
				23	Gentiobiose	1.032	0.038
				24	Glucarate	1.004	-0.041

Table S4.1. List of acquired metabolites from GC-MS analysis with RSD<30% and relative intensity more than three times compare to blank.

No	Metabolite name	Average RT (min)	Average RI	*m/z*
1	Propyleneglycol	5.32	1005.4	117
2	Alanine	6.92	1109.3	116
3	Unknown1	7.47	1151.2	177
4	Unknown2	7.78	1174.1	145
5	Unknown3	7.94	1186.5	281
6	Malonic acid	8.24	1210.6	147
7	Valine	8.41	1225.4	144
8	Unknown4	9.30	1304.5	117
9	Glyceric acid	9.69	1343.0	189
10	Threonine	10.19	1393.0	117
11	Unknown5	10.34	1409.5	131
12	Malic acid	11.16	1499.2	147
13	Unknown6	11.29	1514.7	117
14	Pyroglutamic acid	11.45	1534.6	156
15	Unknown7	11.51	1541.5	129
16	Unknown8	11.65	1558.5	247
17	Unknown9	11.67	1561.1	117
18	Isobutyl acetate*	11.72	1567.1	117
19	Unknown11	11.77	1572.3	129
20	Threonic acid	11.83	1579.1	147
21	Unknown12	11.84	1580.6	179
22	3-Hydroxy-3-methylglutarate	12.12	1614.8	147
23	Fucose*	12.24	1630.3	117
24	Unknown14	12.39	1649.9	217
25	Unknown15	12.57	1672.8	117

26	Unknown16	12.58	1673.6	217
27	Xylose	12.58	1674.0	103
28	Lyxose	12.63	1681.0	103
29	Asparagine	12.66	1684.3	116
30	Arabionose	12.68	1687.3	103
31	Ribose	12.80	1702.5	103
32	Xylitol	13.04	1735.6	217
33	Ribitol	13.18	1753.5	217
34	Unknown17	13.29	1768.9	217
35	Unknown18	13.31	1772.3	147
36	Unknown19	13.37	1779.8	217
37	Unknown20	13.40	1783.7	103
38	Xylonic acid	13.48	1794.9	292
39	Unknown21	13.55	1803.7	217
40	Unknown22	13.55	1804.9	103
41	Unknown23	13.59	1809.9	292
42	Isocitric acid+Citric acid	13.81	1841.2	273
43	Unknown24	14.00	1868.0	173
44	Unknown25	14.07	1878.1	245
45	Unknown26	14.07	1879.1	275
46	Quinic acid	14.17	1892.2	345
47	Sorbose	14.26	1905.9	103
48	Unknown27	14.32	1914.4	147
49	Unknown28	14.32	1914.7	307
50	Fructose	14.33	1915.8	217
51	Unknown29	14.33	1916.6	204
52	Glucose	14.45	1934.0	147
53	Unknown30	14.46	1935.7	133
54	Unknown31	14.57	1951.7	349
55	Unknown32	14.57	1952.7	103

56	Galactose+Glucose	14.58	1953.6	147
57	Tyrosine	14.61	1958.8	218
58	Unknown33	14.65	1964.6	204
59	Mannitol	14.68	1969.1	147
60	Unknown34	14.70	1971.7	305
61	Sorbitol	14.73	1976.8	147
62	Galactitol	14.77	1981.7	205
63	Galacturonic acid	14.78	1983.1	333
64	Gluconic acid	15.13	2038.5	147
65	Glucarate	15.27	2060.5	333
66	Inositol	15.72	2133.1	305
67	Unknown35	16.66	2289.6	204
68	Unknown36	16.72	2300.7	217
69	Unknown37	16.87	2327.3	290
70	Unknown38	17.02	2354.2	204
71	Unknown39	17.54	2449.1	259
72	Unknown40	17.66	2470.7	117
73	Unknown41	17.67	2473.4	204
74	Unknown42	17.73	2483.6	129
75	Unknown43	17.95	2526.9	345
76	Unknown44	17.95	2527.0	435
77	Unknown45	18.31	2596.0	204
78	Unknown46	18.46	2626.1	204
79	Sucrose	18.86	2706.6	361
80	Unknown47	19.11	2759.1	217
81	Unknown48	19.17	2771.3	340
82	Unknown49	19.22	2782.0	361
83	Unknown50	19.27	2790.9	361
84	Trehalose	19.39	2817.7	361
85	Unknown51	19.47	2834.1	217

86	Unknown52	19.48	2835.4	259
87	Unknown53	20.01	2952.7	361
88	Unknown54	20.08	2967.7	204
89	Unknown55	20.33	3024.2	204
90	Unknown56	20.93	3159.2	340
91	Unknown57	21.88	3354.1	340
92	Unknown58	23.06	3550.7	98
93	Unknown59	23.57	3622.9	361

Retention indices (RI) were calculated using a standard alkene mixture (C_{10}-C_{40}). All annotated peak RI and mass spectra were compared with GL-science library and NIST-11 MS library with 70% upwards matching score. (*)mark showed the metabolites that putatively identified by Mass Bank of North America from Fiehns database (https://mona.fiehnlab.ucdavis.edu/)

Table S4.2. List of VIP metabolites with the VIP and coefficient score for each model obtained from OPLS regression analysis.

No	Metabolites	VIP Weight	Coefficient Weight	VIP Color flesh	Coefficient color flesh	VIP Color peel	Coefficient color peel
1	Alanine	1.39466	0.0294414	1.52212	-0.0372607	1.05681	-0.0113658
2	Asparagine	1.38837	0.0308905	1.41719	-0.0339464	1.18404	-0.01716
3	Fructose	1.45973	0.0262637	1.50211	-0.0291509	1.29839	-0.0176781
4	Galactose+Glucose	1.47527	0.0273988	1.51262	-0.0298461	1.30514	-0.0179479
5	Gluconic acid	1.45339	-0.0286224	1.50813	0.0341876	1.29755	0.0183359
6	Glucose	1.46462	0.0264998	1.50666	-0.0293284	1.3023	-0.0177804
7	Glyceric acid	1.28118	-0.0206136	1.32147	0.0257521	1.31265	0.0215984
8	Inositol	1.13019	0.0334069	0.996391	-0.0289689	1.0435	-0.0195513
9	Malic acid	1.46278	0.0264668	1.50946	-0.029536	1.30187	-0.0178228
10	Malonic acid	1.04515	0.00147374	1.09732	0.000890974	1.14622	0.0125711
11	Pyroglutamic acid	1.03307	0.0205045	1.22873	-0.032536	0.753617	-0.0070985
12	Quinic acid	1.2905	0.0379908	1.0365	-0.0215679	1.25315	-0.0264449
13	Sorbitol	1.00943	-0.0042090	1.15971	0.0112591	0.968897	0.00980807
14	Sorbose	1.46775	0.0267192	1.50812	-0.0294092	1.30347	-0.0178193
15	Sucrose	1.41492	0.0269014	1.42951	-0.0276688	1.23745	-0.0167513
16	Tyrosine	1.40439	0.0267957	1.43959	-0.0292188	1.26456	-0.0183999
17	Unknown1	1.08005	-0.0139602	1.23532	0.0216678	0.83271	0.00635515
18	Isobutyl acetate	1.27765	-0.0221154	1.05468	0.00842368	1.3815	0.0243311
19	Fucose	1.41224	-0.0294588	1.27576	0.0227554	1.42228	0.0247816
20	Unknown15	0.976378	-0.0034095	1.0983	0.0109553	1.0688	0.0139665
21	Unknown18	1.25105	-0.0145259	1.22478	0.0120672	1.24697	0.016479
22	Unknown22	1.1071	-0.0074431	1.05291	0.00318769	1.3417	0.0232842
23	Unknown27	1.46542	0.0266025	1.50645	-0.0293605	1.30138	-0.0177585
24	Unknown28	1.45146	0.0258669	1.49514	-0.0288972	1.29283	-0.0175474
25	Unknown29	1.49046	0.029259	1.53578	-0.0323845	1.29005	-0.0176326
26	Unknown30	1.46817	0.0268984	1.51219	-0.0298819	1.29915	-0.0177062
27	Unknown32	1.48191	0.028132	1.5195	-0.0306286	1.30472	-0.0180615
28	Unknown40	1.1953	-0.0271425	0.962117	0.0118731	1.22415	0.0220937

29	Unknown42	1.00962	-0.0121975	0.725002	-0.00494769	1.31521	0.0253214
30	Unknown43	1.07718	-0.0127588	1.18668	0.0177469	0.969734	0.0111035
31	Unknown45	1.17025	-0.0161315	1.14845	0.0133361	1.21756	0.0191304
32	Unknown47	1.36336	0.0255872	1.37965	-0.0266592	1.22166	-0.0174828
33	Unknown5	1.0024	-0.0074953	0.888933	0.00275697	1.33334	0.0253603
34	Unknown51	1.495	0.0358116	1.38972	-0.0287255	1.2719	-0.0189307
35	Unknown54	1.25978	-0.015985	1.19838	0.0113956	1.35817	0.0218773
36	Unknown59	1.44308	0.0262282	1.46984	-0.0281209	1.2786	-0.0172741
37	Unknown7	1.08693	-0.0052433	1.04461	0.00106556	1.22217	0.0176111
38	Unknown9	1.29915	-0.0156349	1.21362	0.0106409	1.3983	0.0217736
39	Valine	1.48799	0.0308649	1.56061	-0.0354511	1.23065	-0.0160228
40	Xylitol	1.00311	-0.0138603	1.24711	0.0276288	0.670862	0.00143075